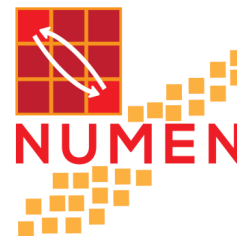
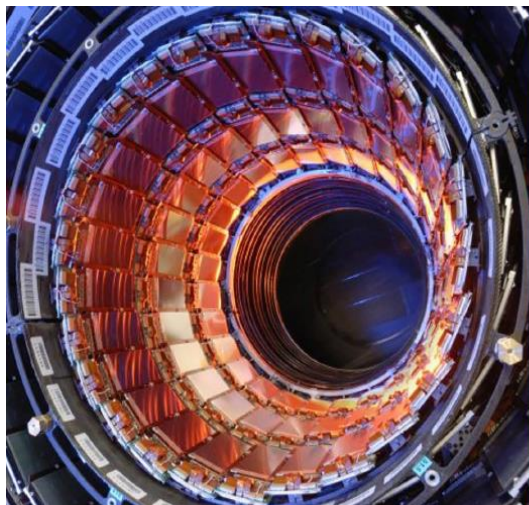


# The NUMEN experiment



**Manuela Cavallaro**

**INFN – Laboratori Nazionali del Sud  
(Italy)**



**XXVI GIORNATE DI STUDIO  
SUI RIVELATORI**

**Scuola F. Bonaudi**

Cogne, 13 – 17 February 2017



## NUMEN

**NU**clear **M**atrix **E**lements for **N**eutrinoless double beta decay



**Physics case:** use of **nuclear reactions** to extract information of the **Nuclear Matrix Elements** entering in the expression relating the  $0\nu\beta\beta$  decay half life to the neutrino absolute mass scale

$$\left(T_{\frac{1}{2}}^{0\nu\beta\beta}(0^+ \rightarrow 0^+)\right)^{-1} = G_{0\nu\beta\beta} \left|M^{0\nu\beta\beta}\right|^2 \left|f(m_i, U_{ei})\right|^2$$

**Pilot experiment** (DOCET) performed at INFN-Laboratori Nazionali del Sud in 2012 to test the feasibility

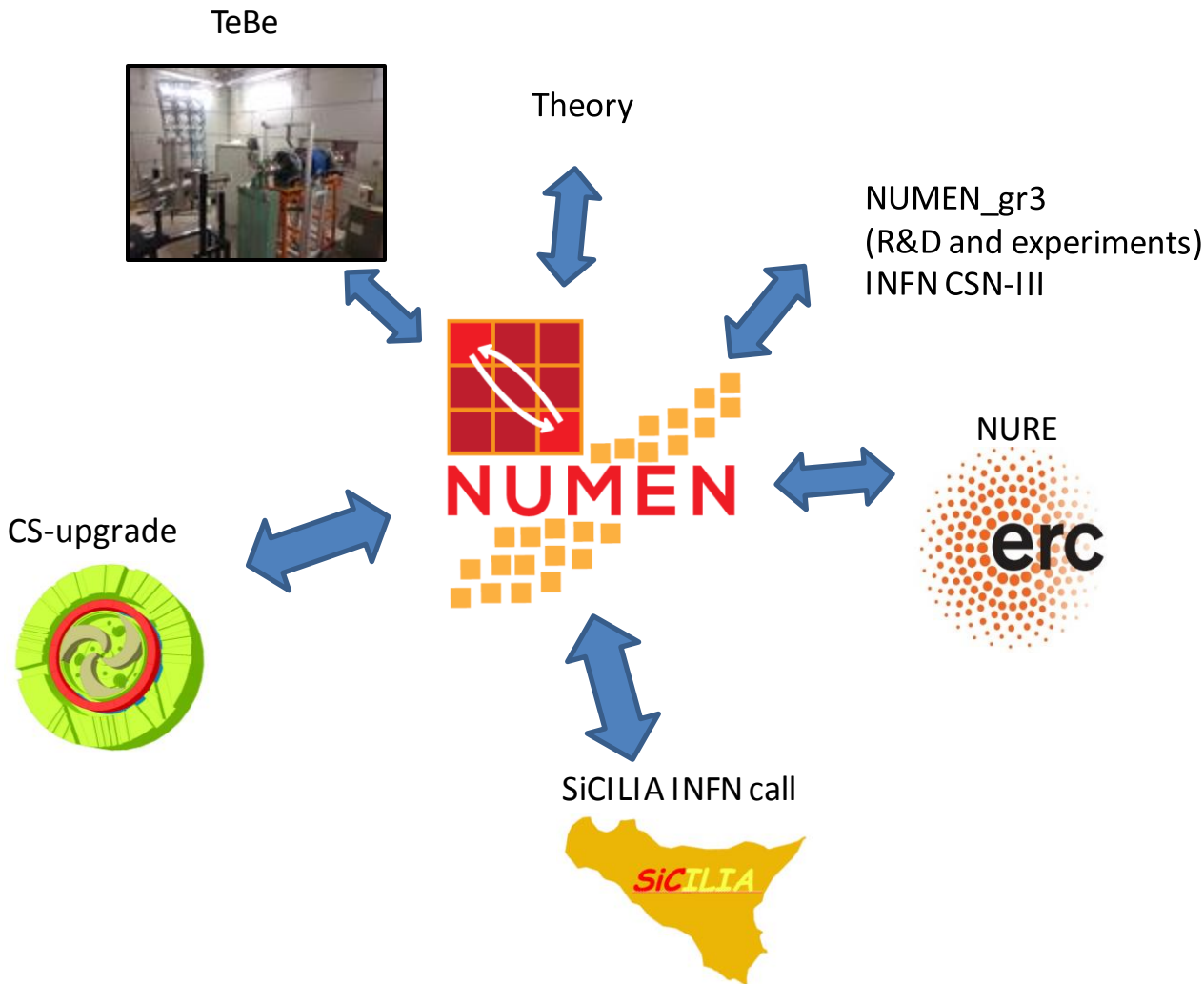
**NUMEN** proposed within the INFN «What Next» initiative in 2014

**NURE project** was approved for funding by ERC-Starting Grant in 2016



# NUMEN

NUclear Matrix Elements for Neutrinoless double beta decay





# NUMEN

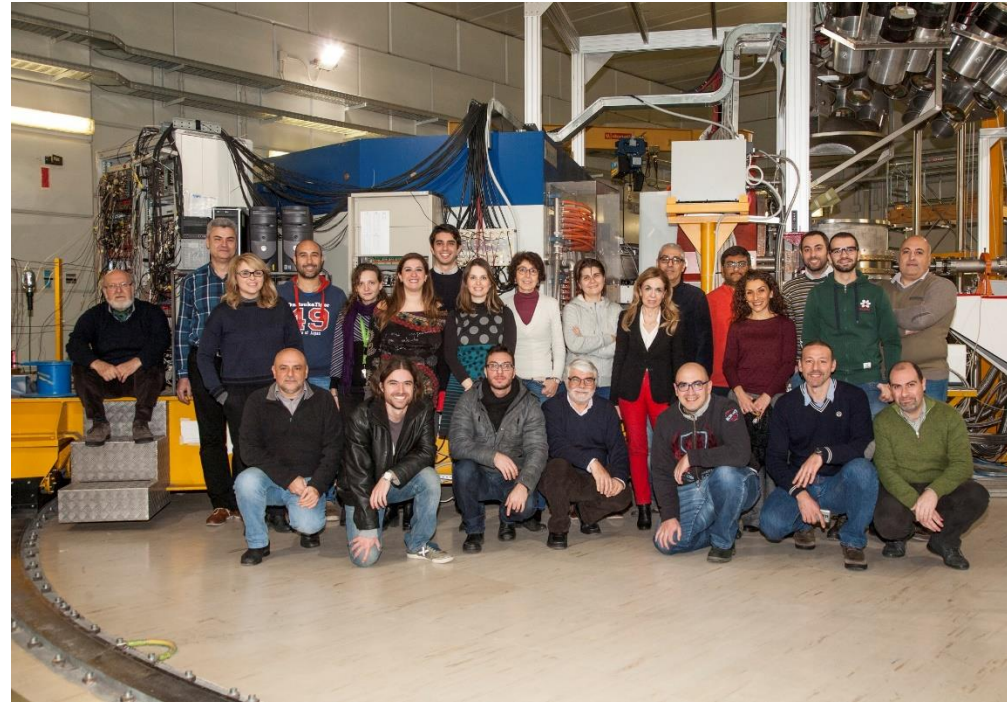
**NUclear Matrix Elements for Neutrinoless double beta decay**



## The collaboration

**Spokespersons:** F. Cappuzzello and C. Agodi

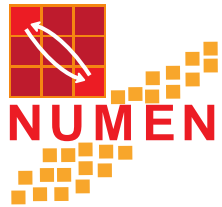
E. Aciksoz, L. Acosta, C. Agodi, X. Aslanoglou, N. Auerbach,  
J. Bellone, R. Bijker, S. Bianco, D. Bonanno, D. Bongiovanni,  
T. Borello, I. Boztosun, V. Branchina, M.P. Bussa, L. Busso,  
S. Calabrese, L. Calabretta, A. Calanna, D. Calvo,  
F. Cappuzzello, D. Carbone, M. Cavallaro, E.R. Chávez Lomelí,  
M. Colonna, G. D'Agostino, N. Deshmuk, P.N. de Faria, C. Ferraresi,  
J.L. Ferreira, P. Finocchiaro, A. Foti, G. Gallo, U. Garcia,  
G. Giraud, V. Greco, A. Hacisalihoglu, J. Kotila, F. Iazzi,  
R. Introzzi, G. Lanzalone, A. Lavagno, F. La Via, J.A. Lay,  
H. Lenske, R. Linares, G. Litrico, F. Longhitano, D. Lo Presti,  
J. Lubian, N. Medina, D. R. Mendes, A. Muoio, J. R. B. Oliveira,  
A. Pakou, L. Pandola, H. Petrascu, F. Pinna, F. Pirri, S. Reito,  
D. Rifuggiato, M.R.D. Rodrigues, A. Russo, G. Russo,  
G. Santagati, E. Santopinto, O. Sgouros, S.O. Solakci,  
G. Souliotis, V. Soukeras, S. Tudisco, R.I.M. Vsevolodovna,  
R. Wheadon, V. Zagatto



*Italy, Brazil, Greece, México, Germany, Turkey, Israel, Romania, Spain*

73 members, 9 countries

In Italy: LNS, Catania, Torino, Genova



# NUMEN is a challenging program

**Experiments  
with the MAGNEX  
spectrometer**

**Upgrade of the LNS  
accelerator and beam lines**

**Nuclear reaction theory**

LNS, Genova,  
Germany, Spain, Israel

**R&D on new technologies**

- Detectors
- Reaction target
- Mechanics

INFN-Torino and Politecnico  
Romania, Mexico

# Outlook

- Large acceptance magnetic spectrometry
- The MAGNEX spectrometer at INFN-LNS
- The physics case
- The NUMEN program



I'LL GET TO IT  
TOMORROW



# Magnetic spectrometry

# Main Concepts

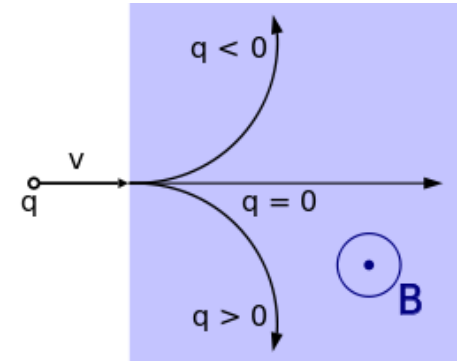
The study of the **motion of charged particles** through a **magnetic field** is a well established technique to explore the **microscopic structure** of the matter.

- ✚ Average motion and the concept of **beam**
- ✚ Analogy between **beam** and **light ray**
- ✚ Optics of charged particle beams and **aberrations**



# Magnetic spectrometry: Using static magnetic fields to learn about microscopic world

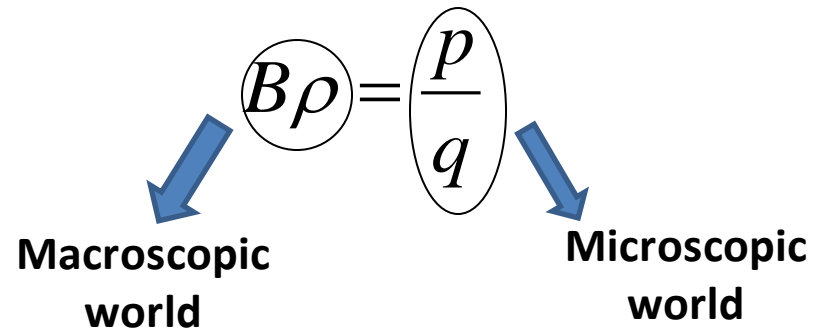
Lorentz force  $\vec{F} = q\vec{v} \wedge \vec{B}$



If  $\vec{v} \perp \vec{B}$  and  $\vec{B}$  is uniform

$$F = qvB = m \frac{v^2}{\rho}$$

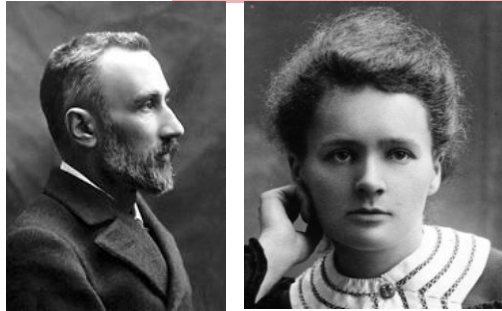
$\rho$   
 curvature radius



- ✚ If **B** is known, a measurement of  $\rho$  corresponds to a measurement of **p/q**
- ✚ If also **q** is known (by supplementary detectors) one gets information about **p** (**momentum spectrometry**)
- ✚ If also the **velocity** of the particle is known, one directly accesses its **mass** (**mass spectrometry**)

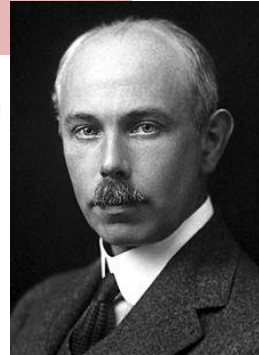
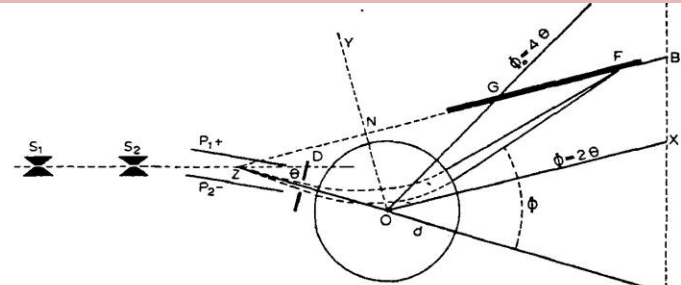
# Some historical background

At least 6 Nobel prizes in physics and chemistry have been awarded to now for studies connected to magnetic spectrometry



**1903 - Marie Skłodowska Curie and Pierre Curie**

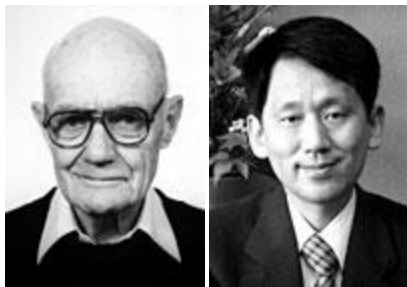
for their joint researches on the **radiation phenomena**



**1922 - Francis William Aston**

for his discovery, by means of his **mass spectrograph**, of isotopes

**1906 - Joseph John Thomson**  
investigations on the conduction  
of electricity by gases



**2002 - JOHN B. FENN and KOICHI TANAKA**

for their development of soft desorption ionisation methods for **mass spectrometric analyses** of biological macromolecules

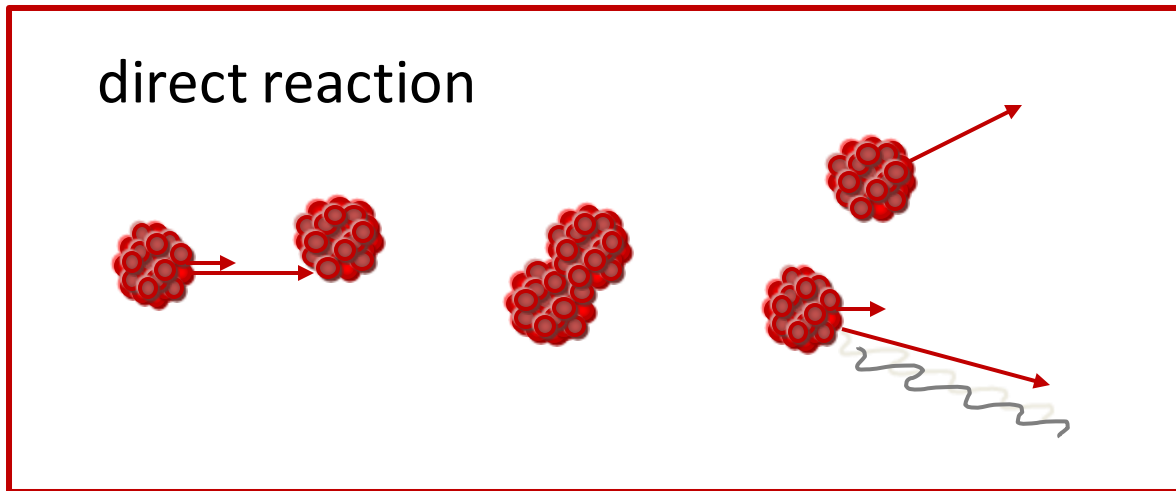
**1989 - Wolfgang Paul**

for the development of  
the ion trap technique



# Magnetic spectrometry and nuclear reactions

Nuclear physics has taken profit by the use of magnets to select and detect the charged particles emitted in a nuclear reaction



✚ Nuclear reactions produce fragments (charged particles) and radiation ( $\gamma$ -rays)

✚ Fragments carry the elementary information of the structure of colliding nuclei and of the reaction mechanism

# Looking for fragments

**what**, at **what angle** and at **what energy**?

Magnetic spectrometers can provide extremely clean information about fragments thanks to their properties:

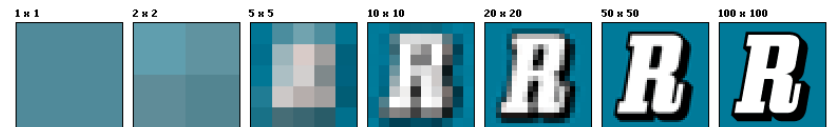
## Selectivity:

- Typically  $10^{9\div 11}$  nuclei/sec (beam intensity) colliding against  $10^{16\div 18}$  nuclei/cm<sup>2</sup> (target thickness)
- Studying a particular reaction is how to look for a needle in a haystack
- Effective suppression of unwanted background
- Possibility to measure at very forward angles (zero-degree) where clearest spectroscopic information

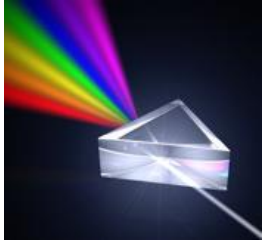


## Resolution:

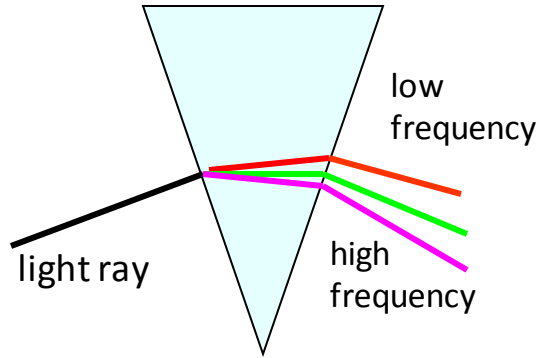
- Both in mass and momentum  
(measuring positions instead of energies)



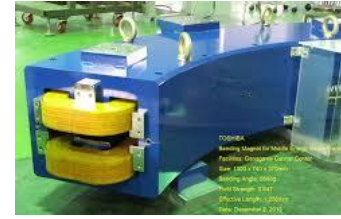
# Some analogy



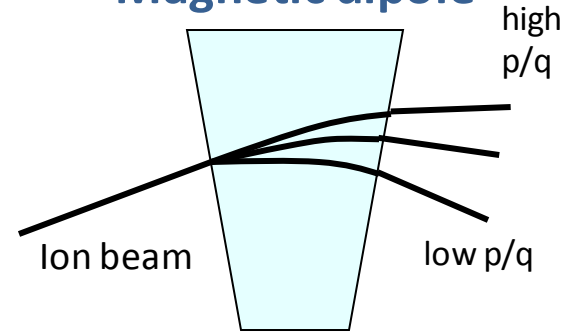
Prism



Deflection depending on the frequency



Magnetic dipole

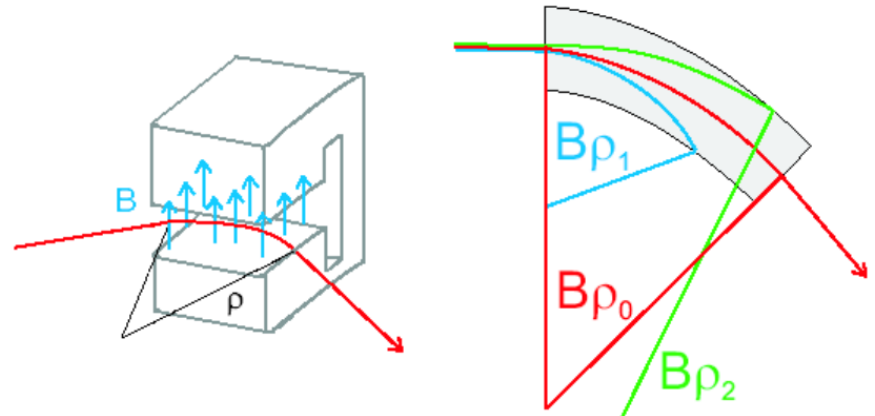


Deflection depending on  $p/q$  (magnetic rigidity)

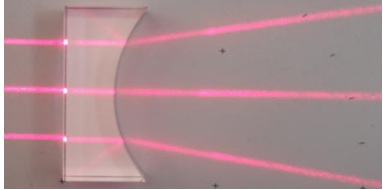
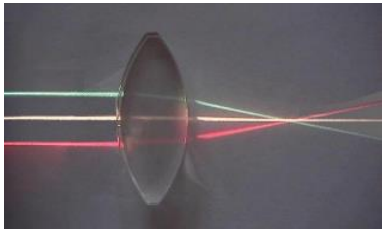
Transform frequency or  $p/q$  intervals in positions

**Dispersive elements**

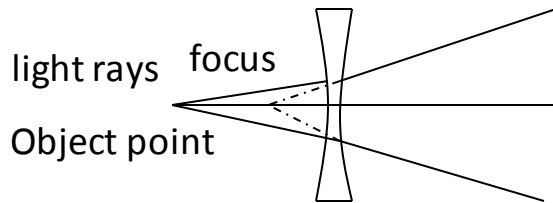
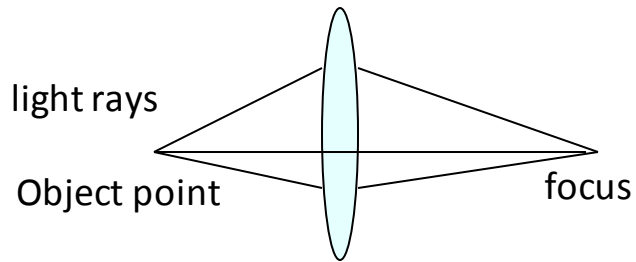
used as analyzers



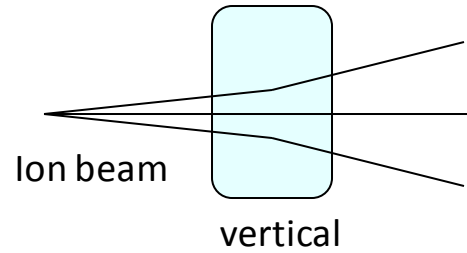
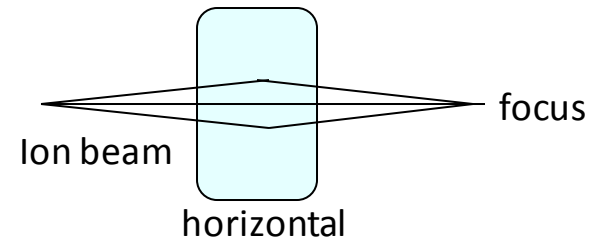
# Some analogy



Convergent and divergent lens

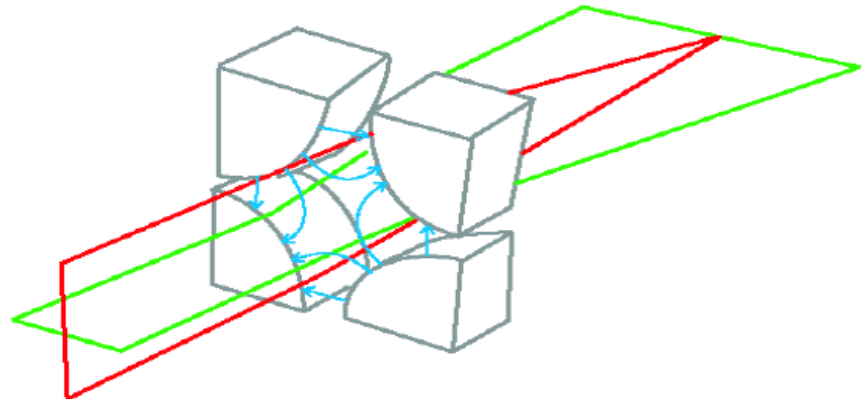


Magnetic quadrupole

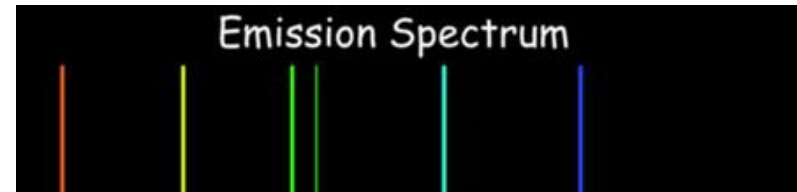
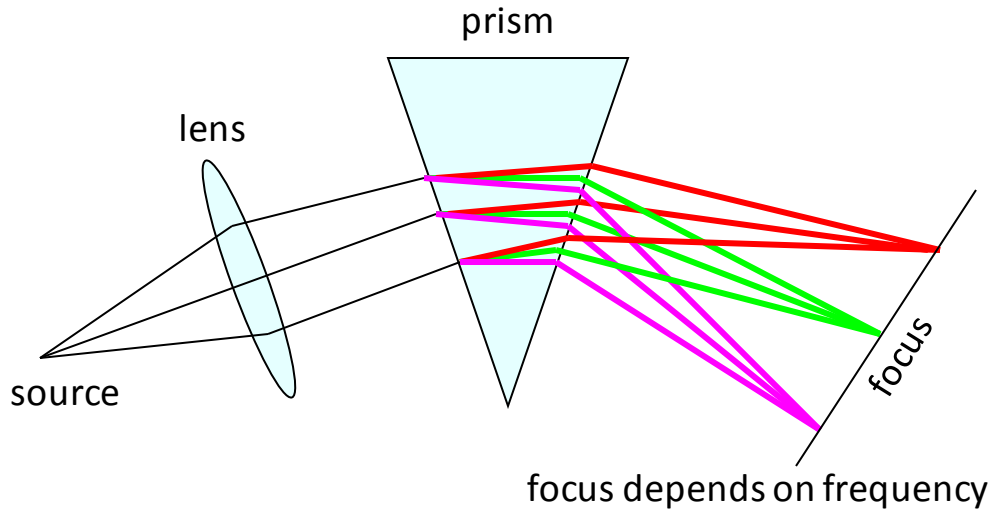


## Focusing elements

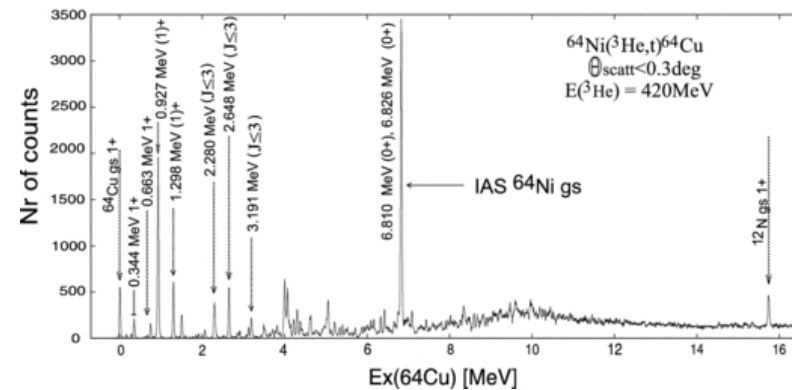
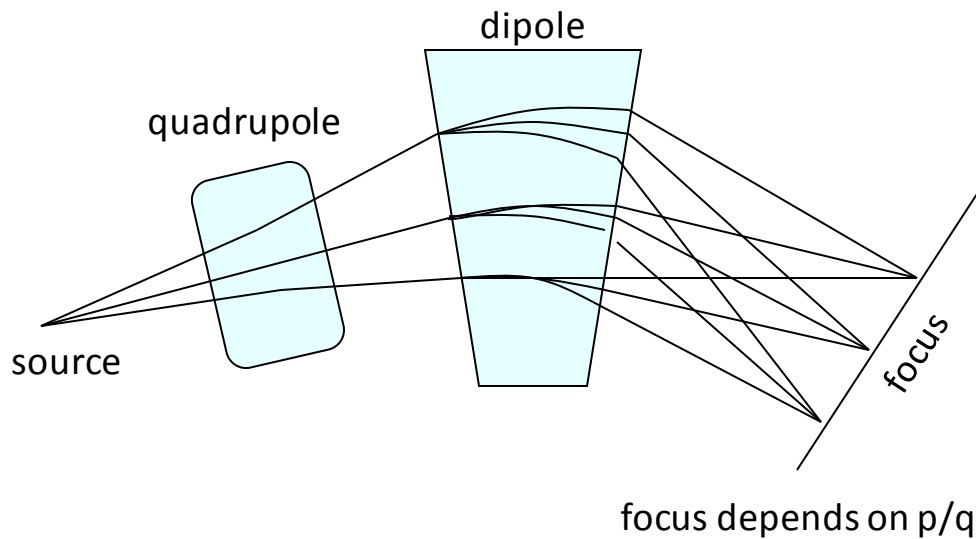
used to concentrate intensity



# Light spectrometer



# Magnetic spectrometer



# Advantages of conventional magnetic spectrometry

- ✚ Good selection of reaction products
- ✚ Possibility to measure near  $0^\circ$
- ✚ High momentum and mass resolution

Magnetic spectrometers quickly became essential tools in nuclear physics laboratories. Different layouts have been established, depending on the optimization of one of these functions.

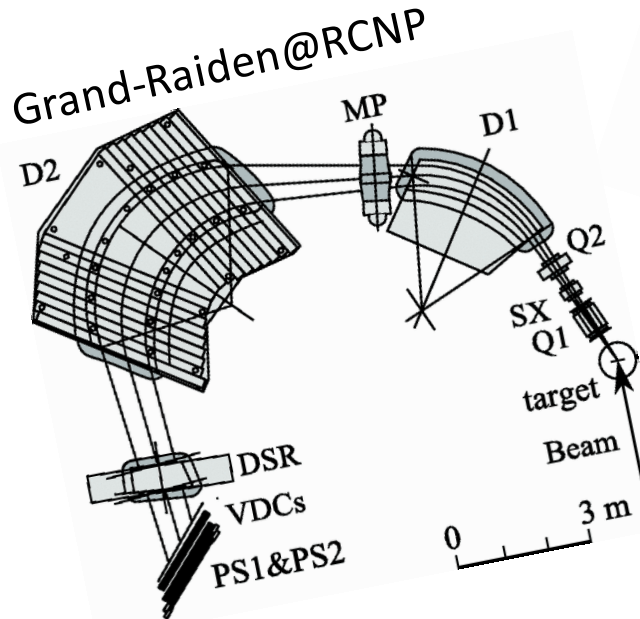
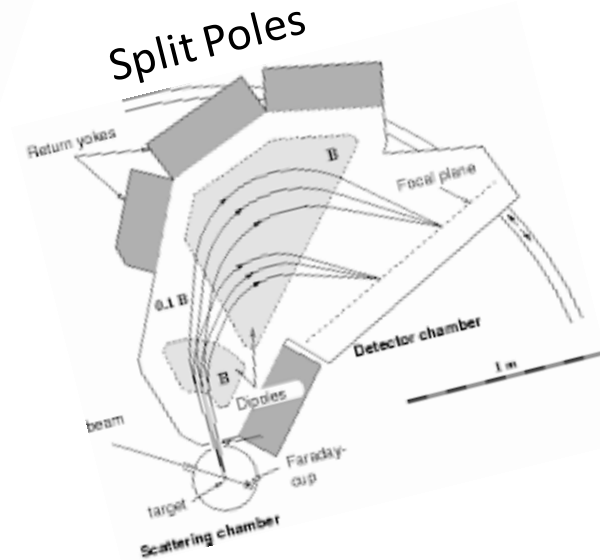
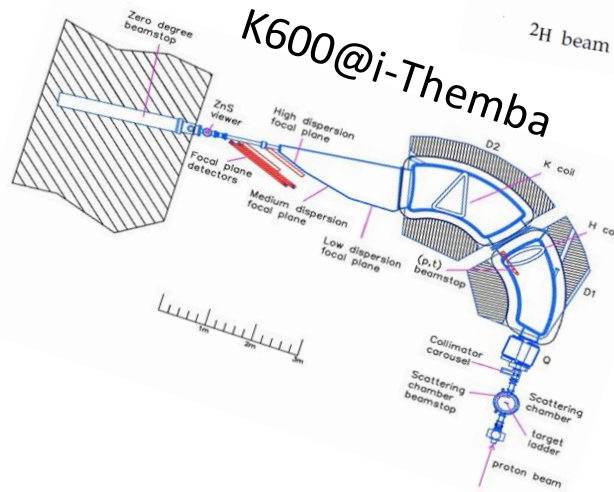
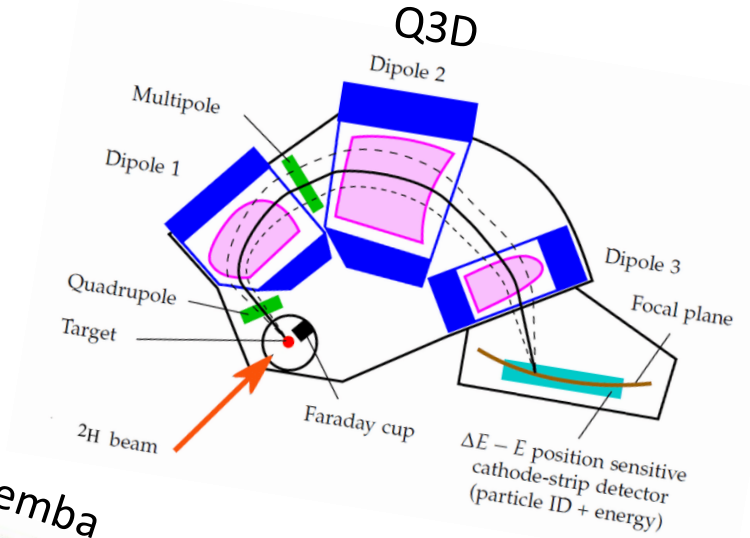


# Examples of magnetic spectrometers

High resolution  $\Delta p/p=1/10000$ ,  $\Delta p/p=1/38000$

Low acceptance  $<10$  msr

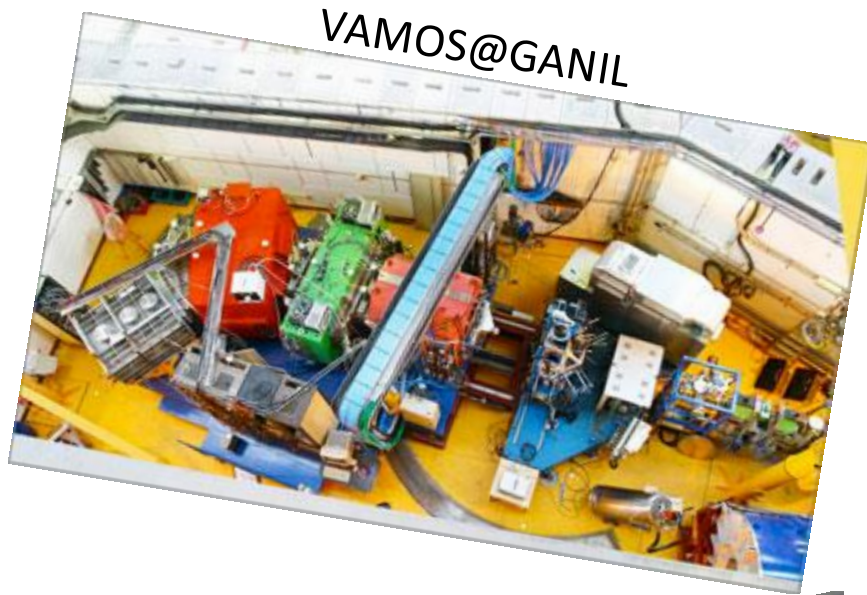
Light ions ( $p$ ,  $d$ ,  $3\text{He}$ )



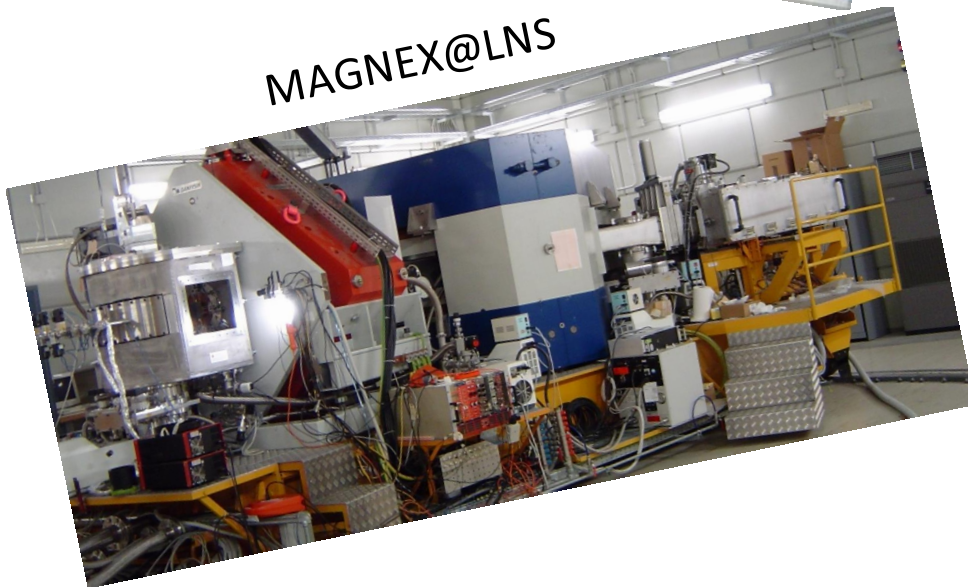
# Necessity to go towards large acceptance

- To detect **rare processes** (products of reactions induced by radioactive ion beams or characterized by low cross-sections)
- Large momentum phase space in a unique setting

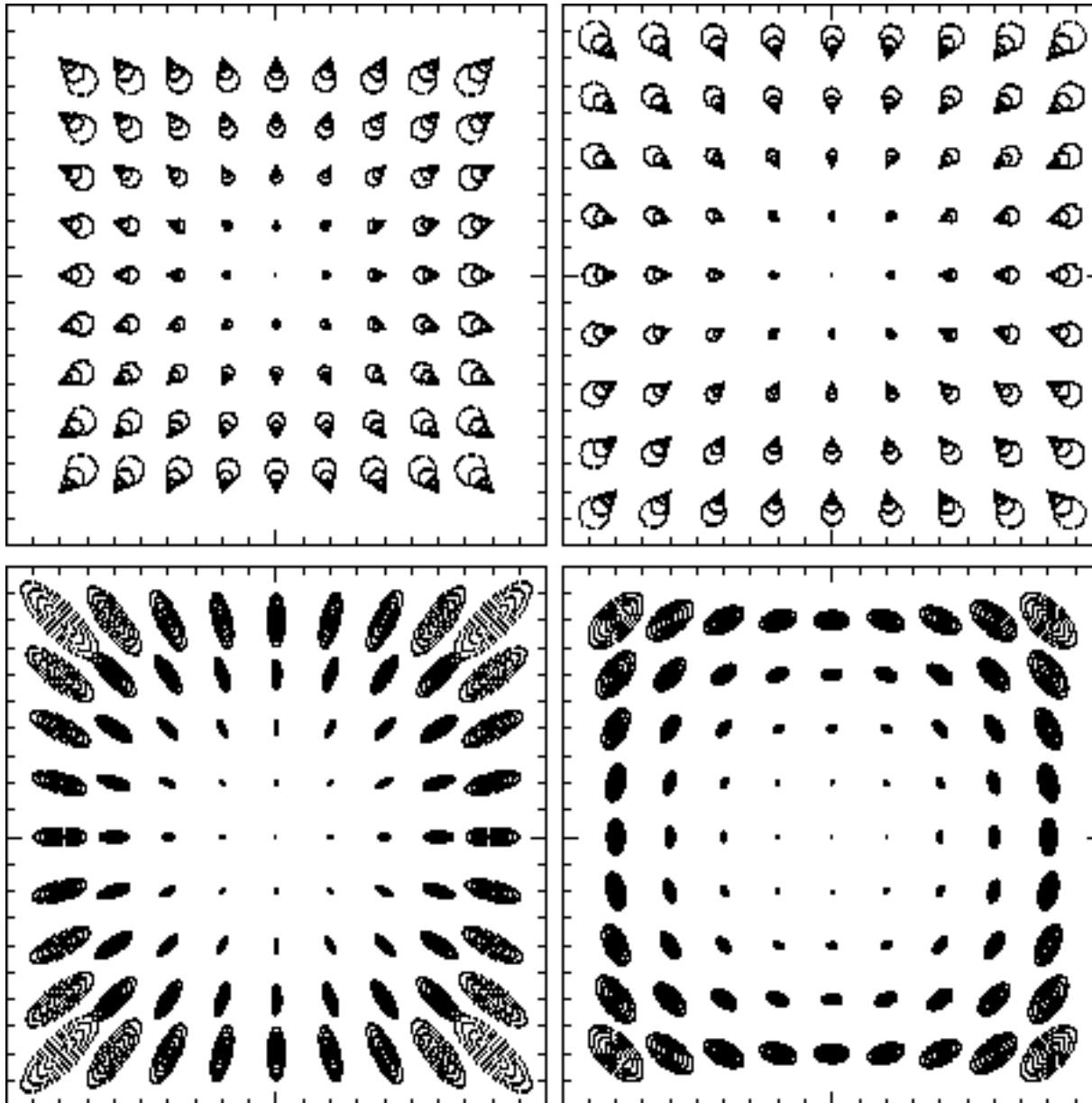
# Examples of large acceptance magnetic spectrometers



Large acceptance 50 msr  
Heavier ions  
Resolution??

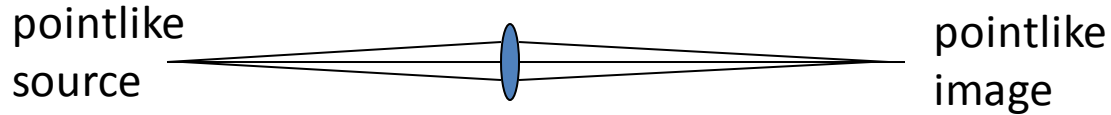


# Large acceptance and aberrations



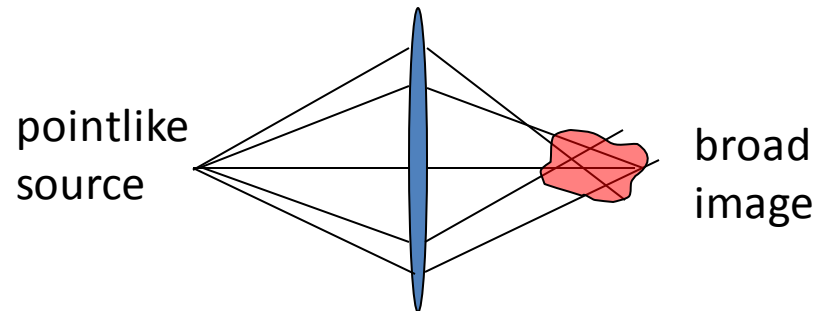
# The large acceptance problem

Small acceptance → High resolution



*All the rays have a common focus*

Large acceptance → aberrations



*Each ray has its own trajectory: focus not anymore a useful concept*

# The large acceptance problem

The motion of a charged particle beam, under the action of magnetic fields, can be described as the dynamical evolution of the representative hyper-volume

$$F : \vec{X}_i \rightarrow \vec{X}_f$$



Taylor expansion

$$x_i(f) = \sum_j R_{ij} x_j(i) + \sum_{j,k} T_{ijk} x_j(i) x_k(i) + \dots$$

**Aberrations**

$F$  transport matrix

$$\mathbf{X}_i = (x_i, \theta_i, y_i, \phi_i, l_i, \delta_i)$$

$$\mathbf{X}_f = (x_f, \theta_f, y_f, \phi_f, l_f, \delta_f)$$

$x, \theta, y, \phi$  horizontal and vertical coordinates and angles at the impact point of the ion trajectory with a plane normal to the central trajectory,

$l$  trajectory length

$\delta = (p - p_0)/p_0$ , is the fractional momentum, where  $p_0$  is the reference momentum and  $p$  is the actual one.

# The large acceptance problem

$$x_i(f) = \sum_j R_{ij} x_j(i) + \sum_{j,k} T_{ijk} x_j(i) x_k(i) + \dots$$

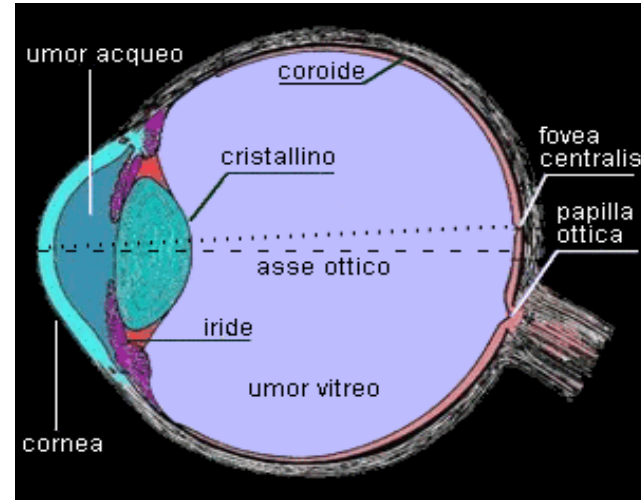
**Aberrations**

First order matrix elements:

$$(a|b) = \frac{\partial a_f}{\partial b_i}$$

$$R = \begin{pmatrix} (x|x) & (x|\theta) & (x|y) & (x|\varphi) & (x|\ell) & (x|\delta) \\ (\theta|x) & (\theta|\theta) & (\theta|y) & (\theta|\varphi) & (\theta|\ell) & (\theta|\delta) \\ (y|x) & (y|\theta) & (y|y) & (y|\varphi) & (y|\ell) & (y|\delta) \\ (\varphi|x) & (\varphi|\theta) & (\varphi|y) & (\varphi|\varphi) & (\varphi|\ell) & (\varphi|\delta) \\ (\ell|x) & (\ell|\theta) & (\ell|y) & (\ell|\varphi) & (\ell|\ell) & (\ell|\delta) \\ (\delta|x) & (\delta|\theta) & (\delta|y) & (\delta|\varphi) & (\delta|\ell) & (\delta|\delta) \end{pmatrix}.$$

# Natural recipes for large acceptance: Human versus fly eyes



Large acceptance optical devices:

- ✚ Many small lenses in the fly versus a unique large one for man.
- ✚ Strong aberrations for us.
- ✚ Aberrations greatly compensated by **brain reconstruction** of the image
- ✚ Reconstruction based on neural networks and a **long learning step**
- ✚ What about a **“clever” spectrometer**?



# Clever Spectrometers

Tracking instead of  
focusing

Spectrometer reconstructing a net image by an optically aberrated one

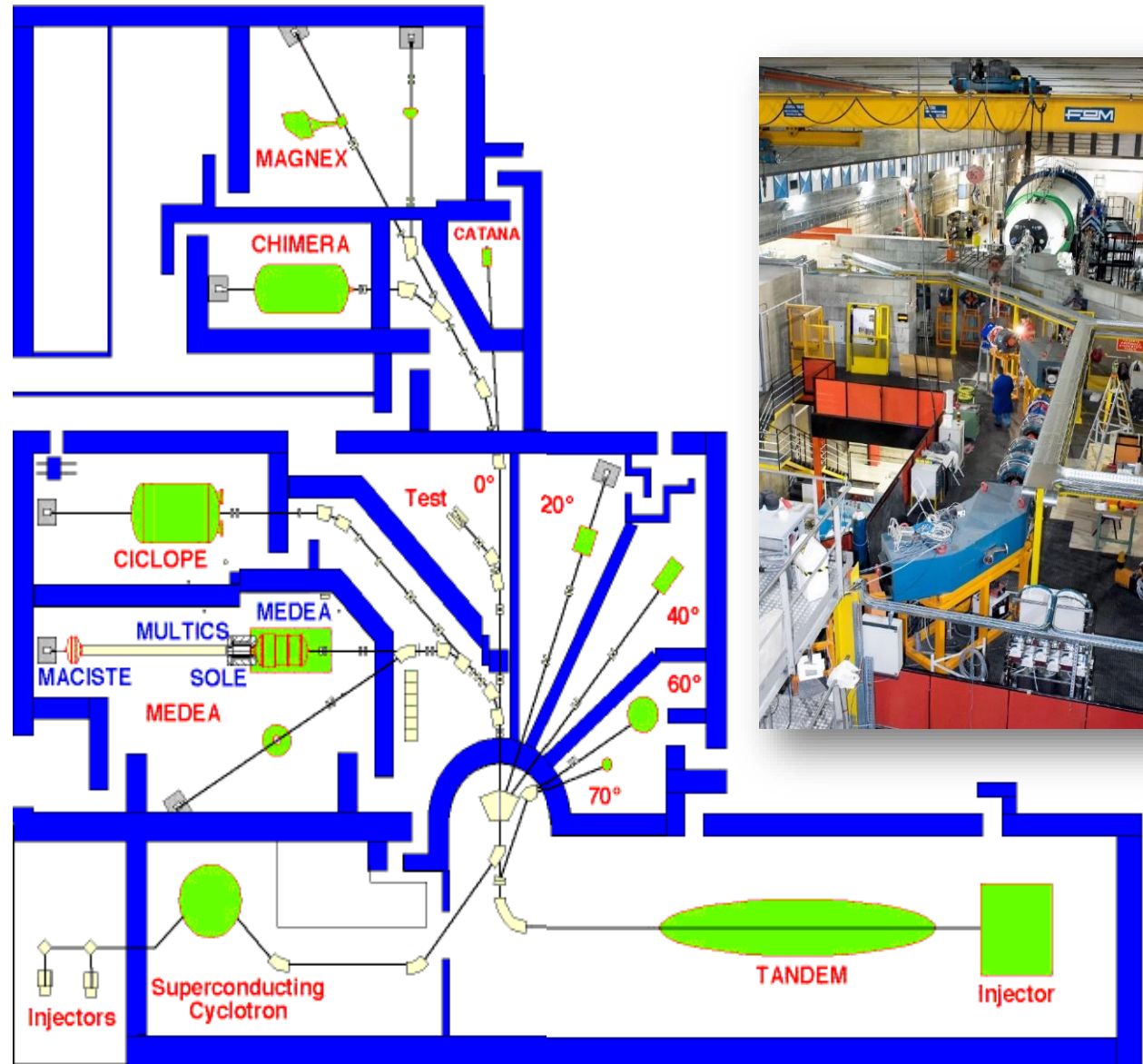


# The MAGNEX spectrometer

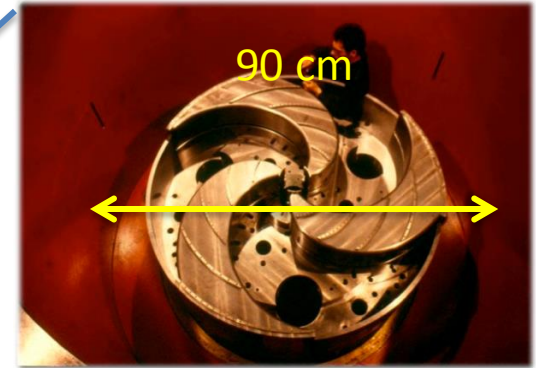
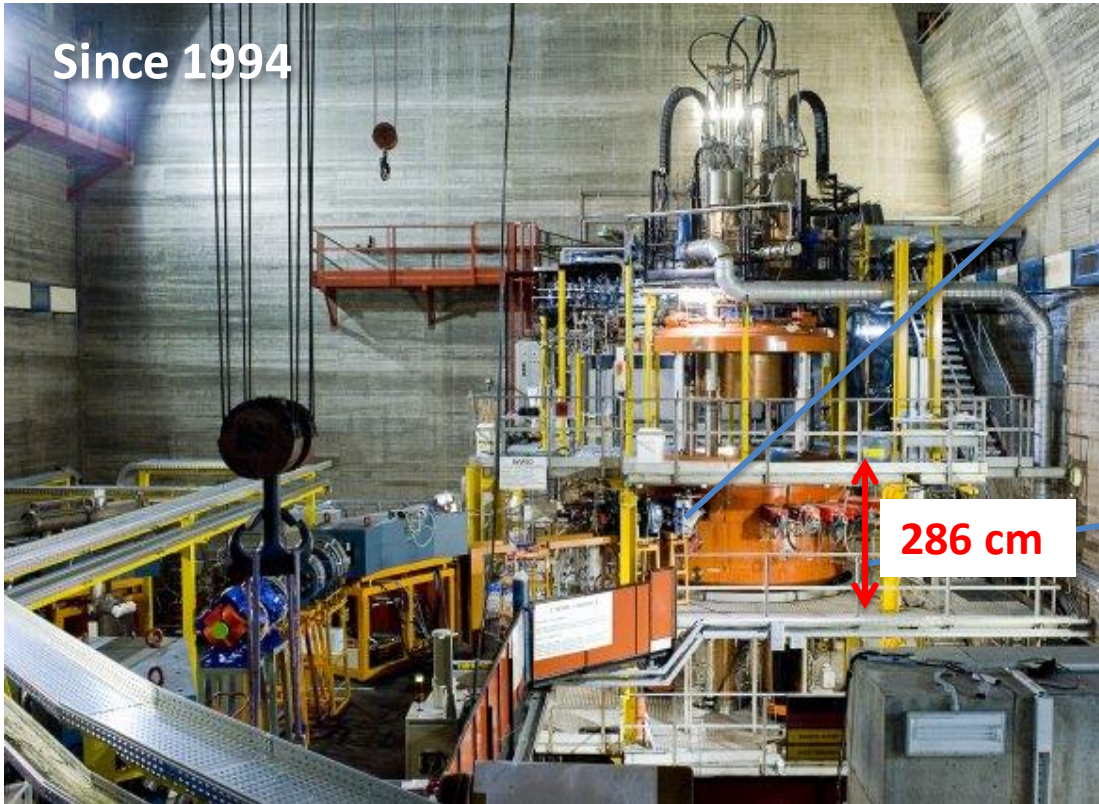


**Catania  
INFN  
Laboratori Nazionali del Sud**

# The LNS laboratory in Catania



# Superconducting cyclotron K800

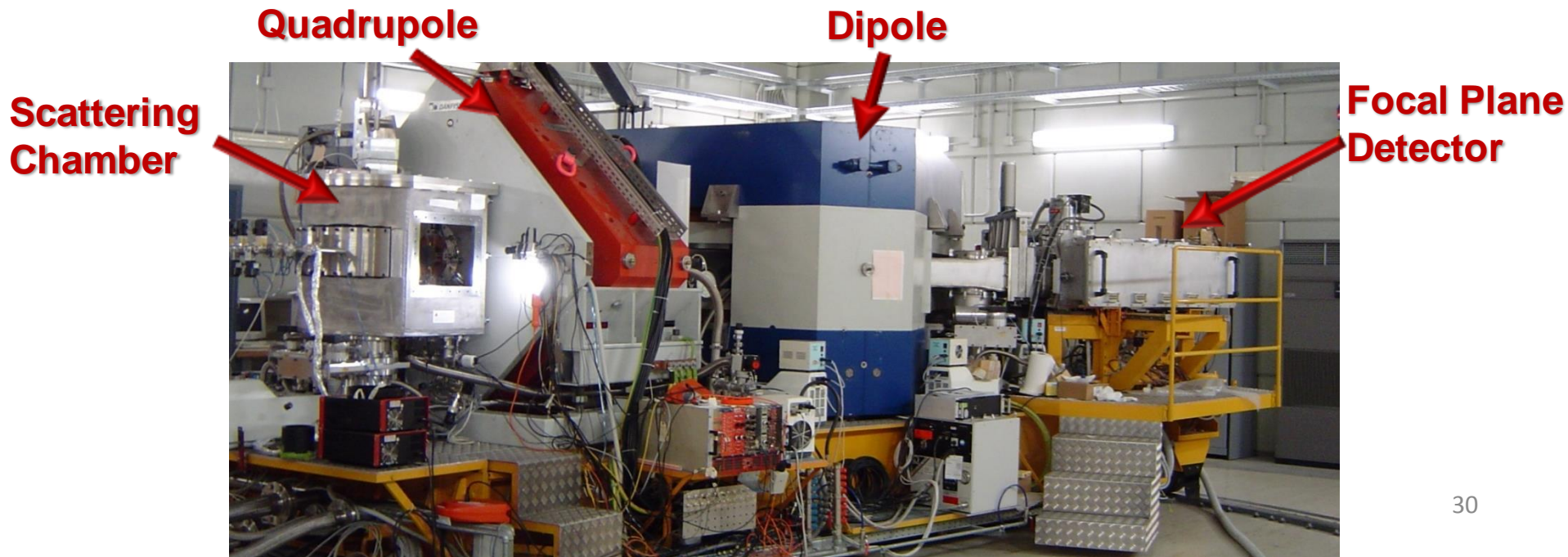


- 176 Tons
- Max magnetic field: 4.8 T

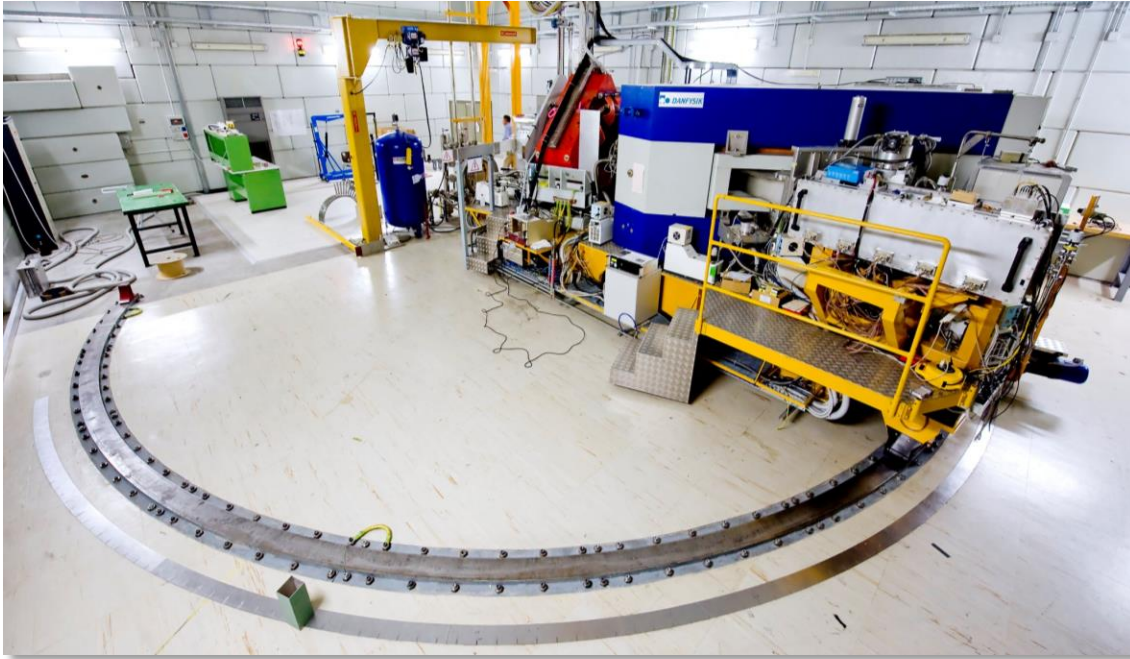
- Accelerating ion beams from proton to Uranium at energy up to 80 MeV/A
- Superconducting magnets with Niobium-Titanium coils in liquid Helium at 4.2 K

# MAGNEX: a large acceptance QD spectrometer

- ❖ **The Quadrupole:** vertically focusing  
(Aperture radius 20 cm, effective length 58 cm. Maximum field strength 5 T/m)
- ❖ **The Dipole:** momentum dispersion (and horizontal focus)  
(Mean bend angle  $55^\circ$ , radius 1.60 m. Maximum field  $\sim 1.15$  T)
- ❖ **The surface coils,** located between the dipole pole faces and the inner high vacuum chamber, giving tunable quadrupolar and sextupolar corrections



# MAGNEX characteristics



Measured resolution:  
Energy  $\Delta E/E \sim 1/1000$   
Angle  $\Delta\theta \sim 0.3^\circ$   
Mass  $\Delta m/m \sim 1/160$

We have measured in  
a **wide mass range**  
(from protons to  
medium-mass nuclei)

Optical characteristics	Measured values
Angular acceptance (Solid angle)	<b>50 msr</b>
Angular range	<b><math>-20^\circ - +85^\circ</math></b>
Momentum (energy) acceptance	<b><math>-14\%</math>, <math>+10\%</math> (<math>-28\%</math>, <math>+20\%</math>)</b>
Momentum dispersion for $k = -0.104$ (cm/%)	<b>3.68</b>
Maximum magnetic rigidity	<b>1.8 T m</b>

# The large acceptance problem

$$F : \vec{X}_i \rightarrow \vec{X}_f$$

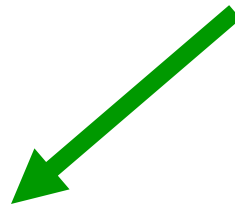
$F$  transport matrix

Large acceptance

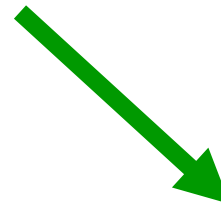


**Aberrations**

$$x_i(f) = \sum_j R_{ij} x_j(i) + \sum_{j,k} T_{ijk} x_j(i) x_k(i) + \dots \quad \text{Up to } 10^\circ \text{ order}$$



Careful hardware design  
(to minimize the aberrations)

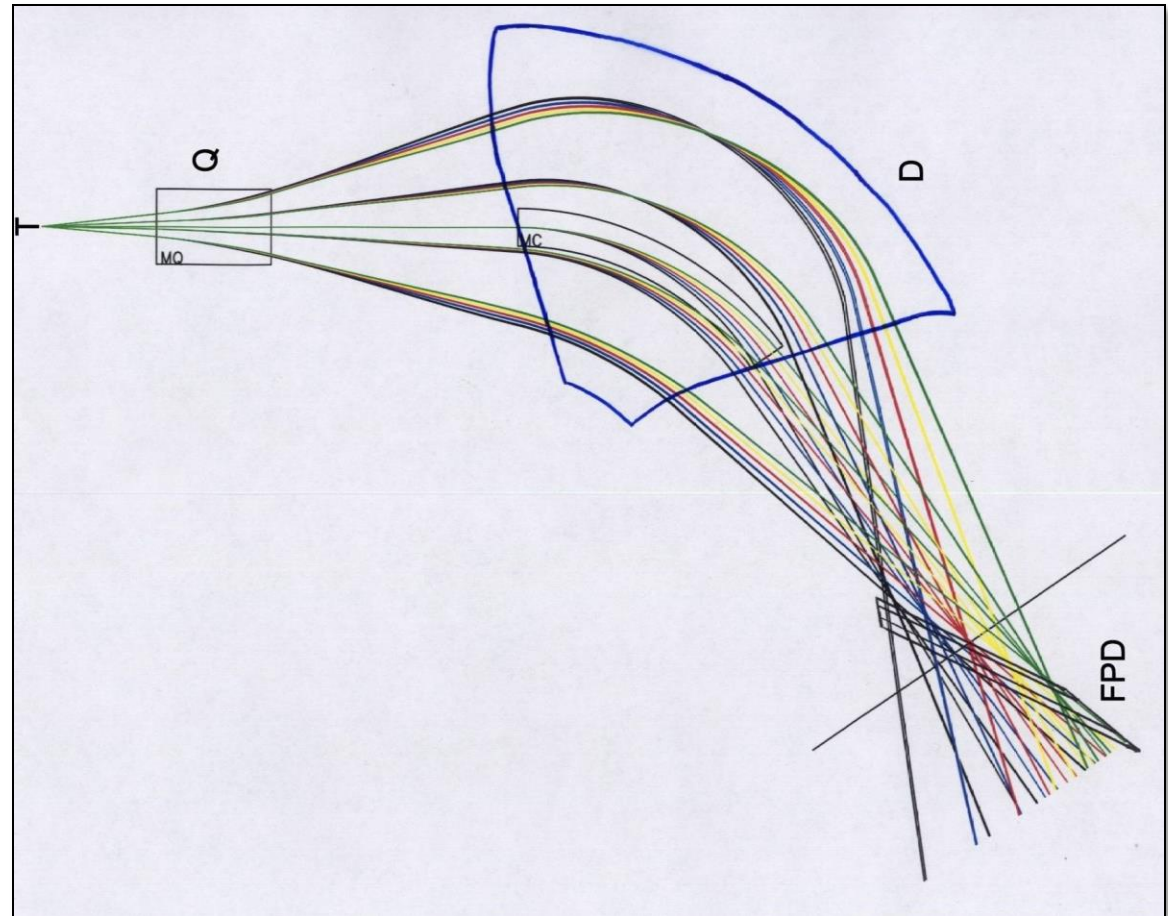


Software ray-reconstruction  
(to know the aberrations)



# Hardware minimisation of aberrations

- Rotation of the focal plane detector of  $59^\circ$
- Shift of the focal plane detector



# Hardware minimisation of aberrations

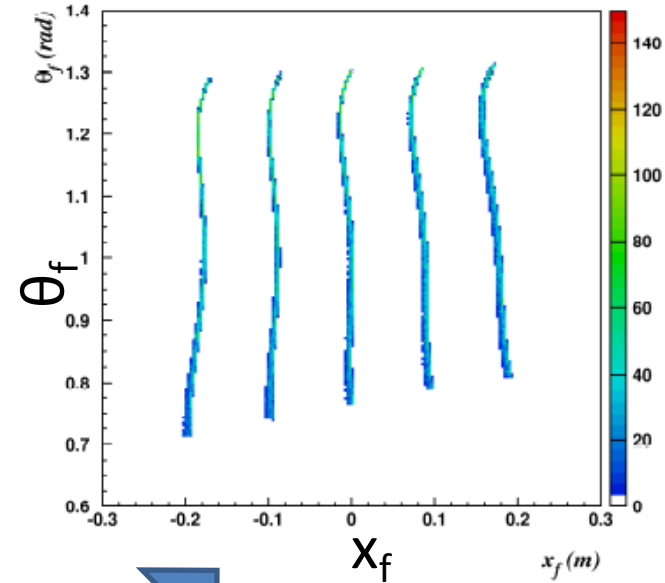
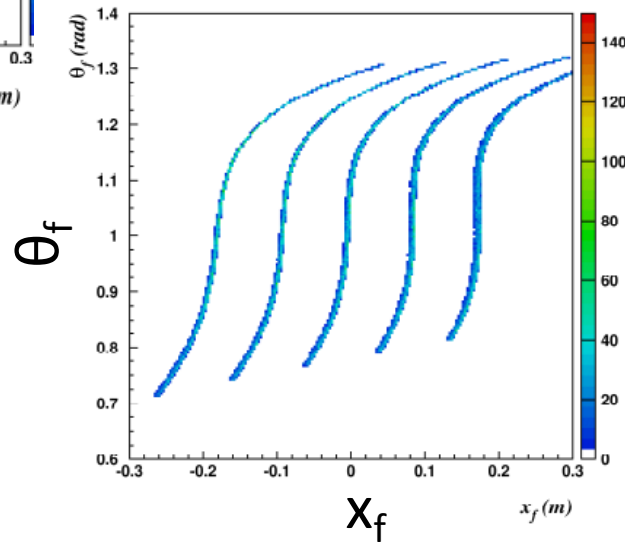
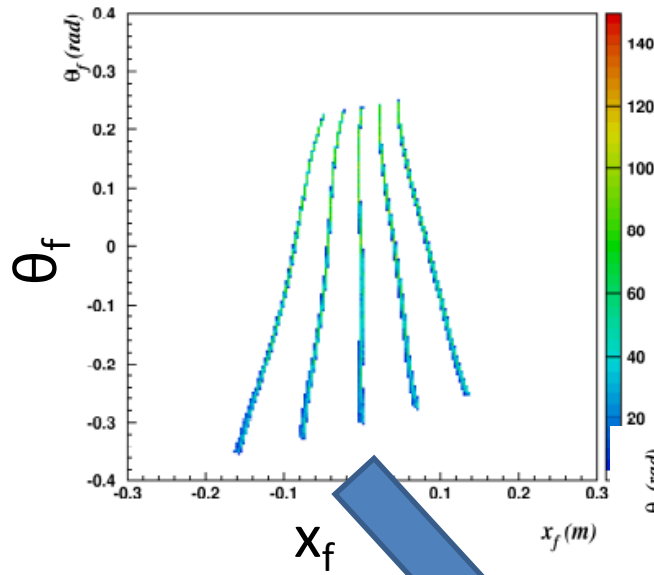
- Introduction of surface coils in the dipole pole tips



- Shaping of dipole entrance and exit boundaries (8<sup>th</sup> order polynomial)



# Hardware minimisation of aberrations



# The large acceptance problem

$$F : \vec{X}_i \rightarrow \vec{X}_f$$

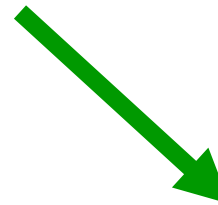
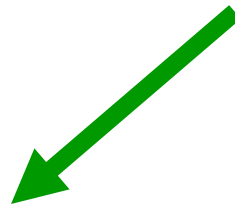
$F$  transport matrix

Large acceptance



**Aberrations**

$$x_i(f) = \sum_j R_{ij} x_j(i) + \sum_{j,k} T_{ijk} x_j(i) x_k(i) + \dots \quad \text{Up to } 10^\circ \text{ order}$$



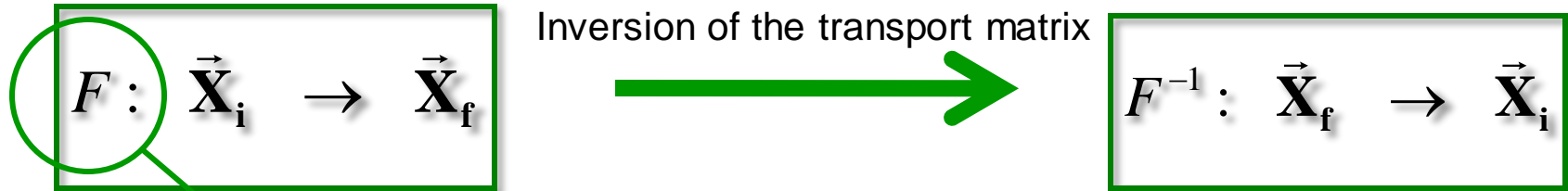
Careful hardware design  
(to minimize the aberrations)

Software ray-reconstruction  
(to know the aberrations)

# Software ray-reconstruction

## ALGEBRIC RAY-RECONSTRUCTION

- ✓ Solution of the **equation of motion** for each detected particle
- ✓ **Inversion** of the transport matrix
- ✓ Application to the final **measured parameters**

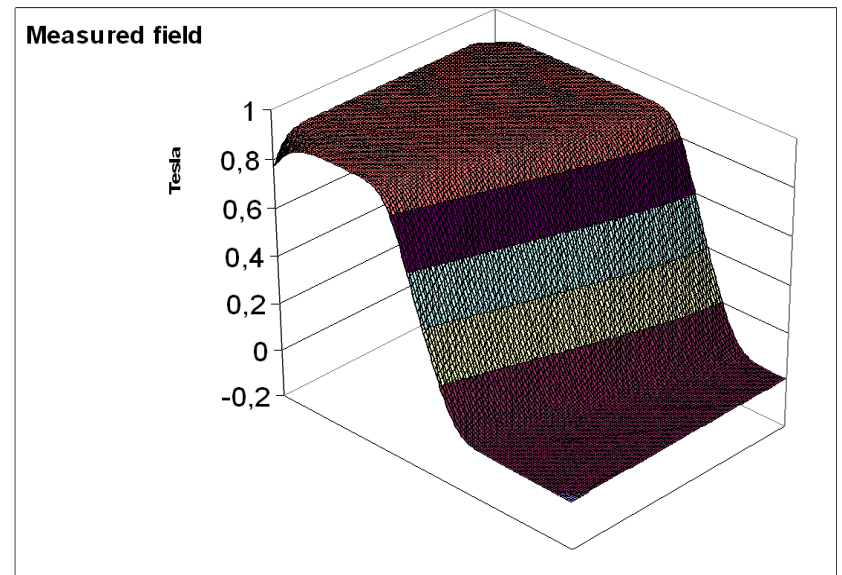
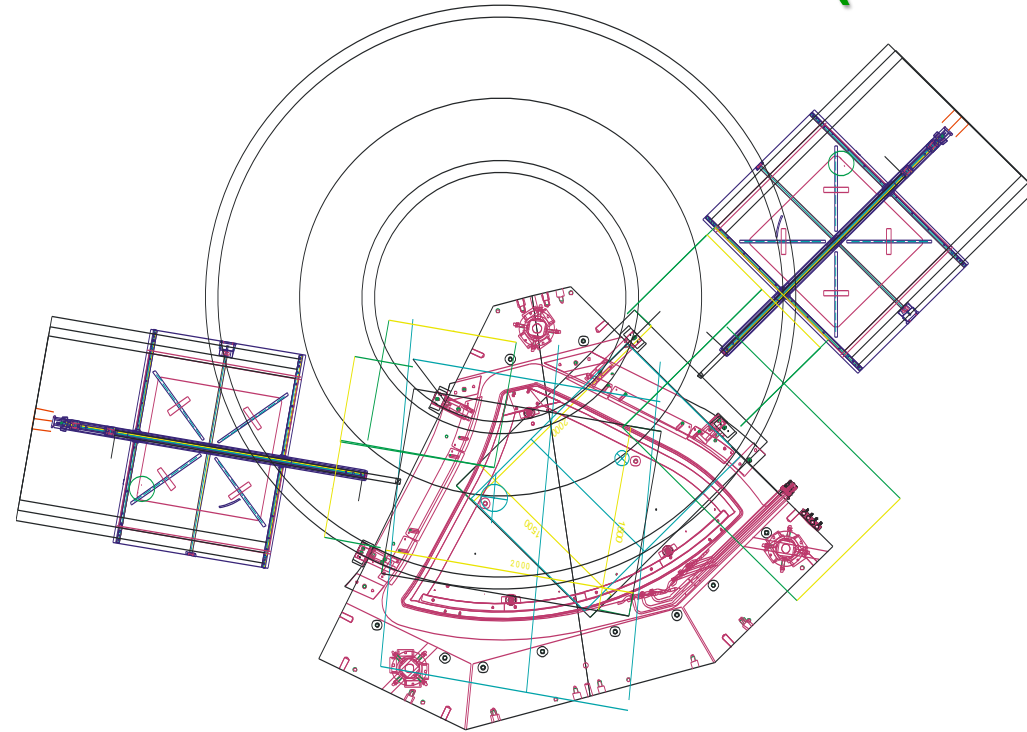


- 1) Detailed knowledge of the geometry and magnetic field

# 1) Detailed knowledge of the magnetic field

## Measurement of the field (3D map)

Measurements at Danfysik  
240000 points  
2 months (night and day)



## Interpolation of the field

Regular function up to  $10^{\circ}$  order

*A.Lazzaro et al., NIMA 570 (2007) 192*

*A.Lazzaro et al., NIMA 585 (2008) 136*

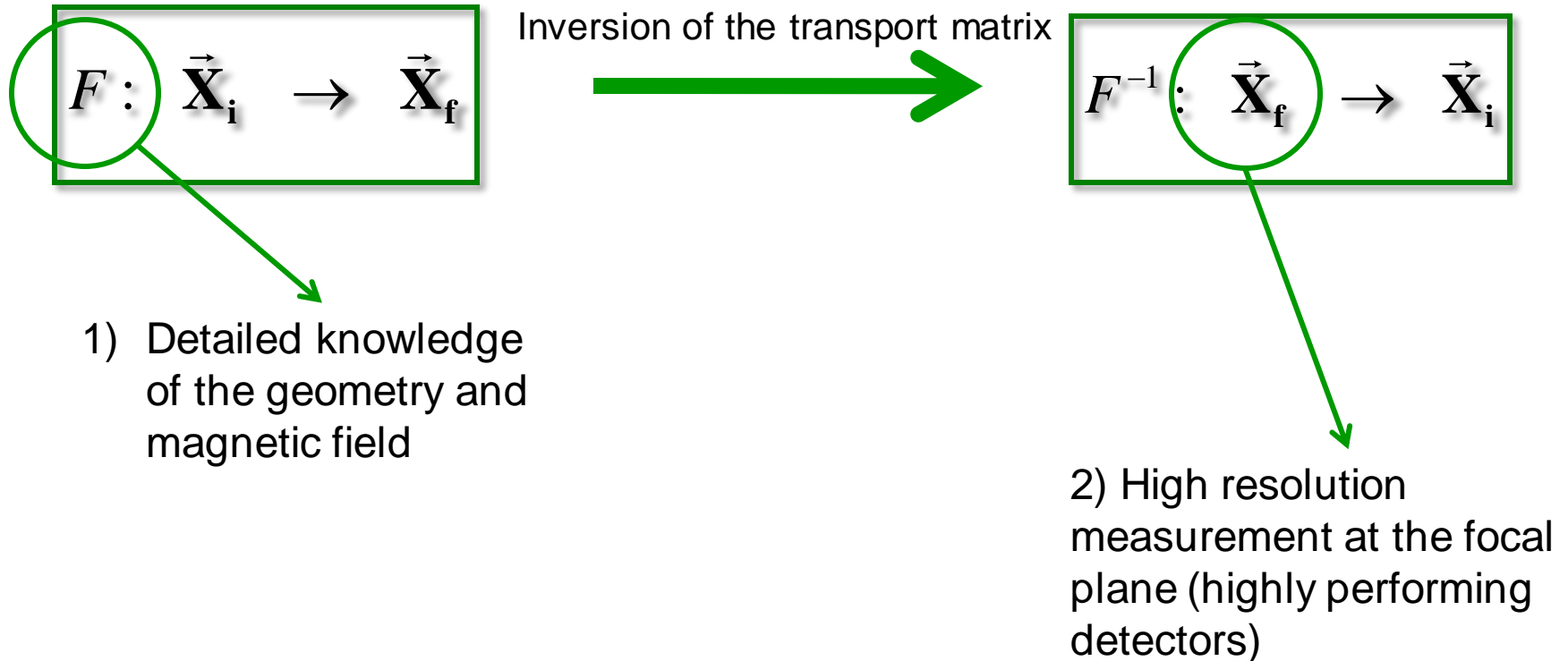
*A.Lazzaro et al., NIMA 591 (2008) 394*

*A.Lazzaro et al., NIMA 602 (2009) 494*

# Software ray-reconstruction

## ALGEBRIC RAY-RECONSTRUCTION

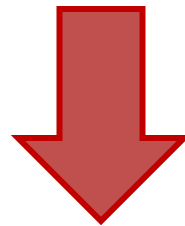
- ✓ Solution of the **equation of motion** for each detected particle
- ✓ **Inversion** of the transport matrix
- ✓ Application to the final **measured parameters**



## 2) MAGNEX Focal Plane Detector

Two tasks to accomplish:

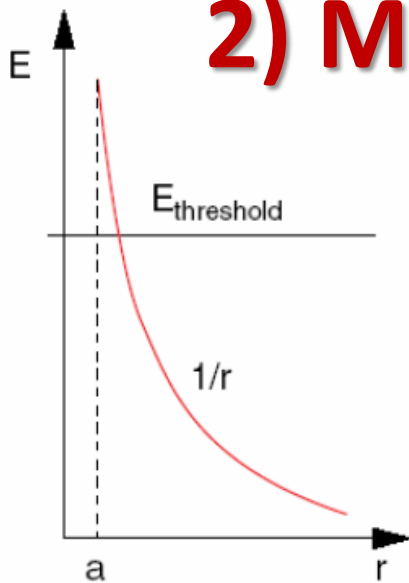
- 1) High resolution measurement at the focal plane of the phase space parameters ( $X_{\text{foc}}, Y_{\text{foc}}, \theta_{\text{foc}}, \phi_{\text{foc}}$ )
- 2) Identification of the reaction ejectiles ( $Z, A$ ) - crucial aspect for heavy ions



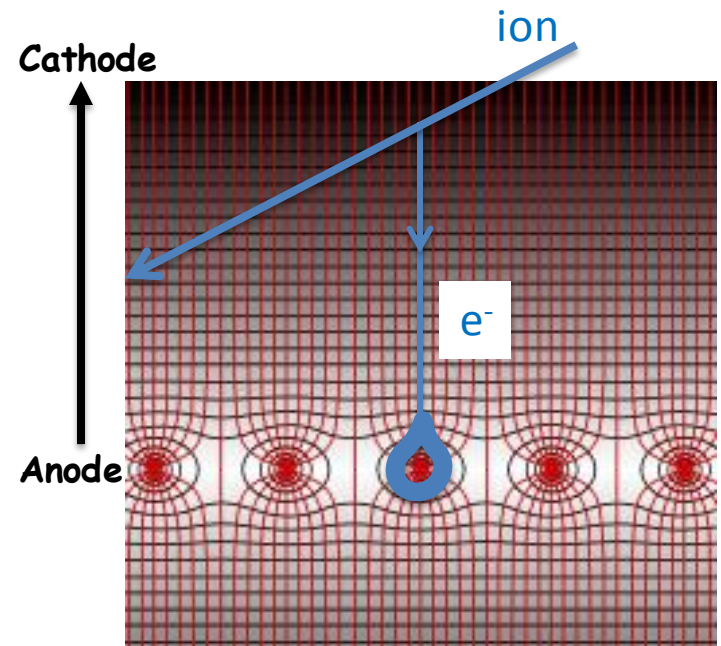
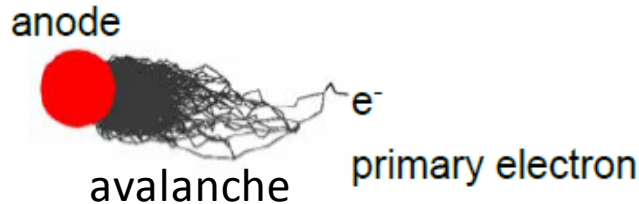
Hybrid detector:  
Gas section: proportional wires and drift chambers  
+  
Stopping wall of silicon detectors



# 2) MAGNEX Focal Plane Detector Wire-based detector



$$E(r) = \frac{CV_0}{2\pi\epsilon_0} \cdot \frac{1}{r}$$



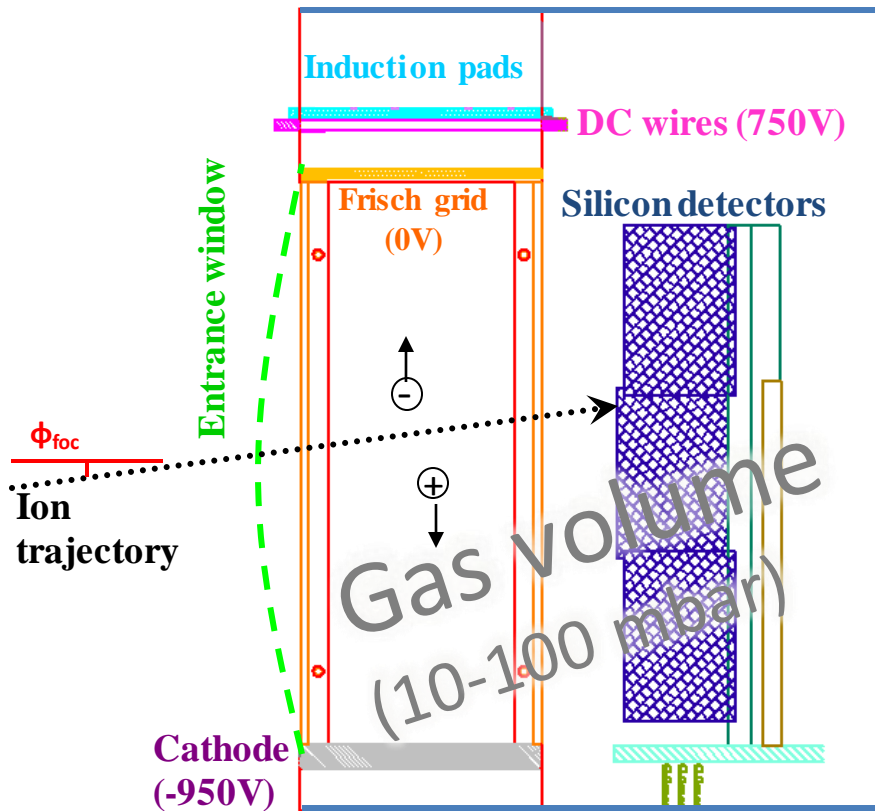
Multi-Wire Proportional Chamber -MWPC

## Properties:

- Flexible geometry and large area ( $\sim m^2$ )
- Cheap
- Many well developed position encoding methods
- Works in magnetic field
- Electron avalanche multiplication (Gain)  $\approx 10^4$ - $10^5$
- Position resolution  $\rightarrow$  down to 100  $\mu m$  for 1 mm wire spacing (limited in size)
- Rate capability  $\approx 10^4$  Hz/ $mm^2$

# 2) MAGNEX Focal Plane Detector

Large volume: 1360mm X 200mm X 96mm



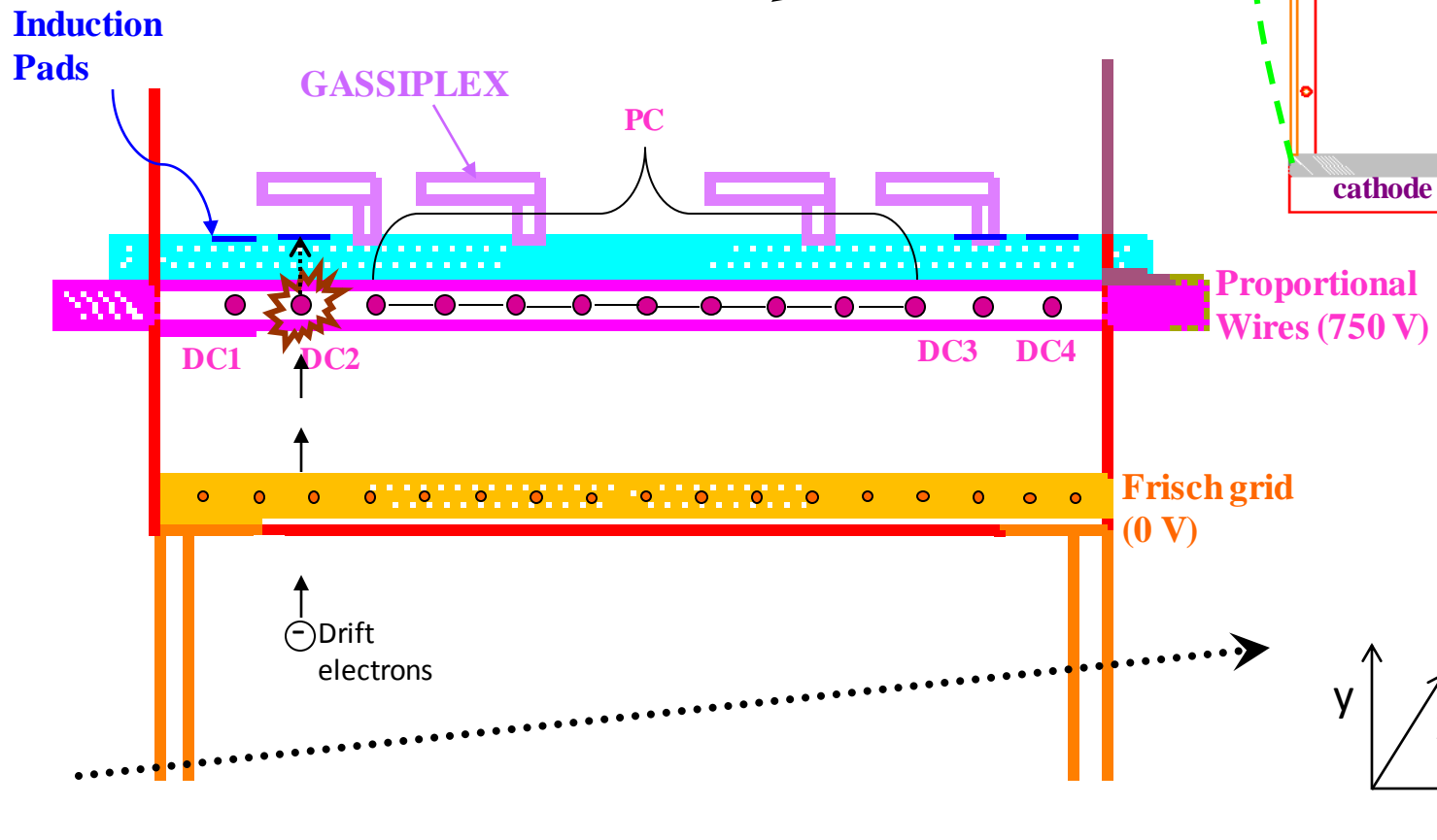
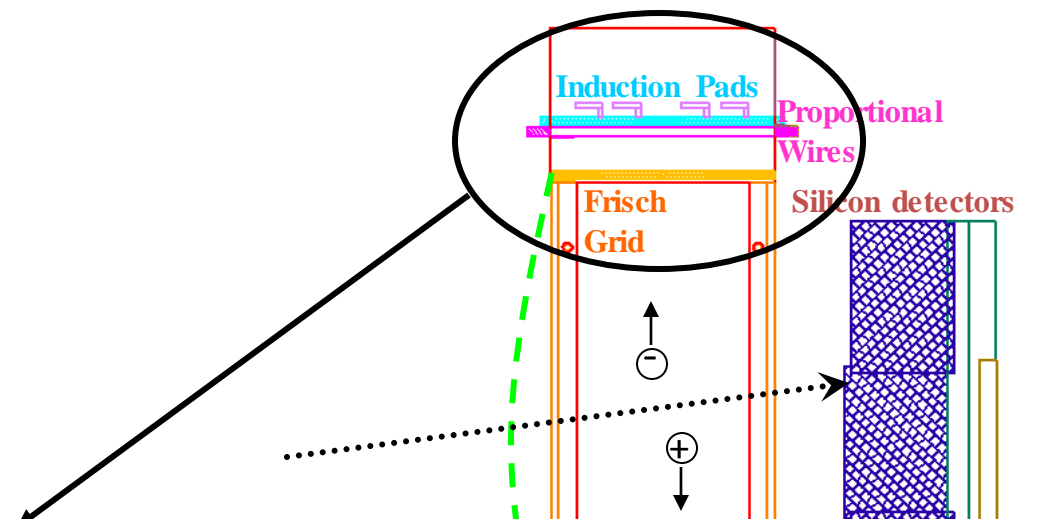
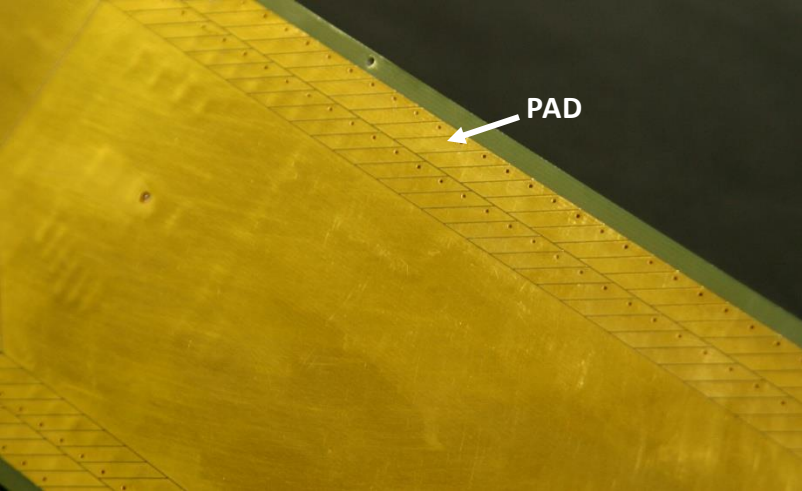
Section view

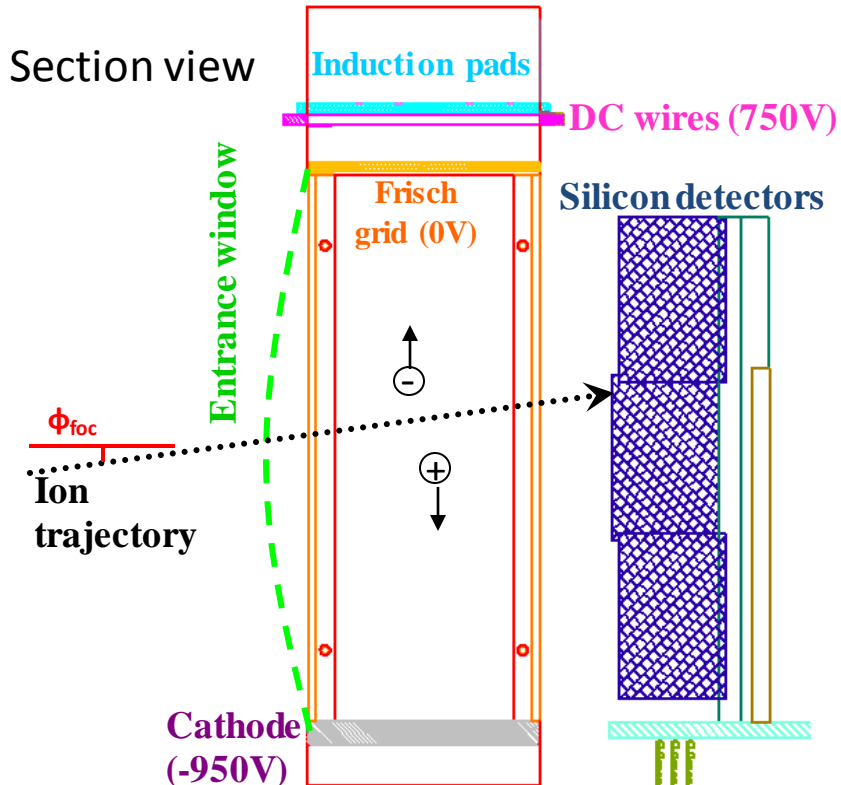


Wall of 60 stopping 7 X 5 cm<sup>2</sup> Silicon detectors  
Covered area 100 X 20 cm<sup>2</sup>  
Thickness 500 – 1000  $\mu$ m

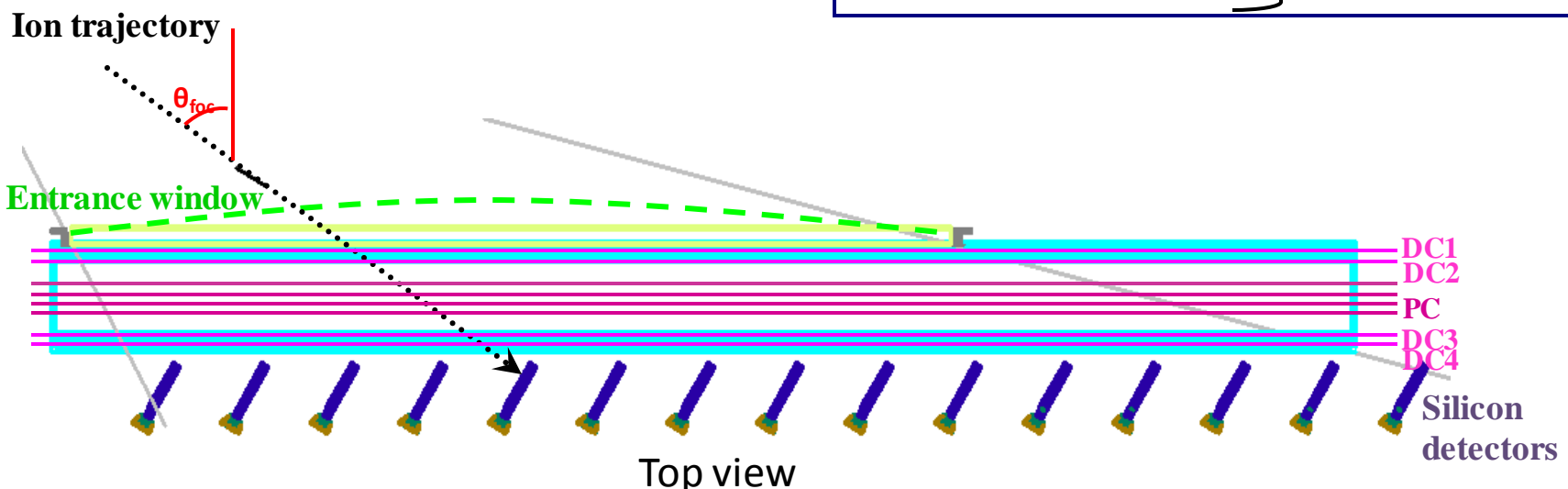
*M.Cavallaro et al. EPJA 48: 59 (2012)*

*D.Carbone et al. EPJA 48: 60 (2012)*





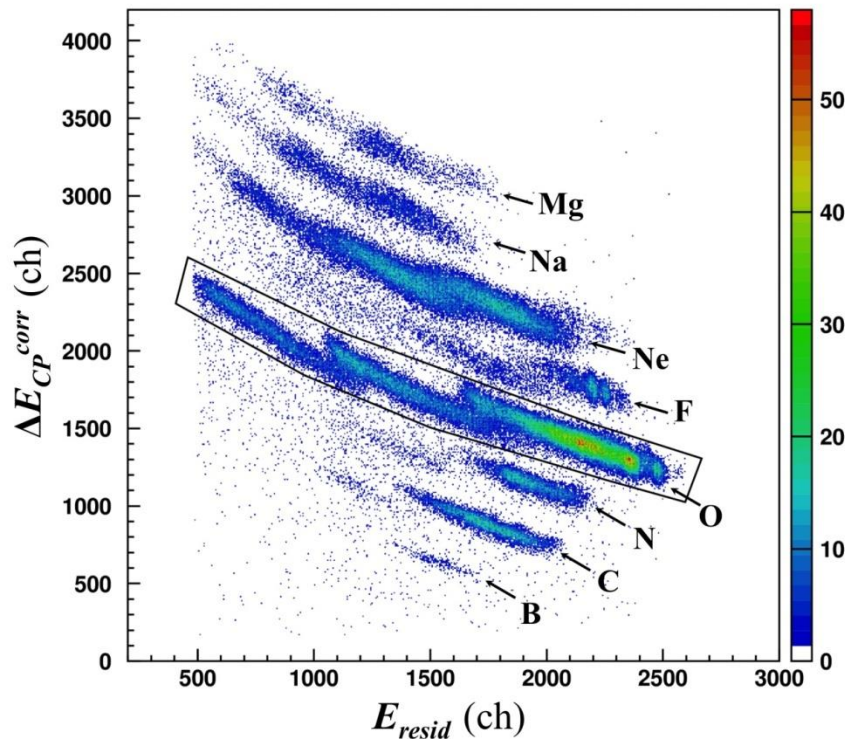
60 Silicon Detectors → $E_{res}$	} Ion identification
5 Proportional Wires → $\Delta E$	
4 Induction Strip → $X_1, X_2, X_3, X_4$ → $X_{foc}, \theta_{foc}$	} Ray- reconstruction
4 Drift Chamber (DC) → $Y_1, Y_2, Y_3, Y_4$ → $Y_{foc}, \phi_{foc}$	



# Particle Identification

*F. Cappuzzello et al., NIMA 621 (2010) 419*

## Z identification

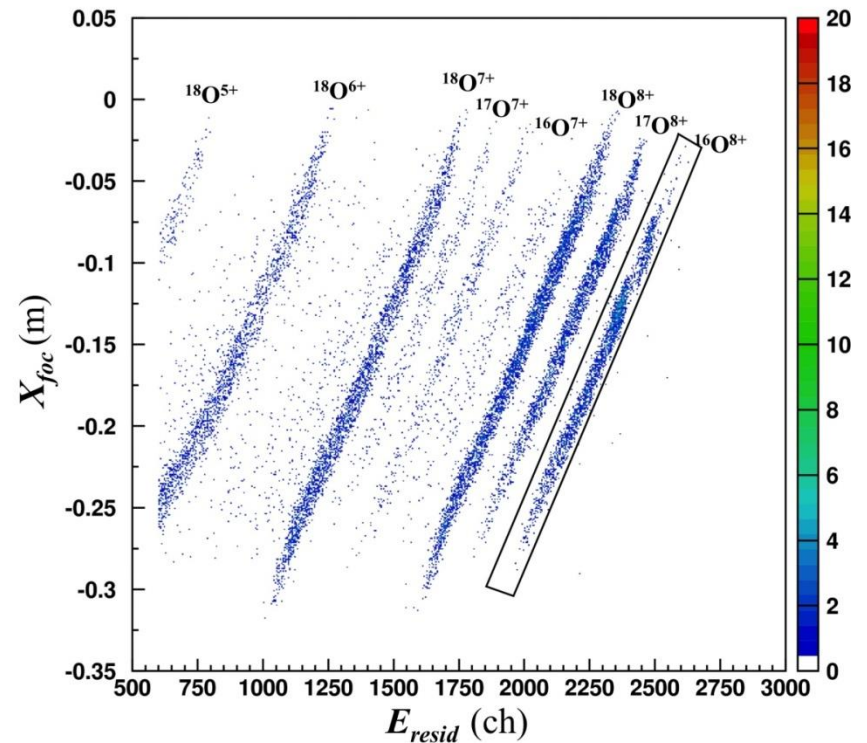


## A identification

$$B\rho = \frac{p}{q}$$



$$X_{foc}^2 \propto \frac{m}{q^2} E_{resid}$$



Mass resolution  $\Delta m/m \sim 1/160$

# MAGNEX FPD characteristics

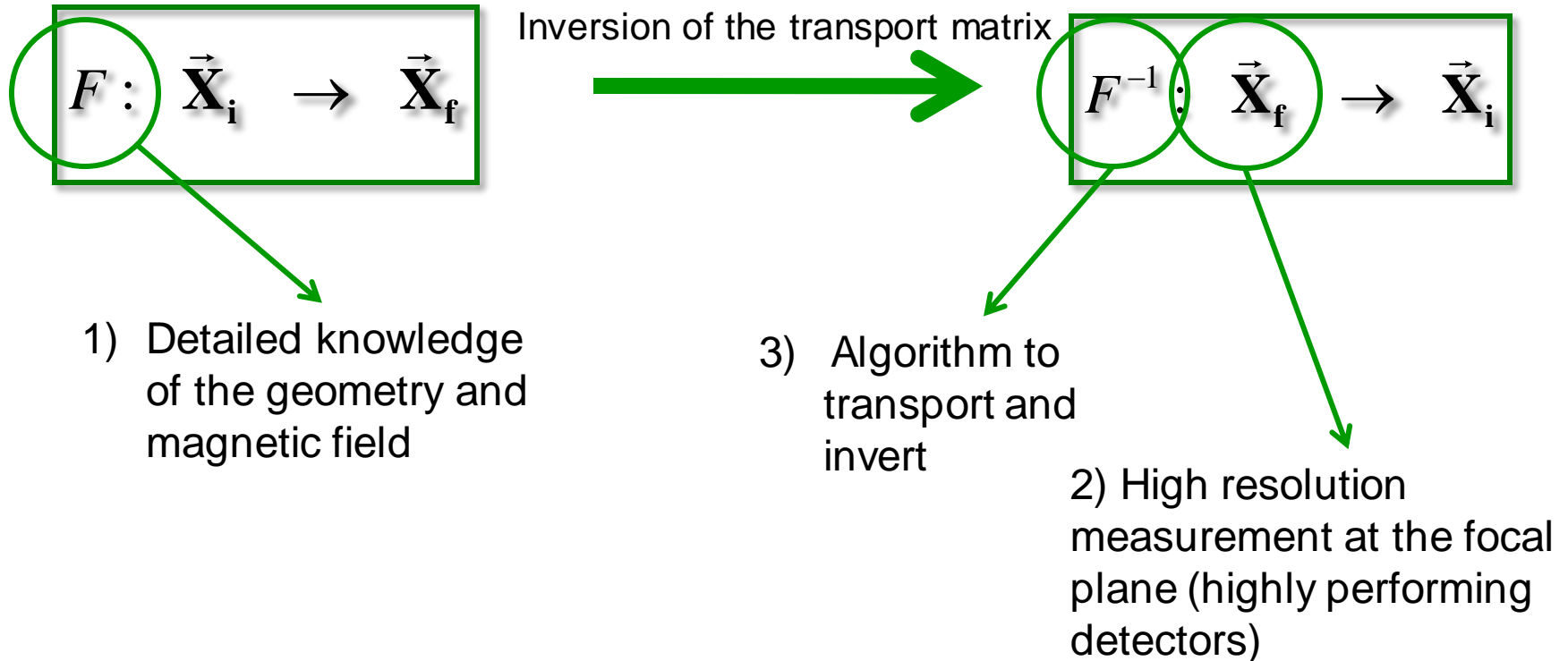
Horizontal and vertical position resolution (FWHM)	0.6 mm
Horizontal and vertical angular resolution (FWHM)	0.3°
Mass resolution <sup>(a)</sup>	0.6%
Explored ion mass range	from $A = 1$ to $A = 48$
Energy loss resolution <sup>(b)</sup>	6.3%
Maximum incident ion rate (uniform distribution)	5 kHz
Maximum incident ion rate (localized in $\sim 1$ cm)	2 kHz

→ For O at 300 MeV  
 $10^4$  Hz/mm<sup>2</sup>

# Software ray-reconstruction

## ALGEBRIC RAY-RECONSTRUCTION

- ✓ Solution of the **equation of motion** for each detected particle
- ✓ **Inversion** of the transport matrix
- ✓ Application to the final **measured parameters**



# 3) Algorithm to transport and invert

ALGEBRIC  
RAY-RECONSTRUCTION

(Differential Algebras)

COSY-INFINITY

Solution of the equation of motion for each detected particle

$$F : \vec{X}_i \rightarrow \vec{X}_f$$

Direct transport map

$\vec{P}_i(E^*, \theta_{lab})$   
Physical Parameters at the target

Target  
QUADRUPOLE

DIPOLE

FPD

$\vec{P}_f(X_{foc}, Y_{foc}, \theta_{foc}, \varphi_{foc})$   
Geometrical Parameters at the FPD

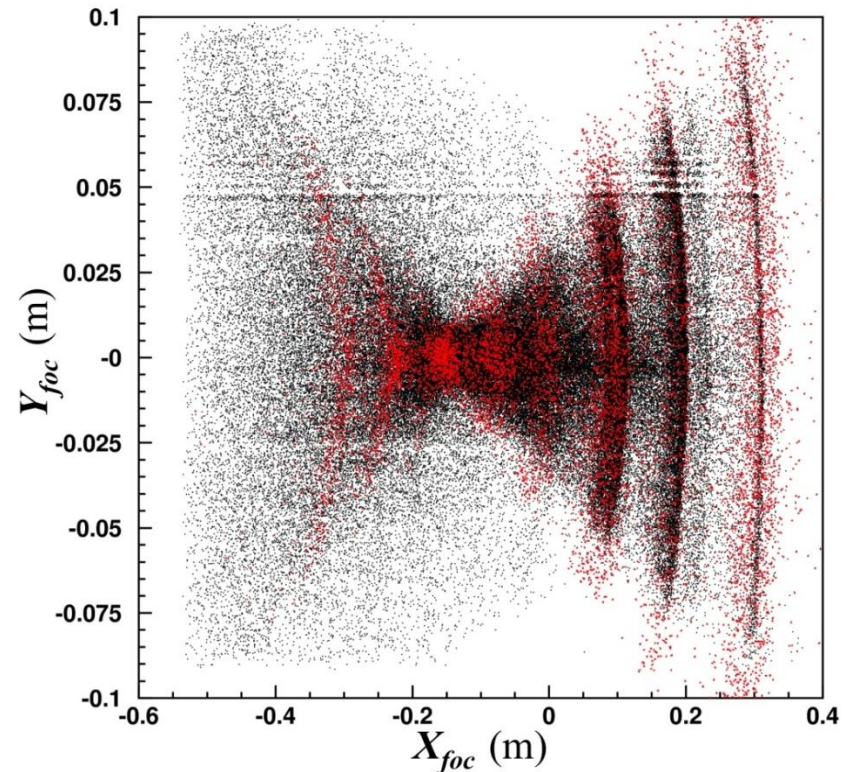
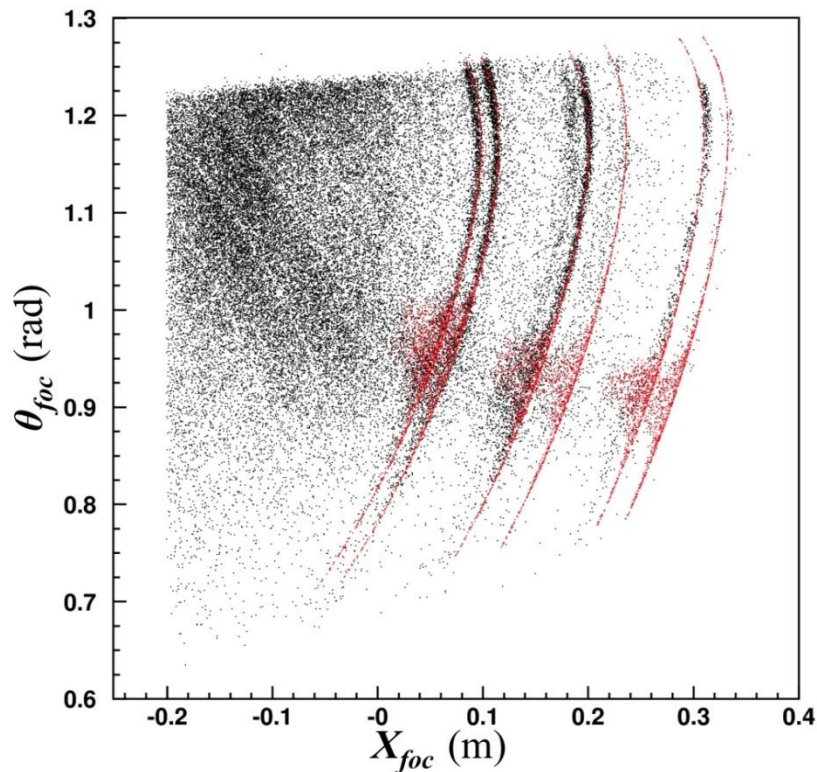


# 3) Algorithm to transport and invert

Examples of parameters at the focal plane

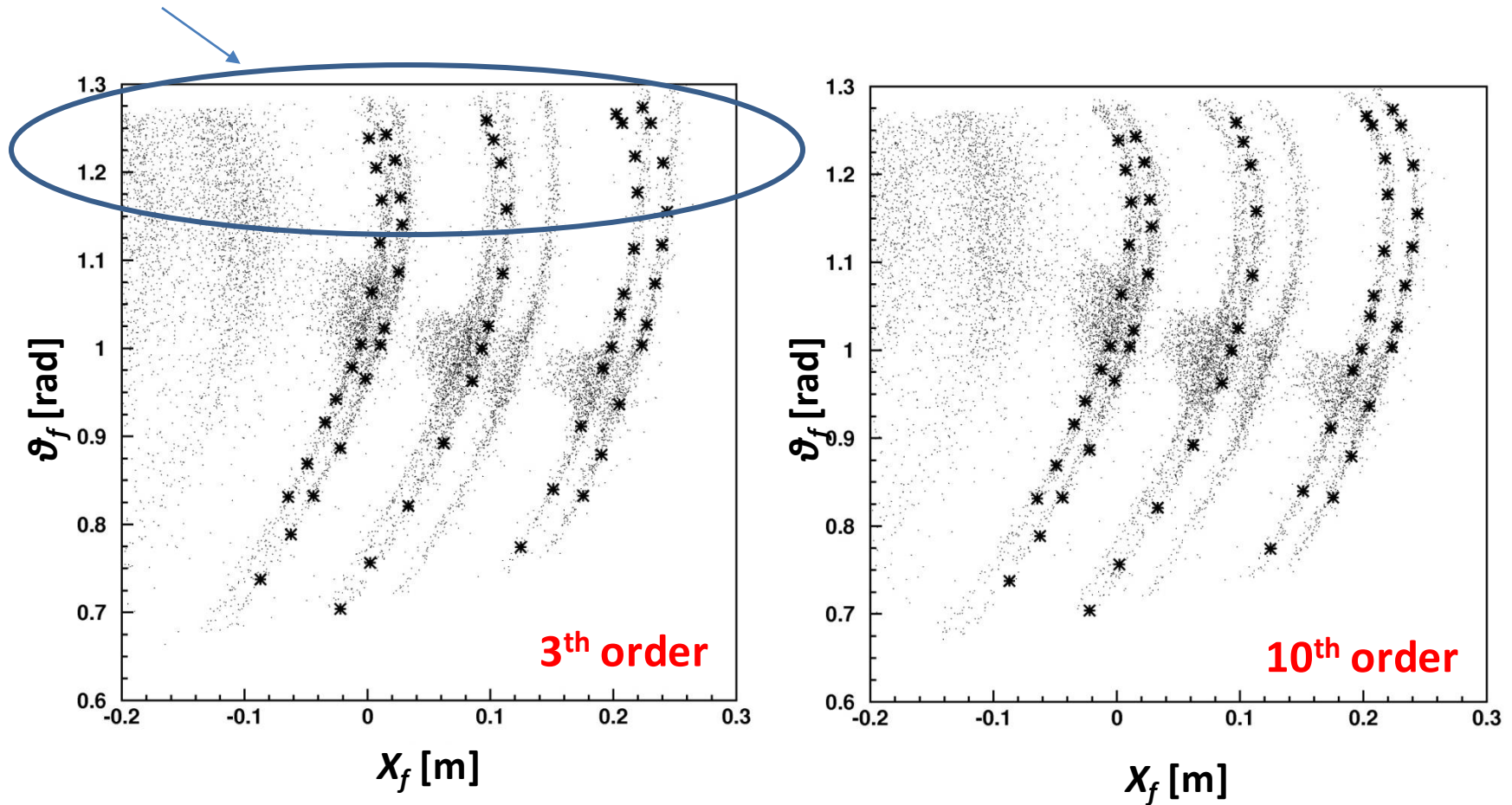
Black: measured parameters

Red: Simulated parameters



# 3) Algorithm to transport and invert

Effect of high order aberrations



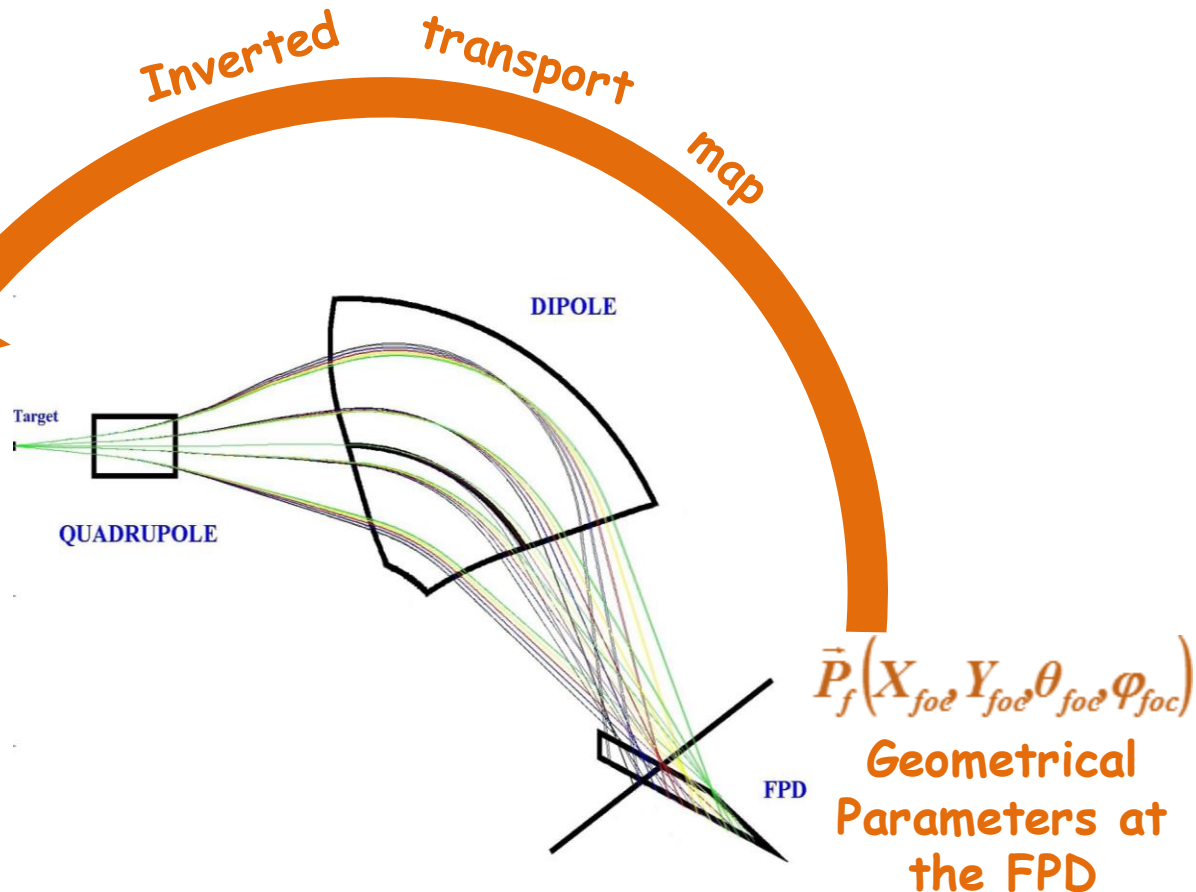
# 3) Algorithm to transport and invert

ALGEBRIC  
RAY-RECONSTRUCTION  
(Differential Algebras)  
COSY-INFINITY

$$F^{-1} : \vec{X}_f \rightarrow \vec{X}_i$$

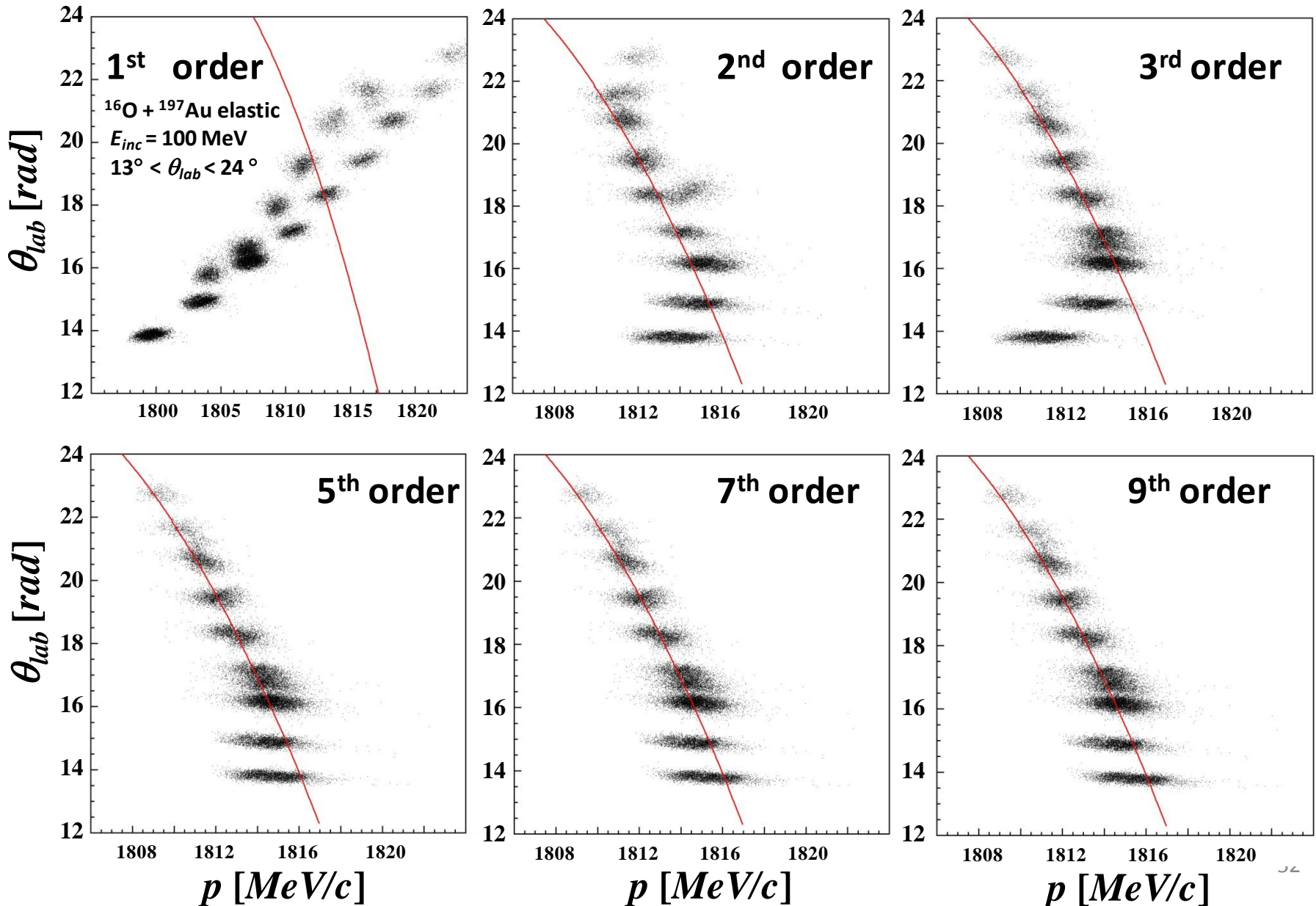
Solution of the equation of motion for each detected particle

$\vec{P}_i(E^*, \theta_{lab})$   
Physical  
Parameters at  
the target



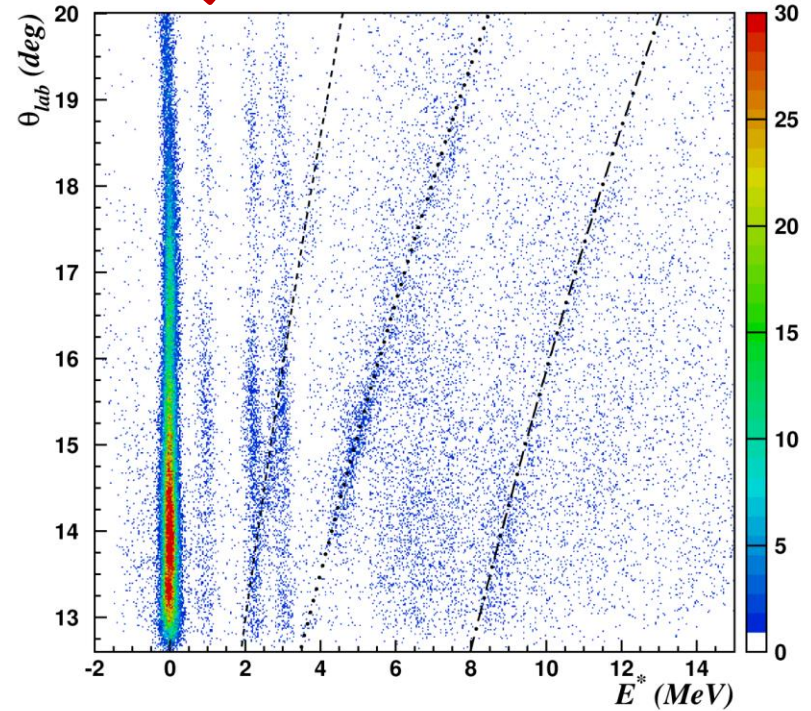
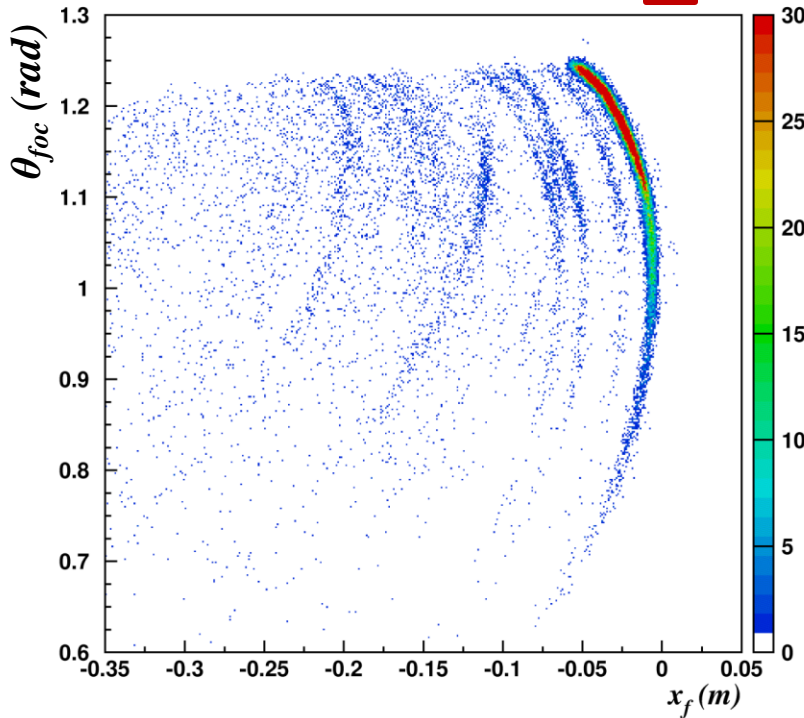
# 3) Algorithm to transport and invert

High order aberrations!



# 3) Algorithm to transport and invert

$^{27}\text{Al}(^{16}\text{O},^{16}\text{O})^{27}\text{Al}$  at 100 MeV  
 $13^\circ < \theta_{\text{lab}} < 20^\circ$



$$E^* = Q - K \left(1 + \frac{M_{\text{ejectile}}}{M_{\text{residual}}}\right) + E_{\text{beam}} \left(1 - \frac{M_{\text{beam}}}{M_{\text{residual}}}\right) + 2 \frac{\sqrt{M_{\text{beam}} M_{\text{ejectile}}}}{M_{\text{residual}}} \sqrt{E_{\text{beam}} K \cos \theta_{\text{lab}}}$$

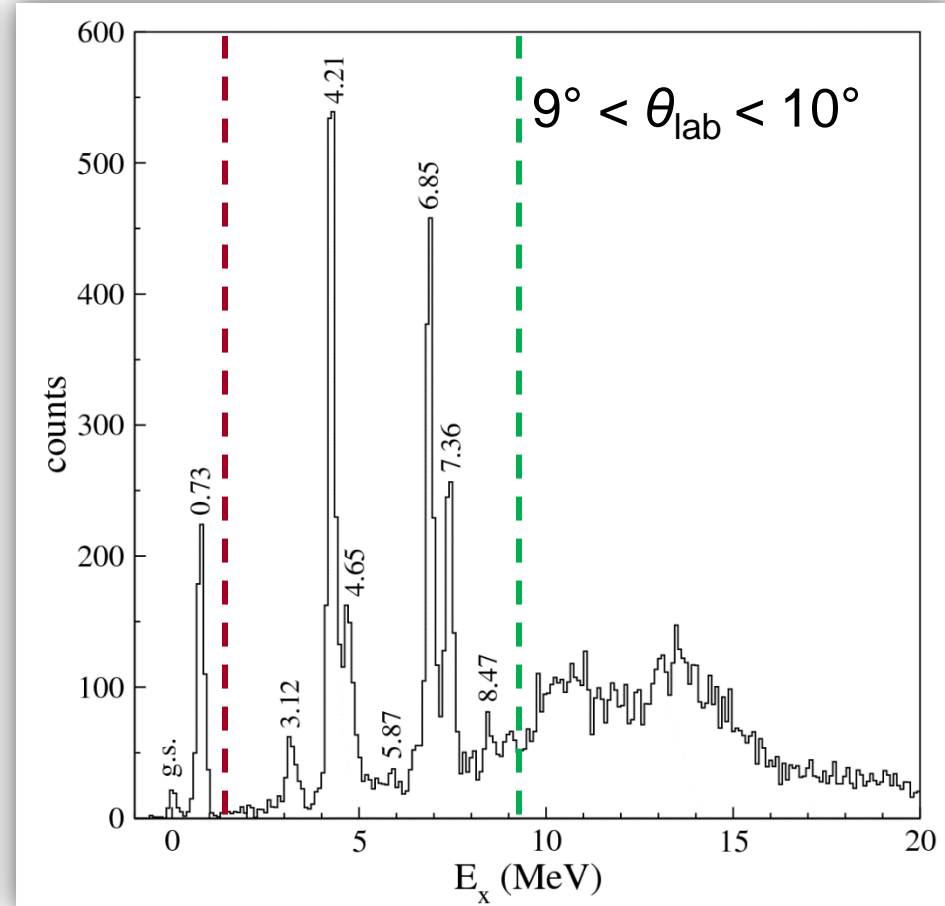
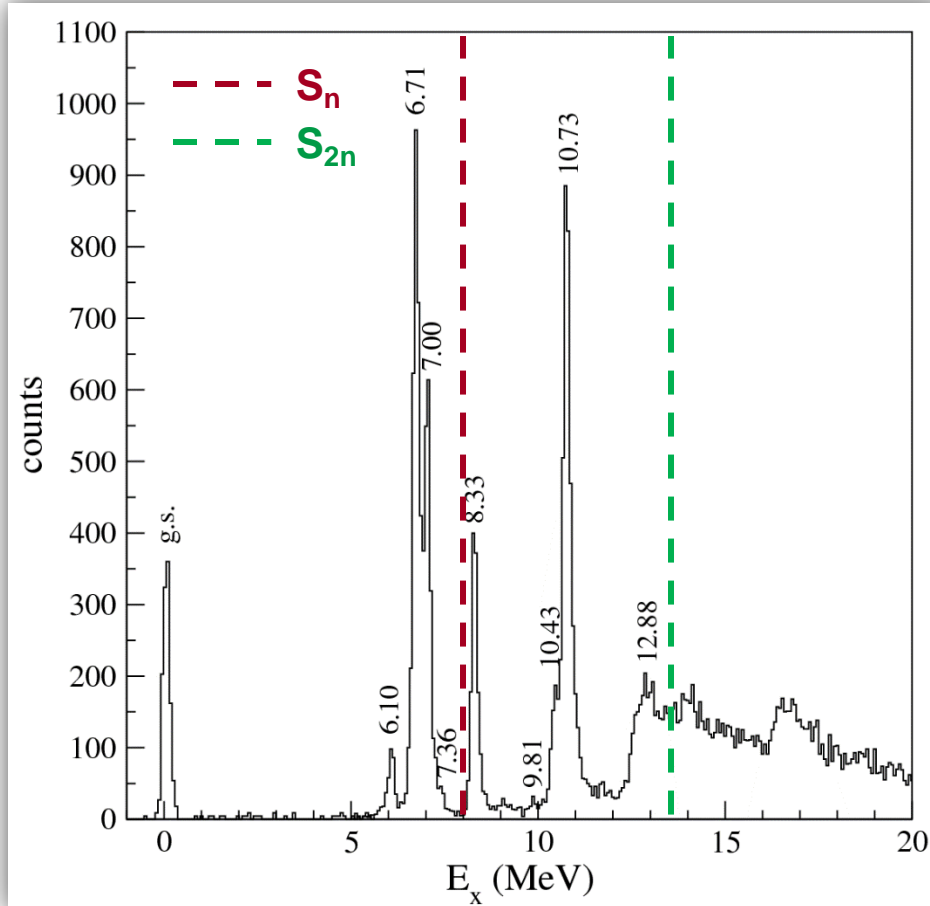
*M. Cavallaro et al., NIMA 648 (2011) 46-51*

*F. Cappuzzello et al., NIMA 638 (2011) 74-82*

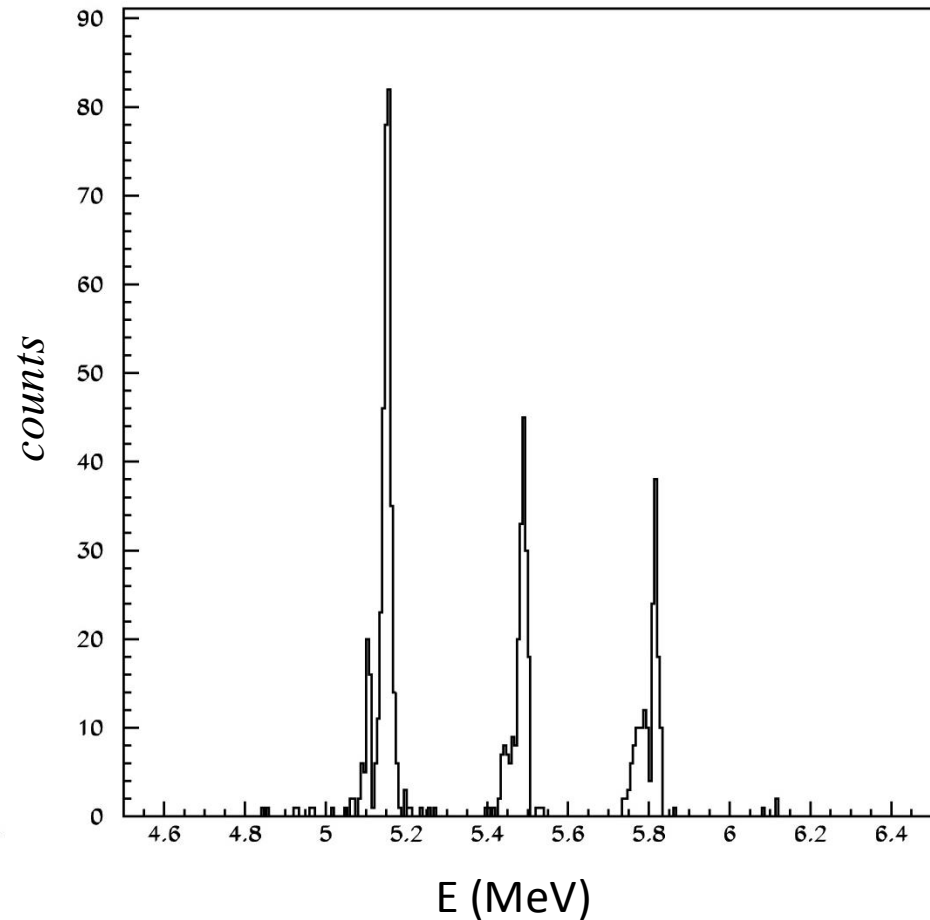
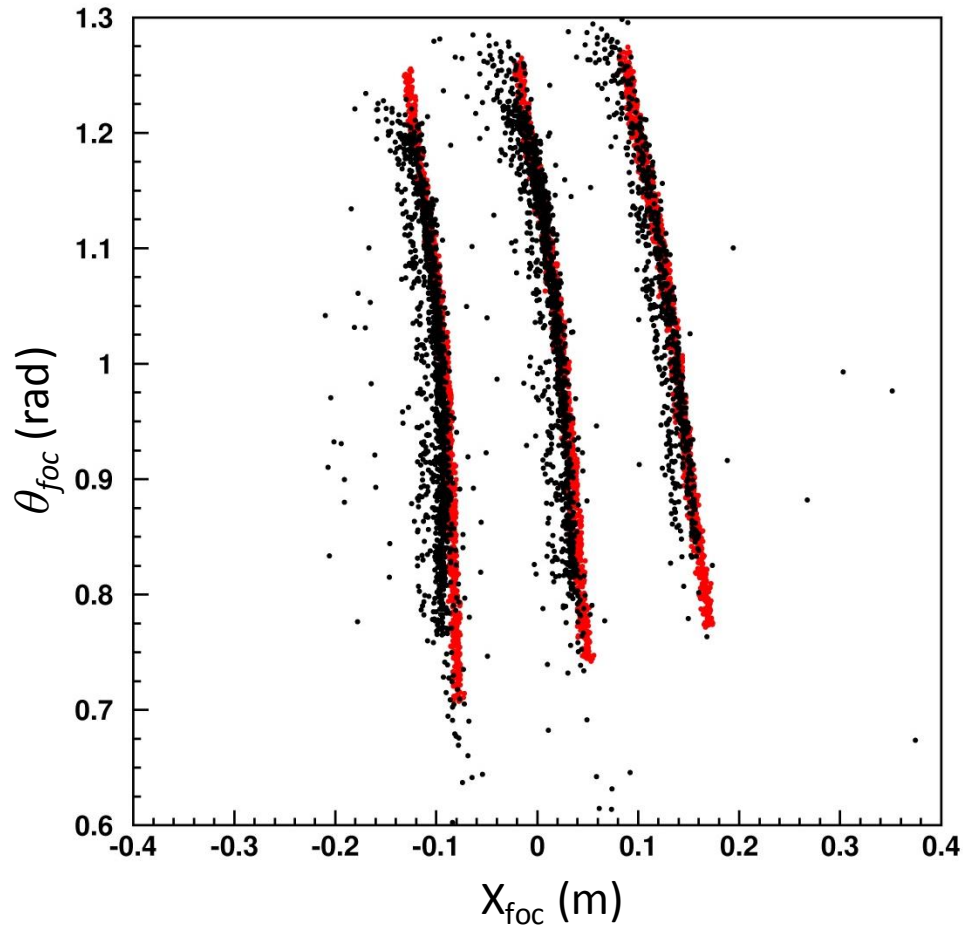
# Typical energy spectra

$^{12}\text{C}(^{18}\text{O}, ^{16}\text{O})^{14}\text{C}$

$^{13}\text{C}(^{18}\text{O}, ^{16}\text{O})^{15}\text{C}$

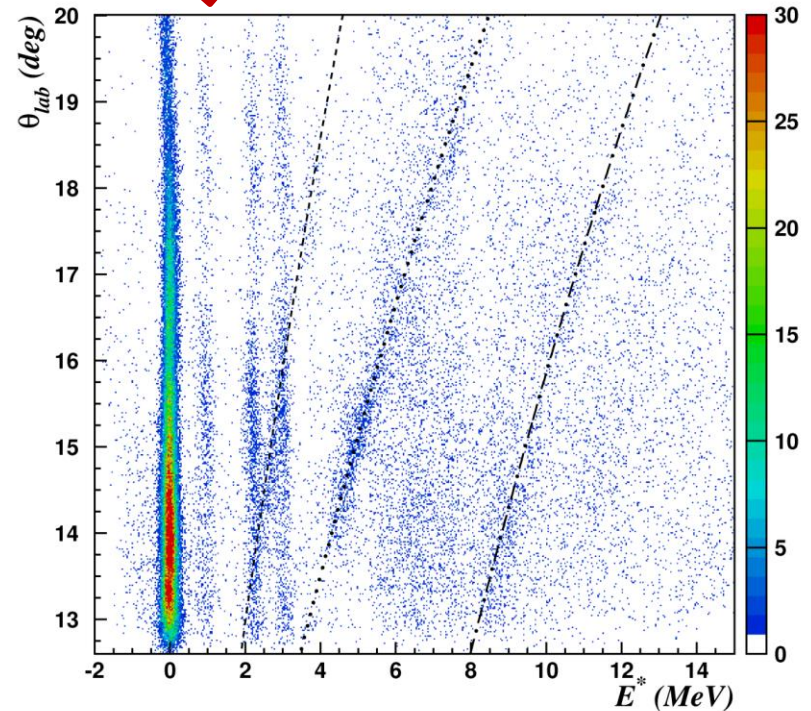
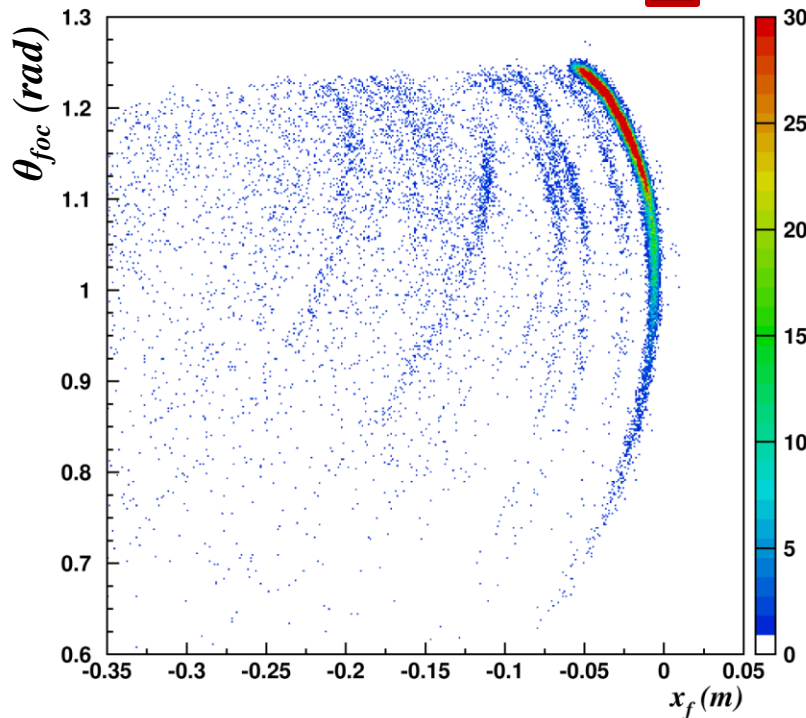


# 3-peaks $\alpha$ -source $^{241}\text{Am}$ + $^{239}\text{Pu}$ + $^{244}\text{Cm}$



# 3) Algorithm to transport and invert

$^{27}\text{Al}(^{16}\text{O},^{16}\text{O})^{27}\text{Al}$  at 100 MeV  
 $13^\circ < \theta_{\text{lab}} < 20^\circ$



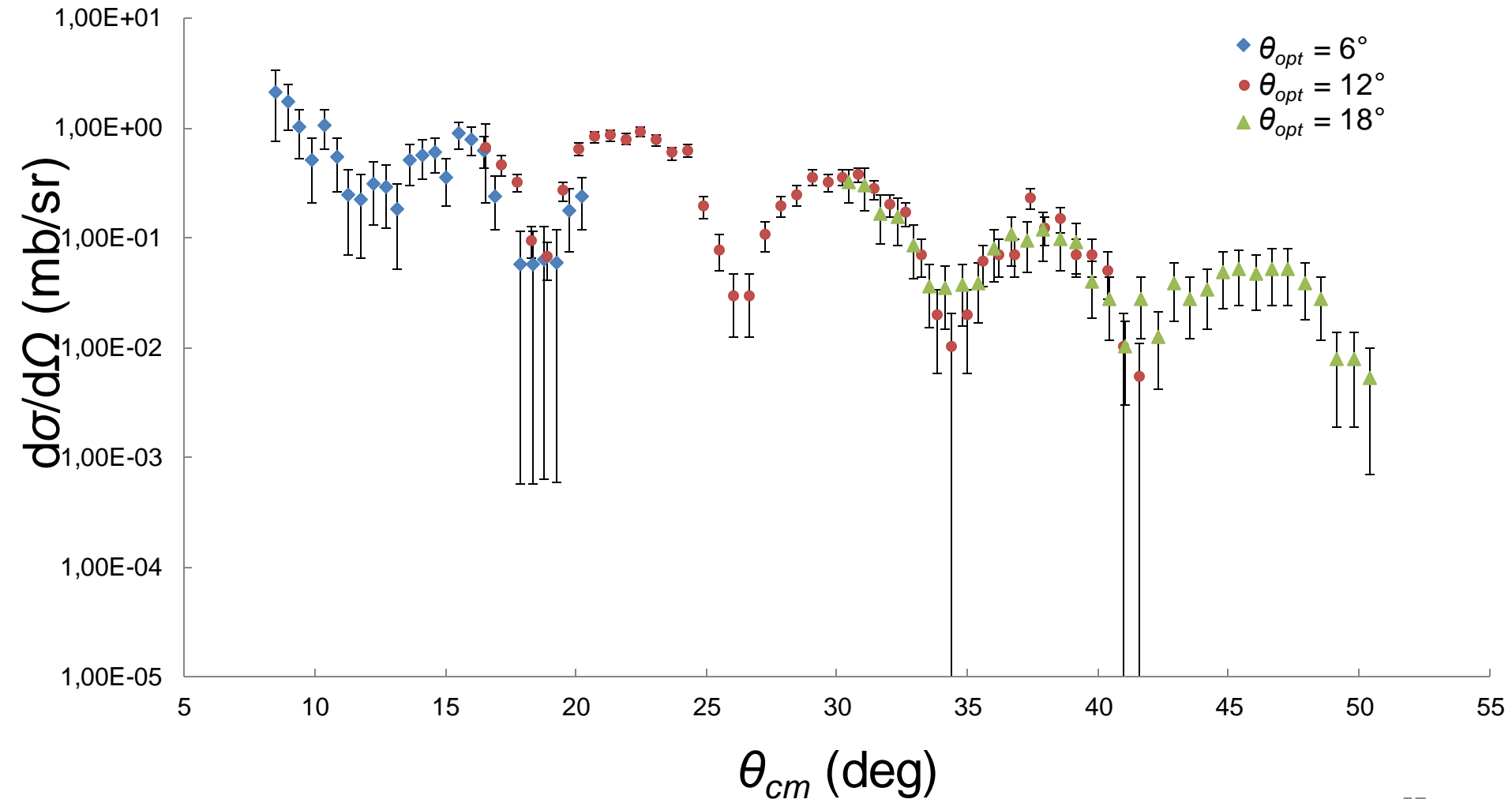
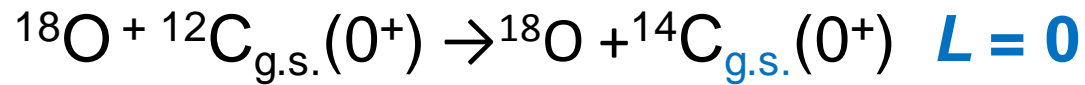
$$E^* = Q - K \left(1 + \frac{M_{\text{ejectile}}}{M_{\text{residual}}}\right) + E_{\text{beam}} \left(1 - \frac{M_{\text{beam}}}{M_{\text{residual}}}\right) + 2 \frac{\sqrt{M_{\text{beam}} M_{\text{ejectile}}}}{M_{\text{residual}}} \sqrt{E_{\text{beam}} K \cos \theta_{\text{lab}}}$$

*M. Cavallaro et al., NIMA 648 (2011) 46-51*

*F. Cappuzzello et al., NIMA 638 (2011) 74-82*



# Typical angular distribution



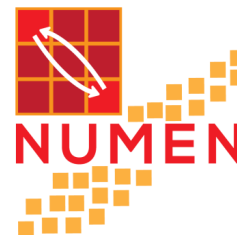
# MAGNEX FPD characteristics

Horizontal and vertical position resolution (FWHM)	0.6 mm
Horizontal and vertical angular resolution (FWHM)	0.3°
Mass resolution <sup>(a)</sup>	0.6%
Explored ion mass range	from $A = 1$ to $A = 48$
Energy loss resolution <sup>(b)</sup>	6.3%
Maximum incident ion rate (uniform distribution)	5 kHz
Maximum incident ion rate (localized in $\sim 1$ cm)	2 kHz

→ For O at 300 MeV  
 $10^4$  Hz/mm<sup>2</sup>

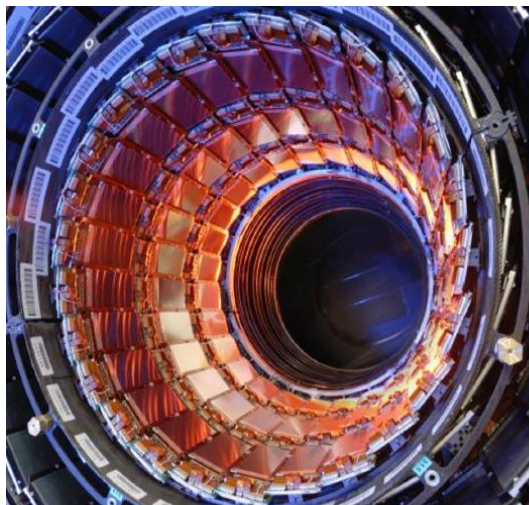


# The NUMEN experiment



**Manuela Cavallaro**

**INFN – Laboratori Nazionali del Sud  
(Italy)**

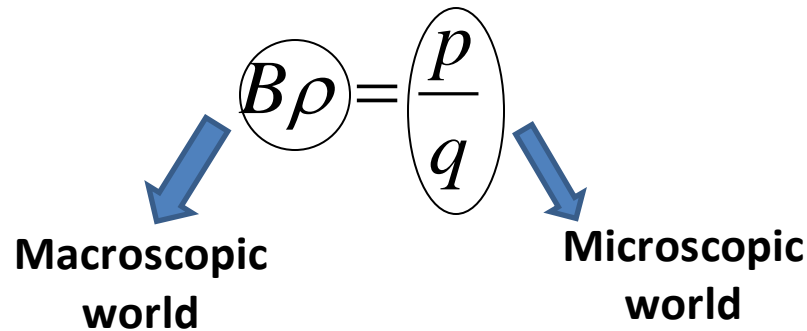


**XXVI GIORNATE DI STUDIO  
SUI RIVELATORI**

**Scuola F. Bonaudi**

Cogne, 13 – 17 February 2017

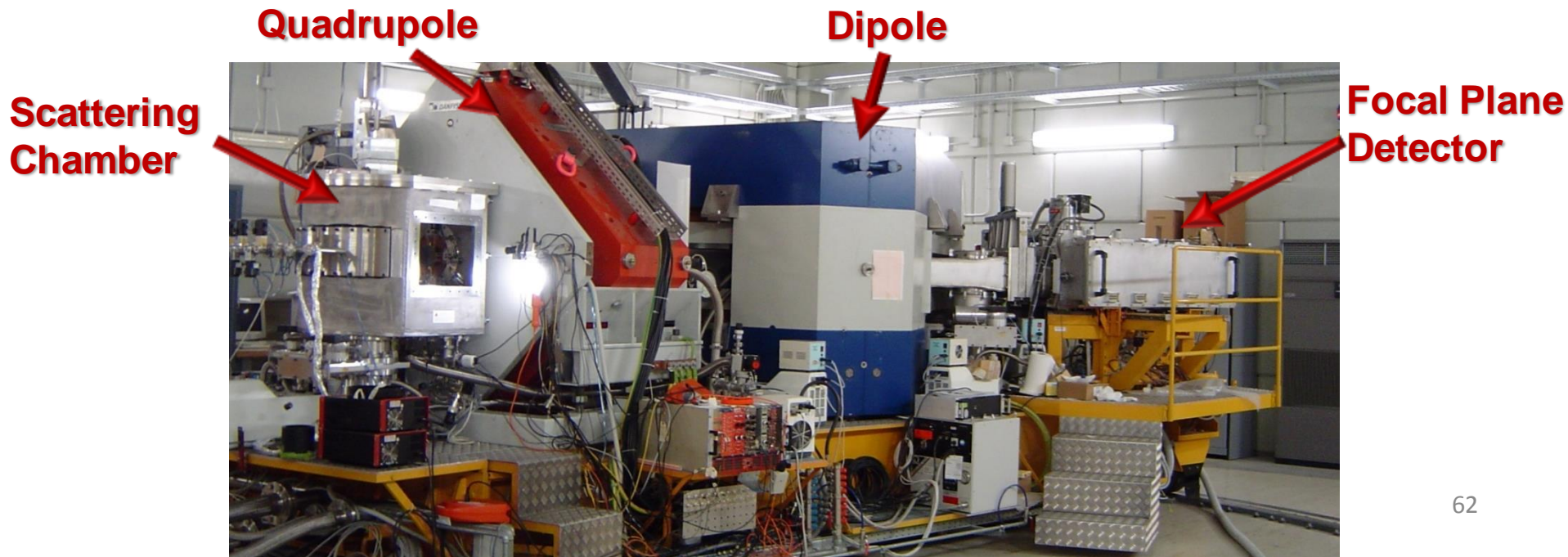
# Advantages of magnetic spectrometry



- + Good selection of reaction products
- + Possibility to measure near  $0^\circ$
- + High momentum and mass resolution

# MAGNEX: a large acceptance QD spectrometer

- ❖ **The Quadrupole:** vertically focusing  
(Aperture radius 20 cm, effective length 58 cm. Maximum field strength 5 T/m)
- ❖ **The Dipole:** momentum dispersion (and horizontal focus)  
(Mean bend angle  $55^\circ$ , radius 1.60 m. Maximum field  $\sim 1.15$  T)
- ❖ **The surface coils,** located between the dipole pole faces and the inner high vacuum chamber, giving tunable quadrupolar and sextupolar corrections



# The large acceptance problem

$$F : \vec{X}_i \rightarrow \vec{X}_f$$

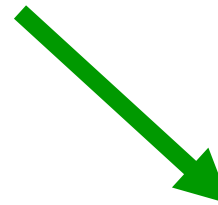
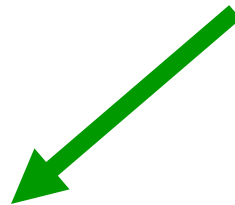
$F$  transport matrix

Large acceptance



**Aberrations**

$$x_i(f) = \sum_j R_{ij} x_j(i) + \sum_{j,k} T_{ijk} x_j(i) x_k(i) + \dots \quad \text{Up to } 10^\circ \text{ order}$$



Careful hardware design  
(to minimize the aberrations)

Software ray-reconstruction  
(to know the aberrations)

# 3) Algorithm to transport and invert

ALGEBRIC  
RAY-RECONSTRUCTION

(Differential Algebras)

COSY-INFINITY

Solution of the equation of motion for each detected particle

$$F : \vec{X}_i \rightarrow \vec{X}_f$$

Direct transport map

$\vec{P}_i(E^*, \theta_{lab})$   
Physical Parameters at the target

Target  
QUADRUPOLE

DIPOLE

FPD

$\vec{P}_f(X_{foc}, Y_{foc}, \theta_{foc}, \varphi_{foc})$   
Geometrical Parameters at the FPD



# 3) Algorithm to transport and invert

ALGEBRIC  
RAY-RECONSTRUCTION

(Differential Algebras)

COSY-INFINITY

$$F^{-1} : \vec{X}_f \rightarrow \vec{X}_i$$

Solution of the equation of motion for each detected particle

Inverted transport map

$\vec{P}_i(E^*, \theta_{lab})$   
Physical Parameters at the target

Target  
QUADRUPOLE

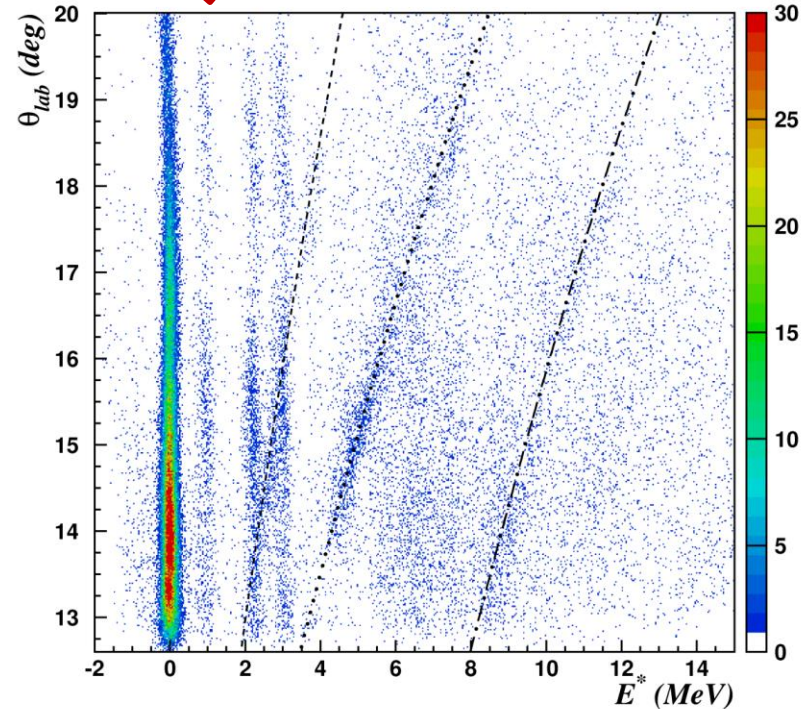
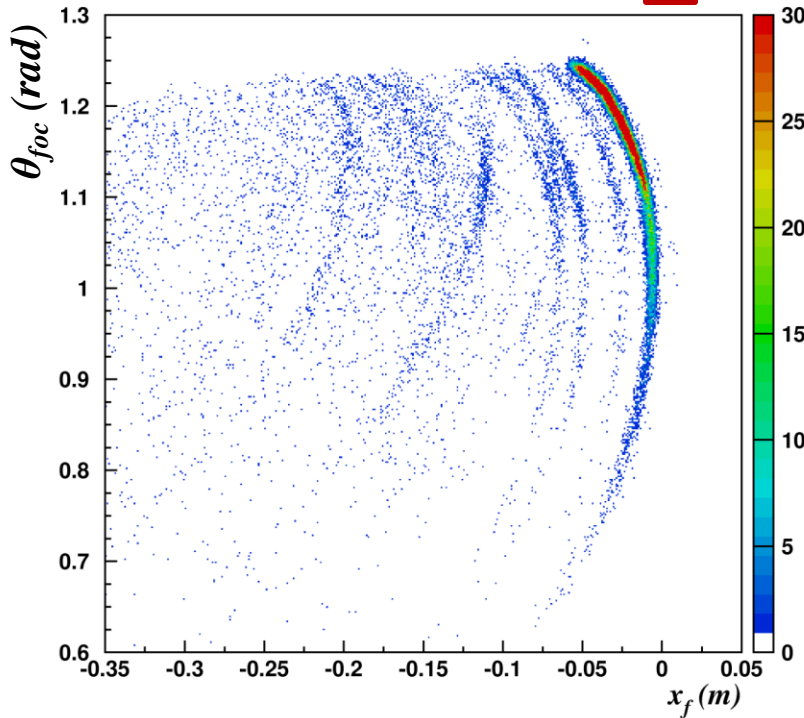
DIPOLE

FPD

$\vec{P}_f(X_{foc}, Y_{foc}, \theta_{foc}, \varphi_{foc})$   
Geometrical Parameters at the FPD

# 3) Algorithm to transport and invert

$^{27}\text{Al}(^{16}\text{O},^{16}\text{O})^{27}\text{Al}$  at 100 MeV  
 $13^\circ < \theta_{\text{lab}} < 20^\circ$



$$E^* = Q - K \left(1 + \frac{M_{\text{ejectile}}}{M_{\text{residual}}}\right) + E_{\text{beam}} \left(1 - \frac{M_{\text{beam}}}{M_{\text{residual}}}\right) + 2 \frac{\sqrt{M_{\text{beam}} M_{\text{ejectile}}}}{M_{\text{residual}}} \sqrt{E_{\text{beam}} K \cos \theta_{\text{lab}}}$$

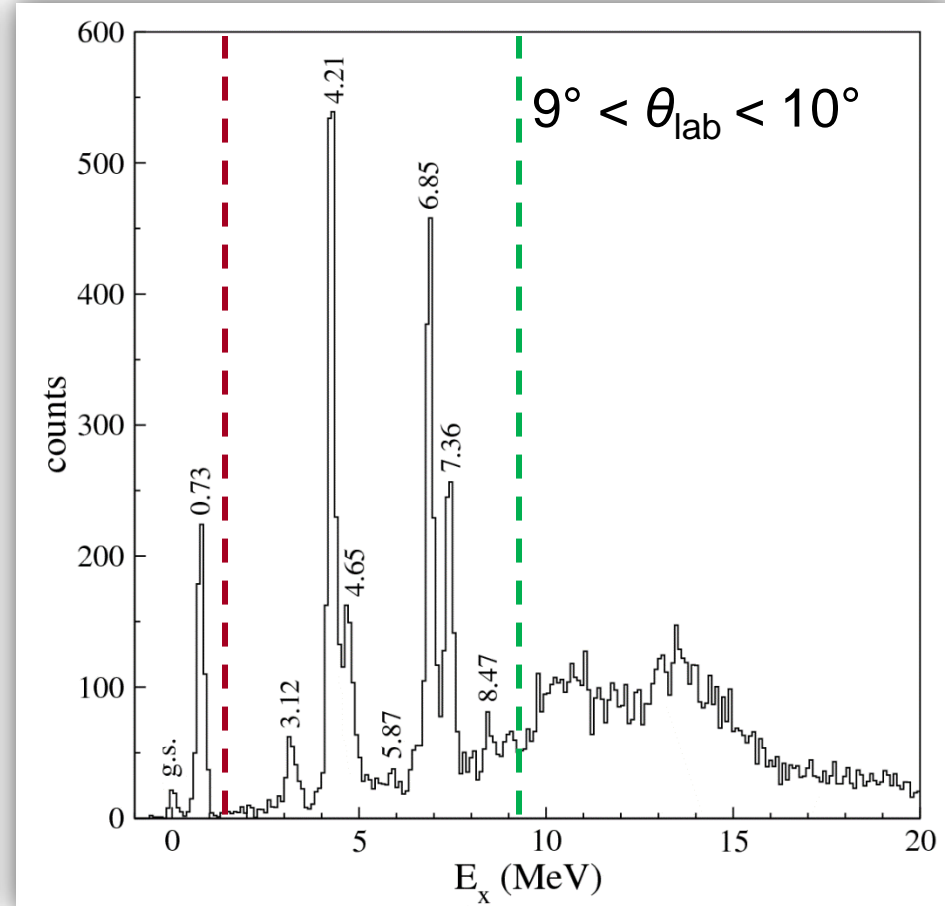
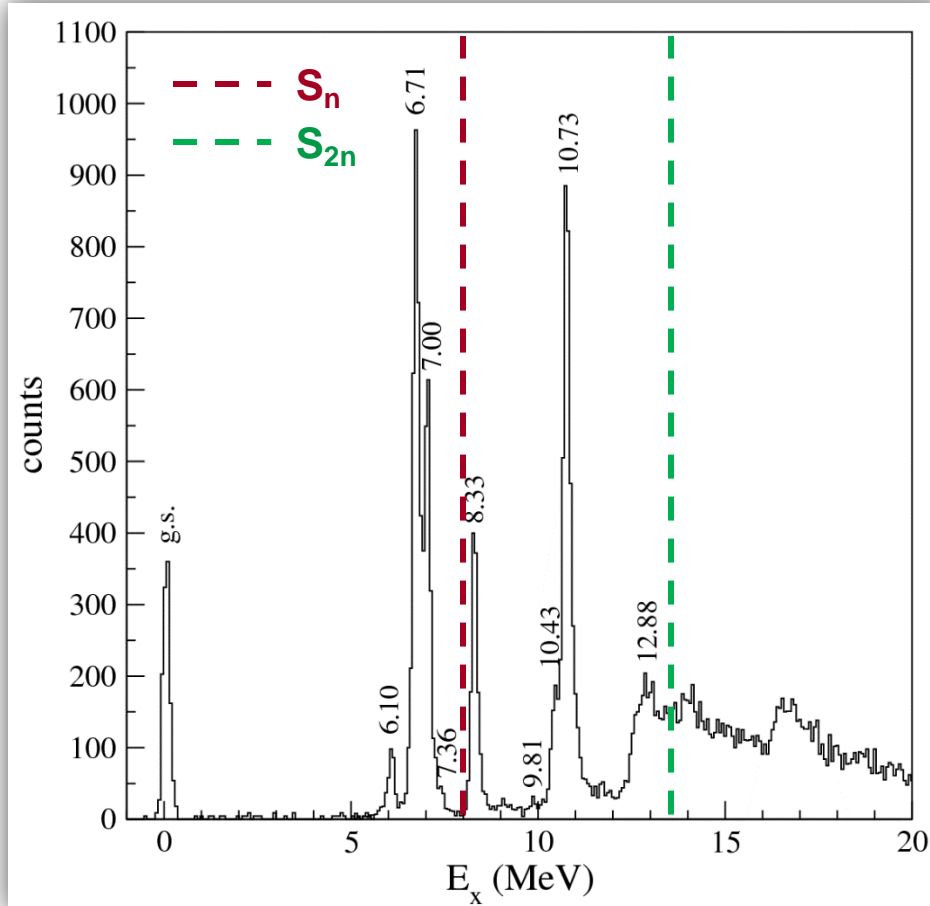
*M. Cavallaro et al., NIMA 648 (2011) 46-51*

*F. Cappuzzello et al., NIMA 638 (2011) 74-82*

# Typical energy spectra

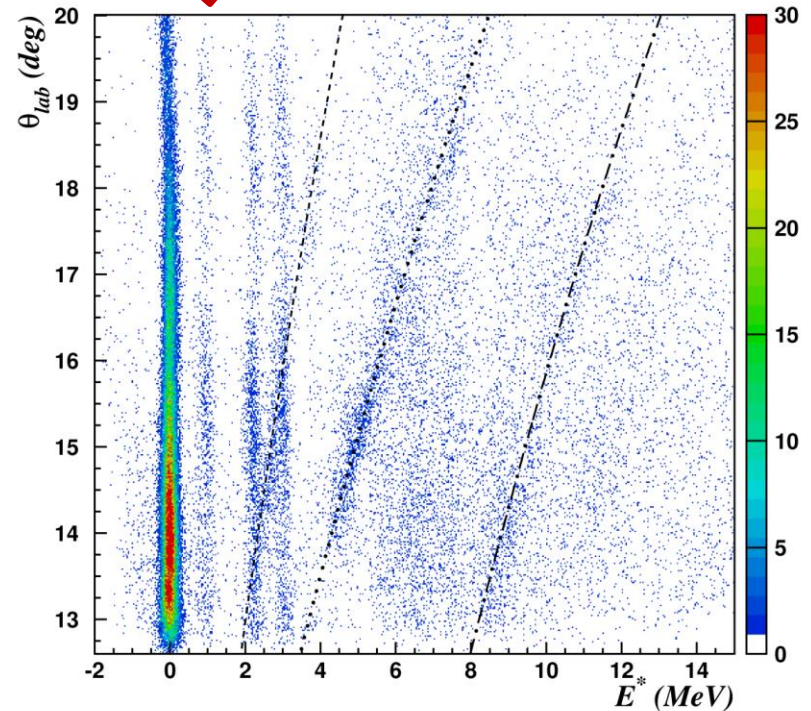
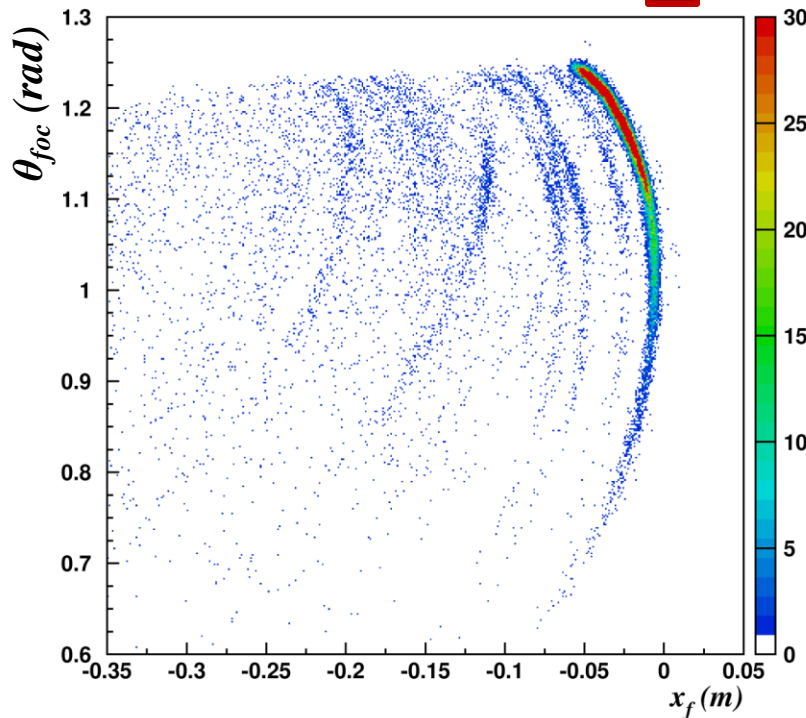
$^{12}\text{C}(^{18}\text{O}, ^{16}\text{O})^{14}\text{C}$

$^{13}\text{C}(^{18}\text{O}, ^{16}\text{O})^{15}\text{C}$



# 3) Algorithm to transport and invert

$^{27}\text{Al}(^{16}\text{O},^{16}\text{O})^{27}\text{Al}$  at 100 MeV  
 $13^\circ < \theta_{\text{lab}} < 20^\circ$

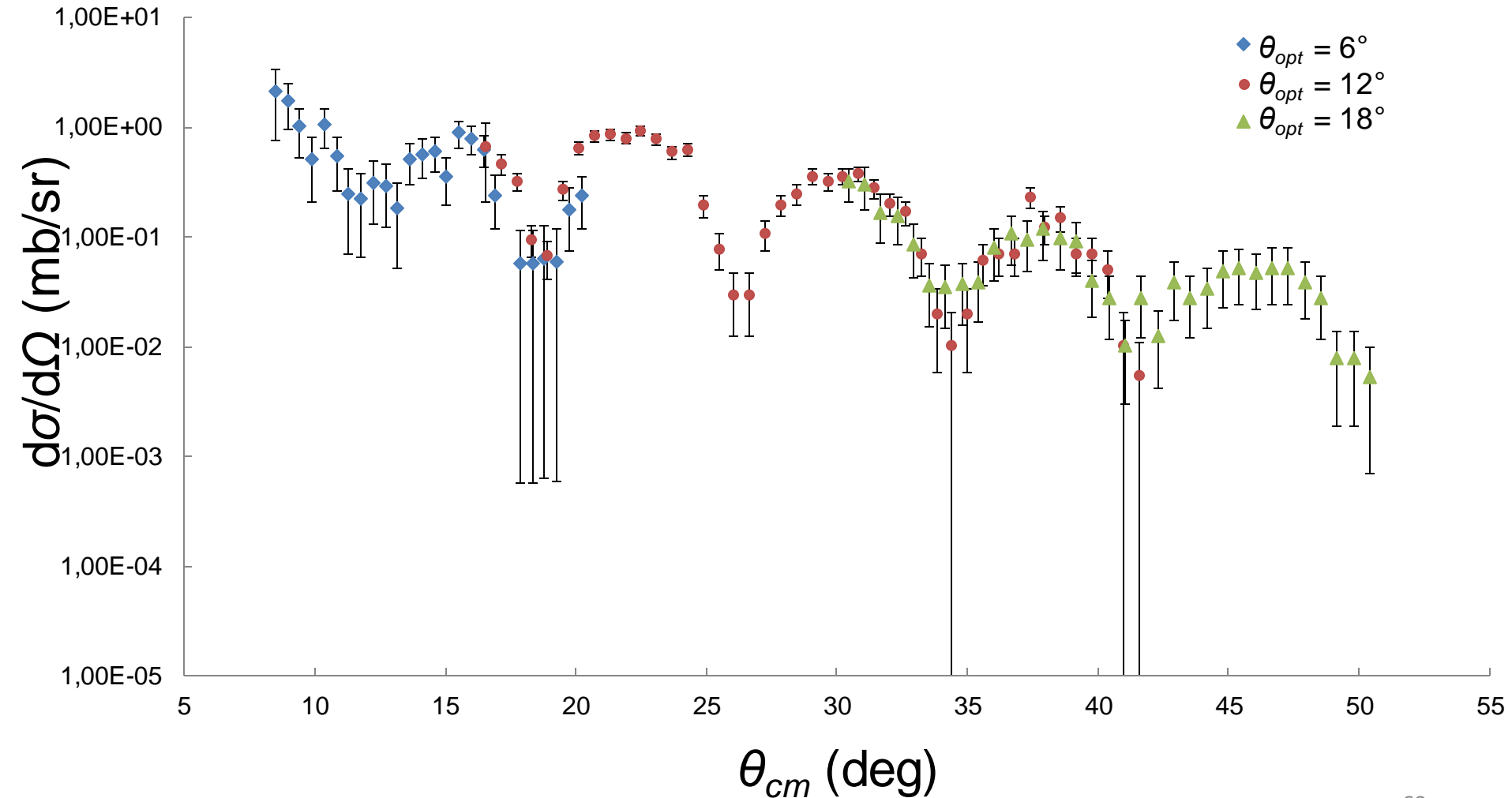
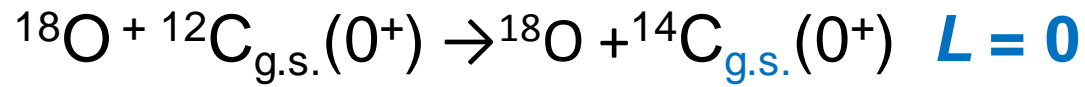


$$E^* = Q - K \left(1 + \frac{M_{\text{ejectile}}}{M_{\text{residual}}}\right) + E_{\text{beam}} \left(1 - \frac{M_{\text{beam}}}{M_{\text{residual}}}\right) + 2 \frac{\sqrt{M_{\text{beam}} M_{\text{ejectile}}}}{M_{\text{residual}}} \sqrt{E_{\text{beam}} K \cos \theta_{\text{lab}}}$$

*M. Cavallaro et al., NIMA 648 (2011) 46-51*

*F. Cappuzzello et al., NIMA 638 (2011) 74-82*

# Typical angular distribution





# **Nuclear Reactions for Neutrinoless Double Beta Decay**

# $0\nu\beta\beta$ decay

Open problem in modern physics:

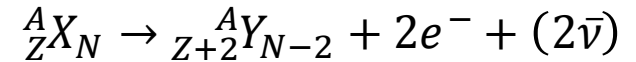
Neutrino absolute mass scale

Neutrino nature



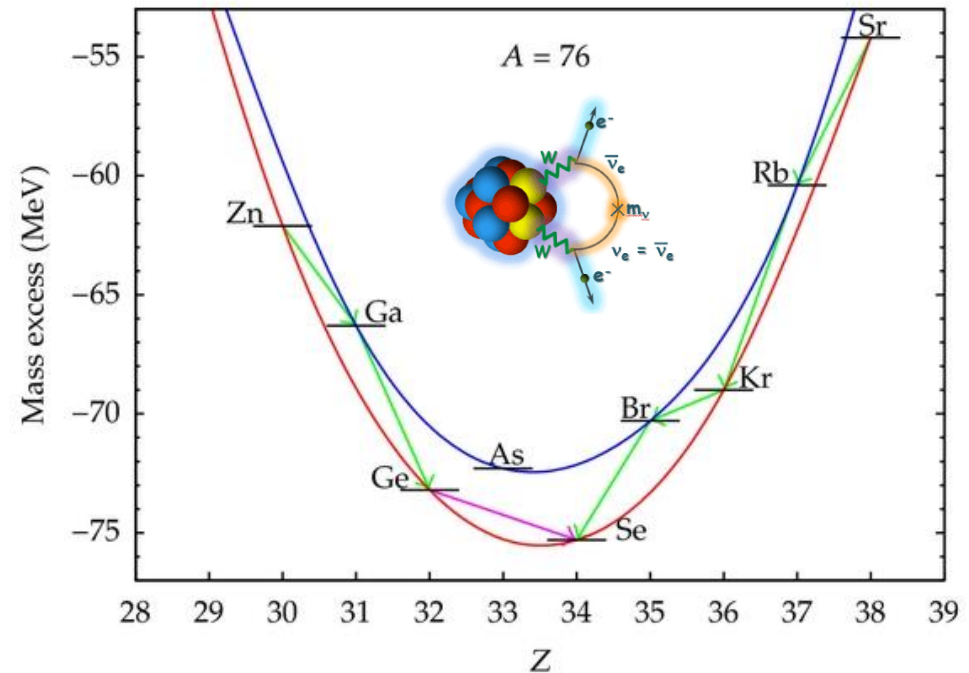
$0\nu\beta\beta$  is considered the most promising approach

**Still not observed**



Beyond standard model

${}^{76}\text{Br}$	${}^{77}\text{Br}$	${}^{78}\text{Br}$	${}^{79}\text{Br}$	${}^{80}\text{Br}$
${}^{75}\text{Se}$	${}^{76}\text{Se}$	${}^{77}\text{Se}$	${}^{78}\text{Se}$	${}^{79}\text{Se}$
${}^{74}\text{As}$	${}^{75}\text{As}$	${}^{76}\text{As}$	${}^{77}\text{As}$	${}^{78}\text{As}$
${}^{73}\text{Ge}$	${}^{74}\text{Ge}$	${}^{75}\text{Ge}$	${}^{76}\text{Ge}$	${}^{77}\text{Ge}$
${}^{72}\text{Ga}$	${}^{73}\text{Ga}$	${}^{74}\text{Ga}$	${}^{75}\text{Ga}$	${}^{76}\text{Ga}$



- ✓ Process mediated by the **weak interaction**
- ✓ Occurring in even-even nuclei where the **single  $\beta$ -decay** is energetically **forbidden**





# Search for $0\nu\beta\beta$ decay. A worldwide race

Experiment	Isotope	Lab	Status
GERDA	$^{76}\text{Ge}$	LNGS [Italy]	Operational
CUORE	$^{130}\text{Te}$	LNGS [Italy]	Construction
Majorana	$^{76}\text{Ge}$	SURF [USA]	Construction
KamLAND-Zen	$^{136}\text{Xe}$	Kamioka [Japan]	Operational
EXO/nEXO	$^{136}\text{Xe}$	WIPP [USA]	Operational
SNO+	$^{130}\text{Te}$	Sudbury [Canada]	Construction
SuperNEMO	$^{82}\text{Se}$ (or others)	LSM [France]	R&D
CANDLES	$^{48}\text{Ca}$	Kamioka [Japan]	R&D
COBRA	$^{116}\text{Cd}$	LNGS [Italy]	R&D
Lucifer	$^{82}\text{Se}$	LNGS [Italy]	R&D
DCBA	many	[Japan]	R&D
AMoRe	$^{100}\text{Mo}$	[Korea]	R&D
MOON	$^{100}\text{Mo}$	[Japan]	R&D

List not complete...

# Nuclear Matrix Elements

$0\nu\beta\beta$  decay half-life

Phase space factor

contains the average  
neutrino mass

$$\left(T_{\frac{1}{2}}^{0\nu\beta\beta}(0^+ \rightarrow 0^+)\right)^{-1} = G_{0\nu\beta\beta} \left|M^{0\nu\beta\beta}\right|^2 \left|f(m_i, U_{ei})\right|^2$$

**Nuclear Matrix Element (NME)**

$$\left|M_{\varepsilon}^{0\nu\beta\beta}\right|^2 = \left|\left\langle\Psi_f\left|\hat{O}_{\varepsilon}^{0\nu\beta\beta}\right|\Psi_i\right\rangle\right|^2$$

Transition probability of  
a **nuclear** process

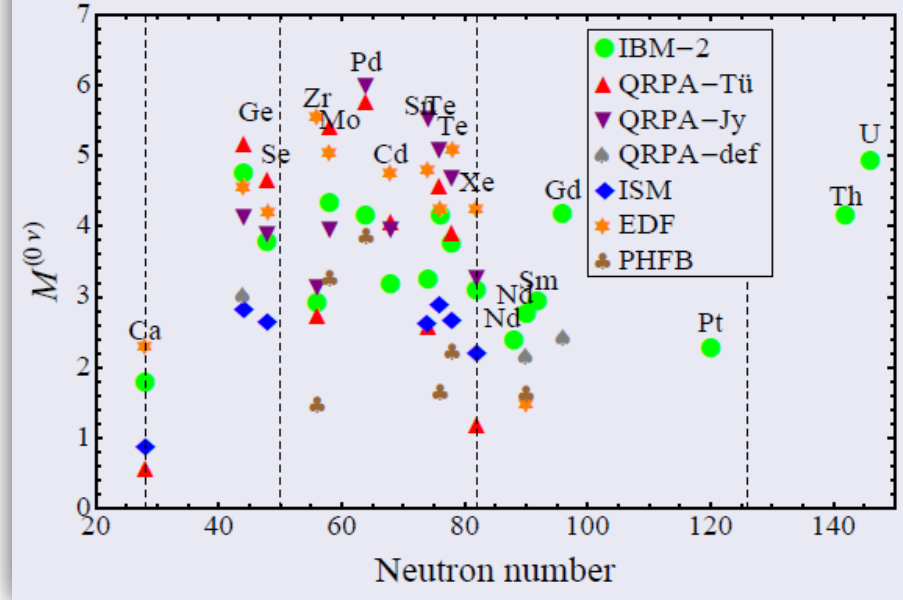
**Nuclear physics plays a key role!**

# Nuclear Matrix Elements

## Nuclear Matrix Element (NME)

$$\left| M_{\varepsilon}^{0\nu\beta\beta} \right|^2 = \left| \left\langle \Psi_f \left| \hat{O}_{\varepsilon}^{0\nu\beta\beta} \right| \Psi_i \right\rangle \right|^2$$

$$M^{(0\nu)} = M_{GT}^{(0\nu)} - \left( \frac{g_V}{g_A} \right)^2 M_F^{(0\nu)} + M_T^{(0\nu)}$$



**Calculations** (still sizeable uncertainties):  
 QRPA, Large scale shell model, IBM, EDF ...

*E. Caurier, et al., PRL 100 (2008) 052503*

*N. L. Vaquero, et al., PRL 111 (2013) 142501*

*J. Barea, PRC 87 (2013) 014315*

*T. R. Rodriguez, PLB 719 (2013) 174*

*F. Simkovic, PRC 77 (2008) 045503.*

...

Warning: Many body WaveFunctions!

# The idea

Is there an **experimental way** to access the NME?

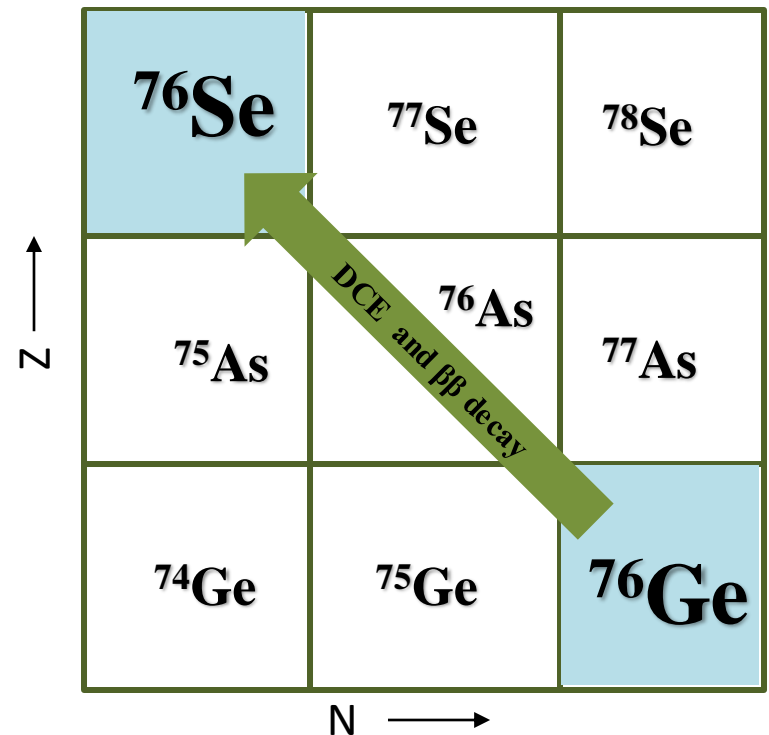
The ERC project NURE:



Nuclear reactions

**Double Charge Exchange reactions (DCE)**

to stimulate in the laboratory the same nuclear transition occurring in  $0\nu\beta\beta$



# $0\nu\beta\beta$ vs HI-DCE



## Differences

- DCE mediated by **strong interaction**,  $0\nu\beta\beta$  by **weak interaction**
- DCE includes **sequential transfer mechanism**

## Similarities

- **Same initial and final states:** Parent/daughter states of the  $0\nu\beta\beta$  decay are the same as those of the target/residual nuclei in the DCE
- **Similar operator:** Short-range Fermi, Gamow-Teller and rank-2 tensor components are present in both the transition operators, with tunable weight in DCE
- **Large linear momentum** ( $\sim 100$  MeV/c) available in the virtual intermediate channel
- **Non-local** processes: characterized by two vertices localized in a pair of valence nucleons
- **Same nuclear medium:** Constraint on the theoretical determination of quenching phenomena on  $0\nu\beta\beta$
- **Off-shell propagation** through virtual intermediate channels

# The project



NURE plans to measure the **absolute cross section** of **HI-DCE** reactions on **nuclei** candidates for  $0\nu\beta\beta$  and to **extract «data-driven» NME**

the measured quantity  
is the **cross section**

details of the  
reaction

$$\frac{d\sigma}{d\Omega}(q, \omega) = f(NME)$$

The extraction of nuclear structure information from measured cross sections is **not trivial** but **feasible**  
**(result of decades of nuclear physics)**

e.g. for single charge-exchange: NME extracted within  
2-5% accuracy by proportionality relation

$$\frac{d\sigma}{d\Omega}(q, \omega) = \hat{\sigma}(E_p, A)F(q, \omega)NME(\alpha) \left\{ \begin{array}{l} E_p \text{ incident energy} \\ q \text{ momentum transfer} \\ \omega \text{ excitation energy} \end{array} \right.$$



# The project

- **Only two transitions of interest for  $0\nu\beta\beta$ :**



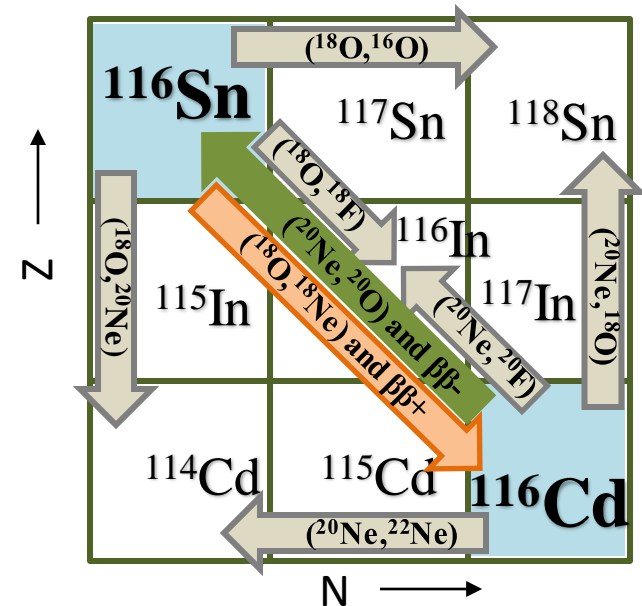
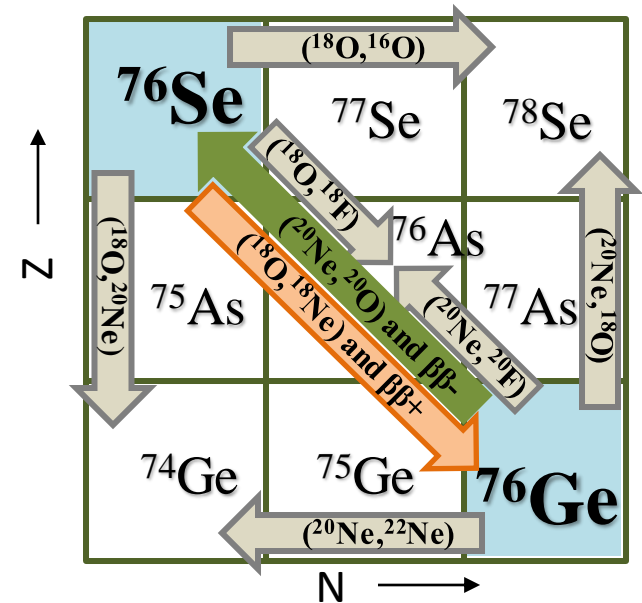
GERDA, MAJORANA, COBRA

- **Two directions:**

$\beta\beta^+$  via  $({}^{18}\text{O}, {}^{18}\text{Ne})$  and  $\beta\beta^-$  via  $({}^{20}\text{Ne}, {}^{20}\text{O})$

- **Complete net** of reactions which can contribute to the DCE cross-section:  
1p-, 2p-, 1n-, 2n-transfer, single cex, DCE

- **Two (or more) incident energies** to study the reaction mechanism

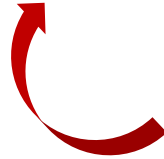


# The context

## Weak interaction probes

$\beta$ ,  $2\nu\beta\beta$ ,

$\mu$ -capture,  
 $\nu$ -nucleus scattering, ...



## Double charge-exchange

induced by **pions** ( $\pi^\pm$ ,  $\pi^\mp$ )

abandoned in the 80's due to the large differences in the momentum transfer and lack of direct GT component in the operators

**Single charge-exchange** reactions induced by light ions ( ${}^3\text{He}, t$ ), ( $d, {}^2\text{He}$ ), ...



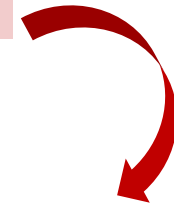
Interesting for  $\beta$ -decay and  $2\nu\beta\beta$ !

## Other researches

to extract information on NME from experimental data and/or constrain the theory

## Transfer reactions

for constraining  $\Psi_i$ ,  $\Psi_f$



## Heavy-ion induced double charge-exchange

limited in the past due to low cross-sections

Renewed interest (RIKEN, Osaka) but low resolution ( $\sim 1.5$  MeV)



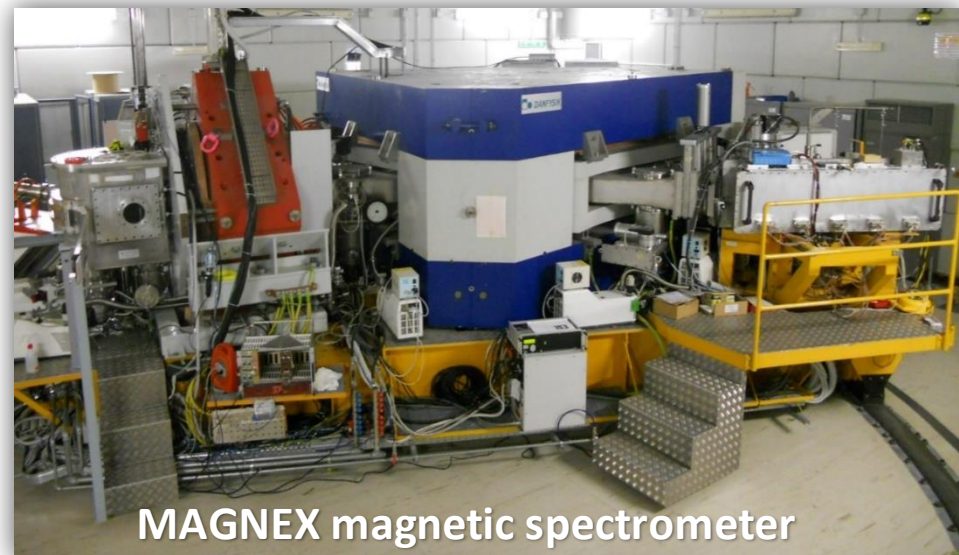
# The pilot experiment



Catania

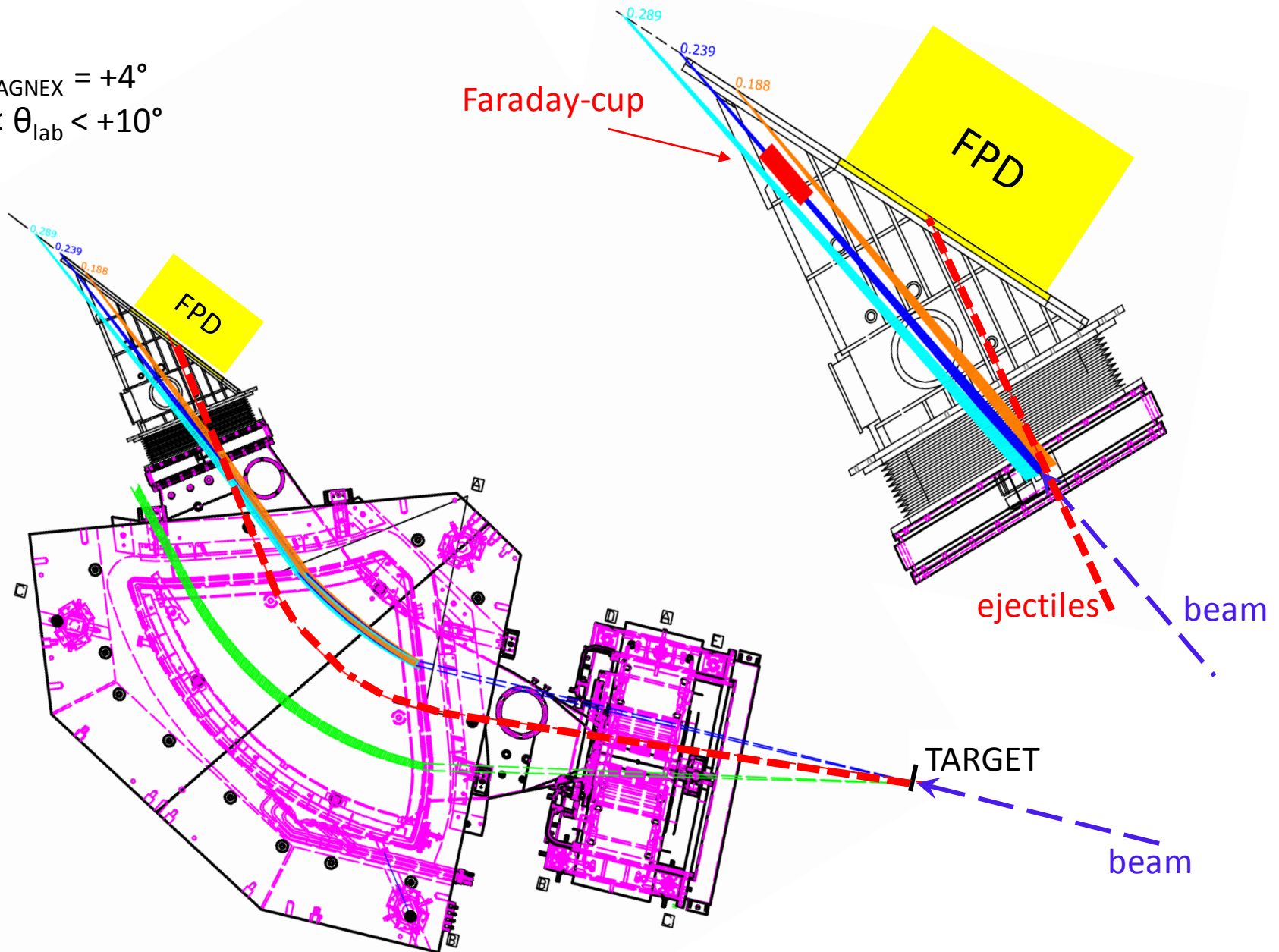
$^{40}\text{Ca}(^{18}\text{O}, ^{18}\text{Ne})^{40}\text{Ar}$  @ 270 MeV

- $^{18}\text{O}^{7+}$  beam from Cyclotron at **270 MeV** (10 pA, 3300  $\mu\text{C}$  in 10 days)
- $^{40}\text{Ca}$  target 300  $\mu\text{g}/\text{cm}^2$
- Ejectiles detected by the MAGNEX spectrometer  $0^\circ < \vartheta_{lab} < 10^\circ$   
corresponding to a momentum transfer ranging from  **$0.17 \text{ fm}^{-1}$  to  $2.2 \text{ fm}^{-1}$**



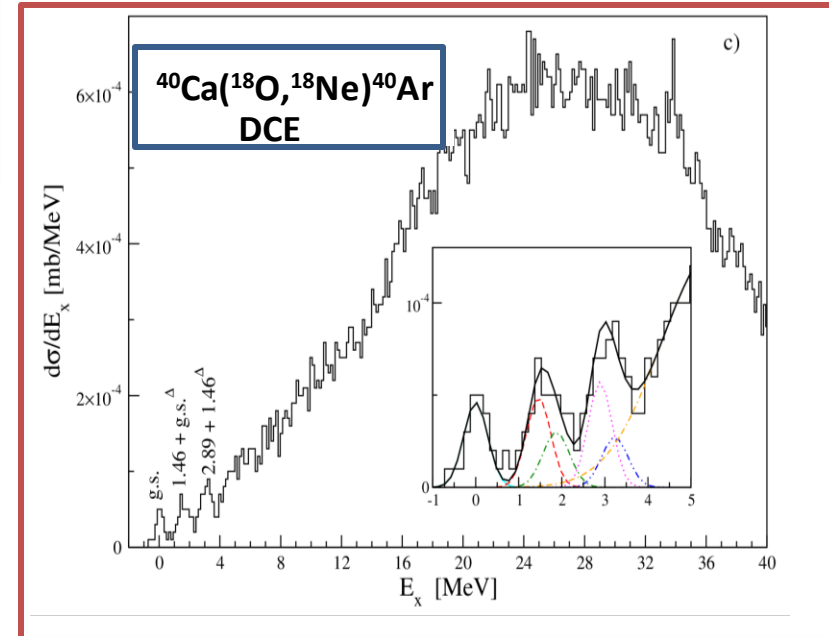
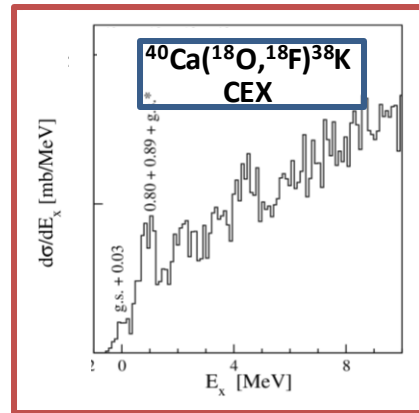
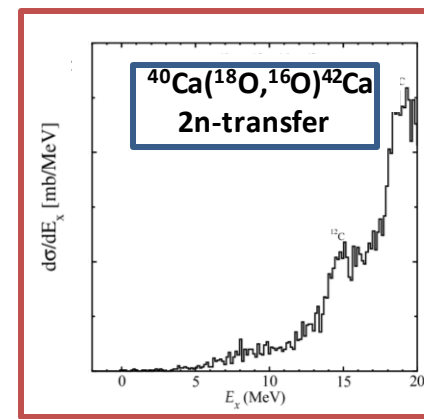
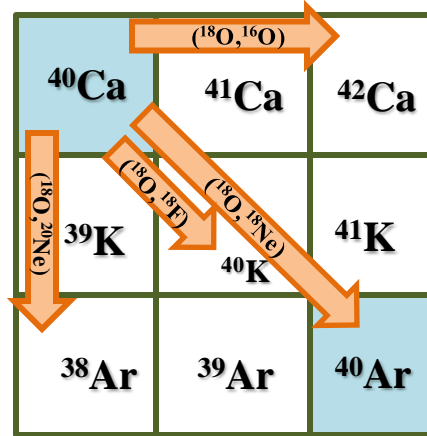
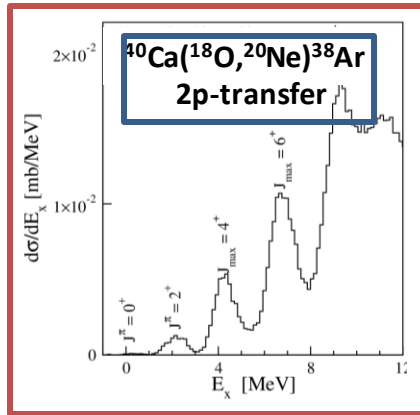
# Zero-degree measurement

$$\Theta_{\text{MAGNEX}} = +4^\circ$$
$$-1^\circ < \theta_{\text{lab}} < +10^\circ$$



# The pilot experiment

$^{18}\text{O} + ^{40}\text{Ca}$  at 270 MeV



- **Experimental feasibility:** zero-deg, resolution (500 keV), low cross-section ( $\mu\text{b}/\text{sr}$ )  
Limitations of the past HI-DCE experiments are overcome!
- **Data analysis feasibility:** the analysis of the DCE cross-section has led to NME compatible with the existing calculations

# Preliminary NME extraction

In the lack of «real» theory...



Under the hypothesis of validity of the factorization

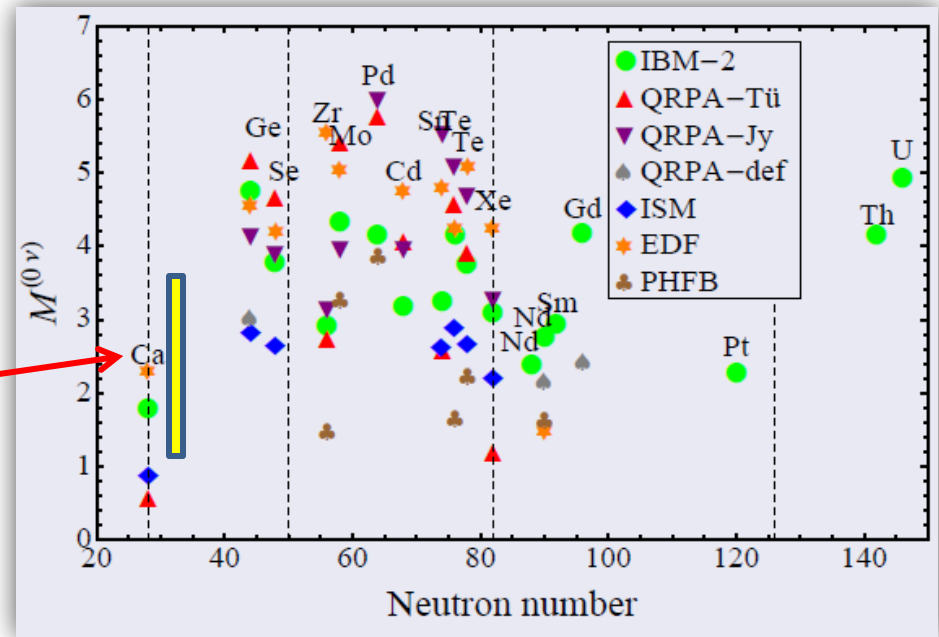
$$\frac{d\sigma}{d\Omega_{DCE}}(q, \omega) = \hat{\sigma}_\alpha^{DCE}(E_p, A) F_\alpha^{DCE}(q, \omega) B_T^{DCE}(\alpha) B_P^{DCE}(\alpha)$$

$$\left| M(^{40}\text{Ca}) \right|^2 = 0.37 \pm 0.18$$

Just to speculate:  
removing Pauli blocking one  
can roughly estimate

$$\left| M^{0\nu\beta\beta}(^{48}\text{Ca}) \right|^2 = 2.6 \pm 1.3$$

Pauli blocking about 0.14 for F and GT

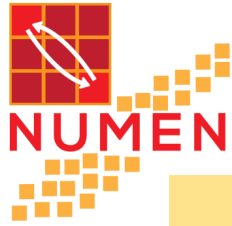


# A broader view

Limitations of NURE:

- Only two systems can be studied in 5 years (due to the **low cross-sections**)
- A more accurate job on the **theory** is needed

# The NUMEN program

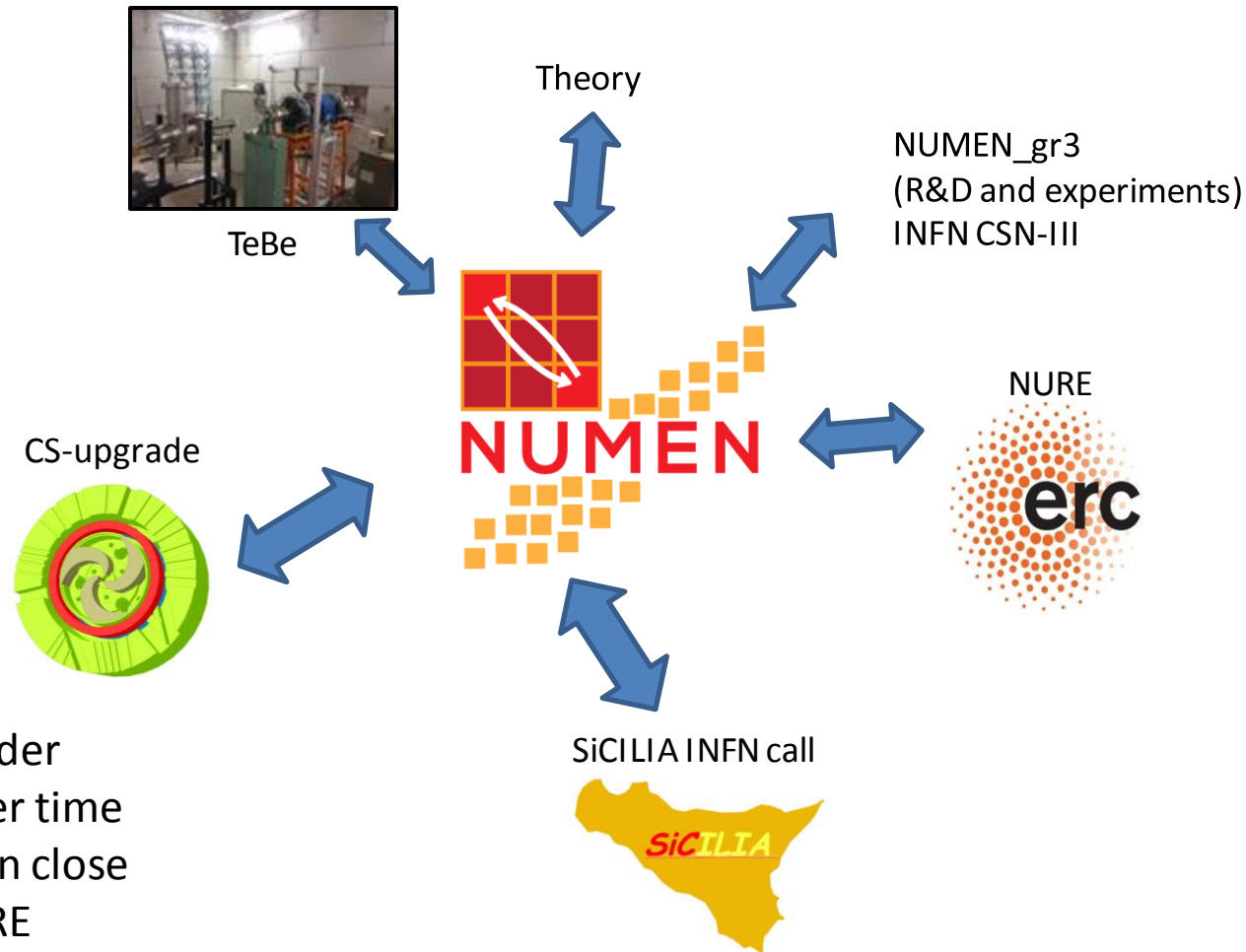


# A broader view



## The NUMEN project

NUclear Matrix Elements for Neutrinoless double beta decay



Operating in a wider context, in a wider time scale (10-15 yr), in close synergy with NURE



# A broader view



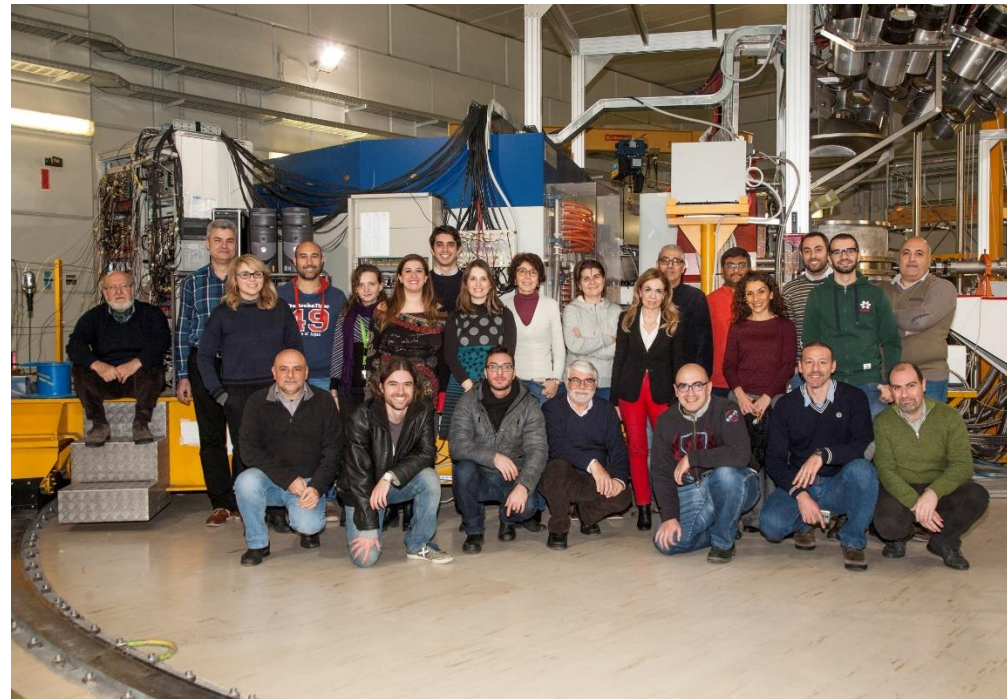
## The NUMEN project

NUclear Matrix Elements for Neutrinoless double beta decay

### The collaboration

**Spokespersons:** F. Cappuzzello and C. Agodi

E. Aciksoz, L. Acosta, C. Agodi, X. Aslanoglou, N. Auerbach,  
J. Bellone, R. Bijker, S. Bianco, D. Bonanno, D. Bongiovanni,  
T. Borello, I. Boztosun, V. Branchina, M.P. Bussa, L. Busso,  
S. Calabrese, L. Calabretta, A. Calanna, D. Calvo,  
F. Cappuzzello, D. Carbone, M. Cavallaro, E.R. Chávez Lomelí,  
M. Colonna, G. D'Agostino, N. Deshmuk, P.N. de Faria, C. Ferraresi,  
J.L. Ferreira, P. Finocchiaro, A. Foti, G. Gallo, U. Garcia,  
G. Giraud, V. Greco, A. Hacisalihoglu, J. Kotila, F. Iazzi,  
R. Introzzi, G. Lanzalone, A. Lavagno, F. La Via, J.A. Lay,  
H. Lenske, R. Linares, G. Litrico, F. Longhitano, D. Lo Presti,  
J. Lubian, N. Medina, D. R. Mendes, A. Muoio, J. R. B. Oliveira,  
A. Pakou, L. Pandola, H. Petrascu, F. Pinna, F. Pirri, S. Reito,  
D. Rifuggiato, M.R.D. Rodrigues, A. Russo, G. Russo,  
G. Santagati, E. Santopinto, O. Sgouros, S.O. Solakci,  
G. Souliotis, V. Soukeras, S. Tudisco, R.I.M. Vsevolodovna,  
R. Wheadon, V. Zagatto



*Italy, Brazil, Greece, México, Germany, Turkey, Israel, Romania, Spain*

73 members, 9 countries



# The Goals of the Research Program



## Main goal (Holy Graal):

Extraction from measured cross-sections of “*data-driven*” information on NME for all the systems candidate for  $0\nu\beta\beta$

## Secondary goals:



- **Constraints** to the existing theories of NMEs
- Model-independent **comparative information** on the sensitivity of half-life experiments
- Complete study of the **reaction mechanism**

BY-PRODUCTS



# A broader view



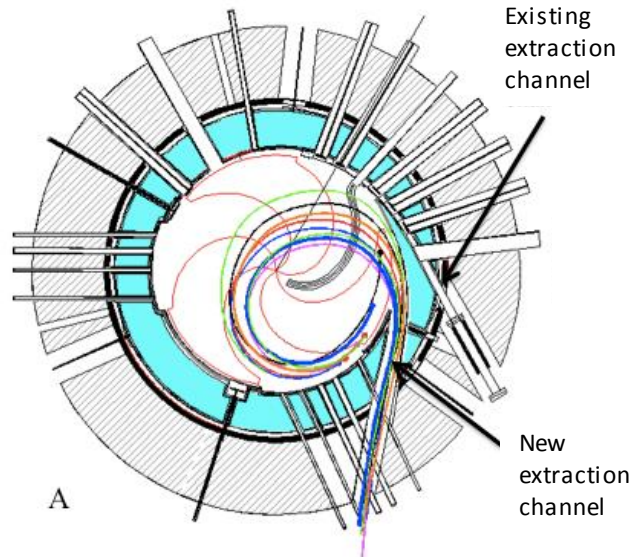
## The NUMEN project

**NU**clear **M**atrix **E**lements for **N**eutrinoless double beta decay

- **Phase1:** The experimental **feasibility** (completed)
- **Phase2:** **Experimental exploration** of few cases (NURE) and **work on theory** (running until 2021)
- **Phase3:** **Facility upgrade** (Cyclotron, MAGNEX, beam line, ...) to work with two orders of magnitude more intense beam
- **Phase4:** **Systematic experimental campaign** on all the systems with the upgraded facility

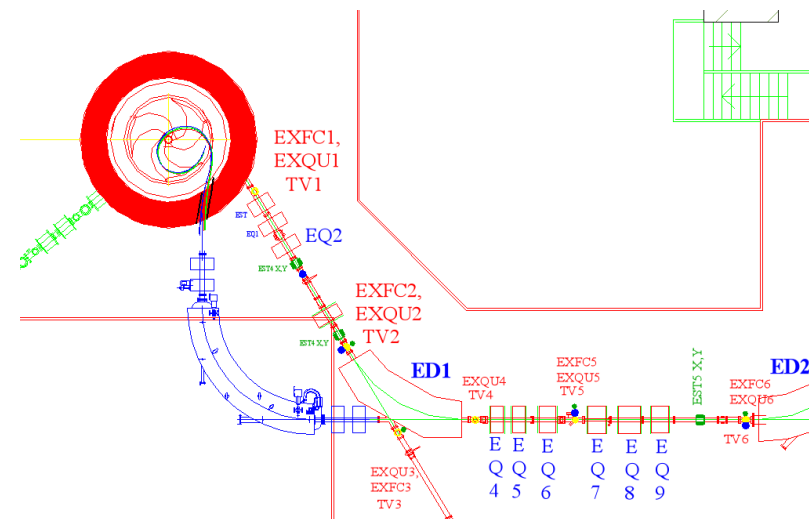
# Upgrade of LNS facilities: The CS accelerator

- **CS** accelerator current (from 100 W to 5-10 kW);



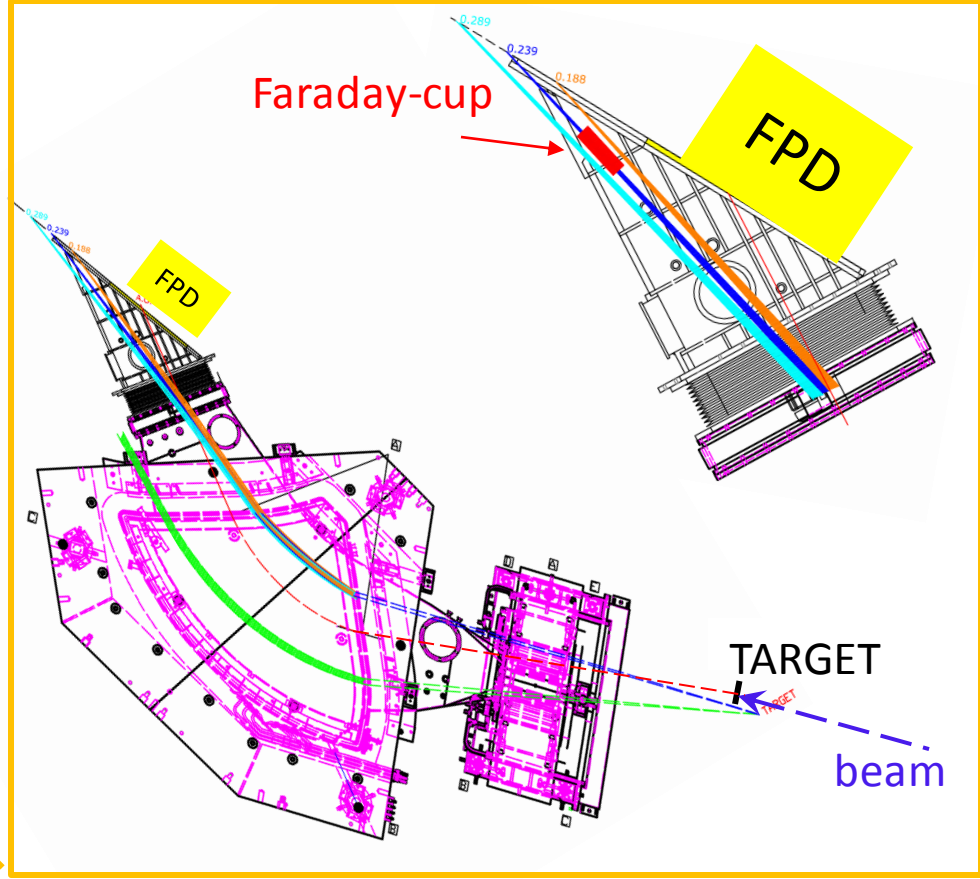
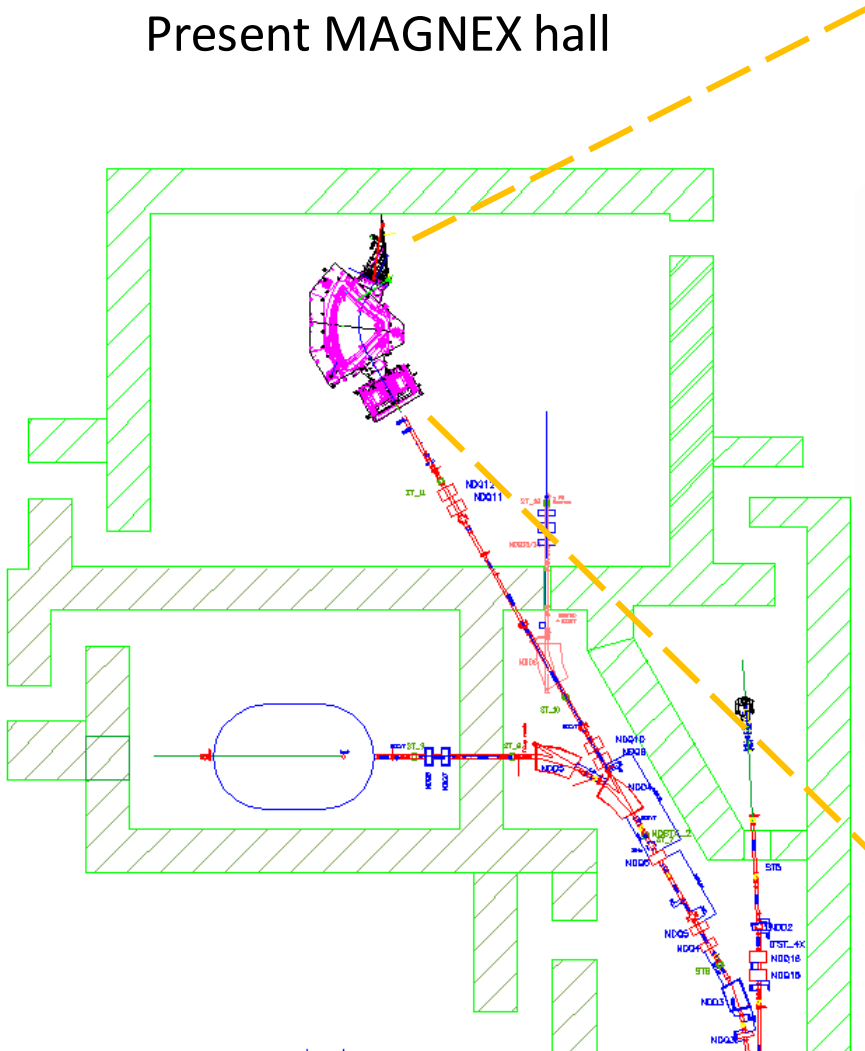
From **electrostatic extraction**  
(low efficiency 50%) to  
**extraction by stripping** (>99%)

- **beam transport line**  
transmission efficiency to  
nearly 100%



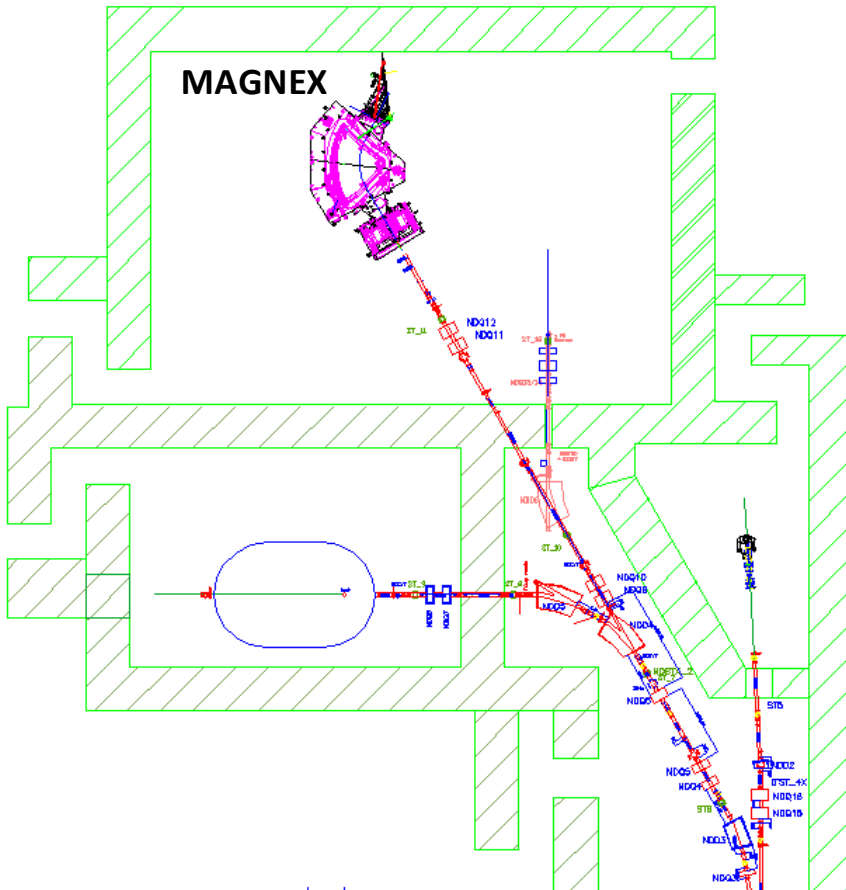
# Beam dump inside the MAGNEX hall

Present MAGNEX hall

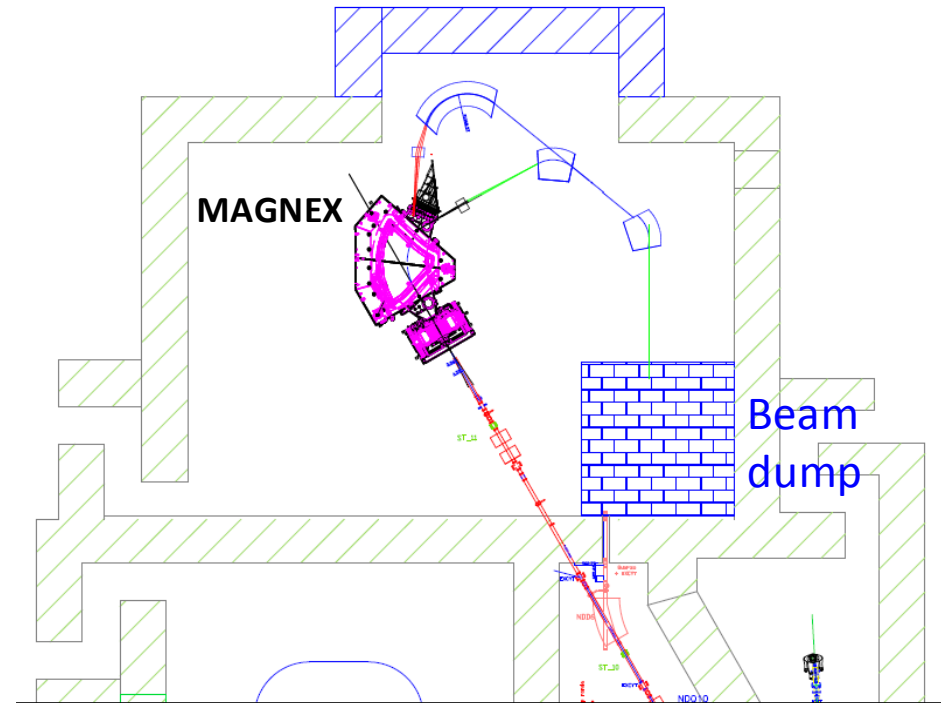


# Beam dump inside the MAGNEX hall

Present MAGNEX hall



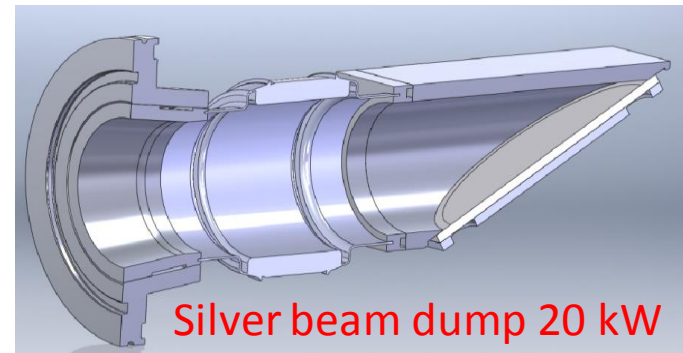
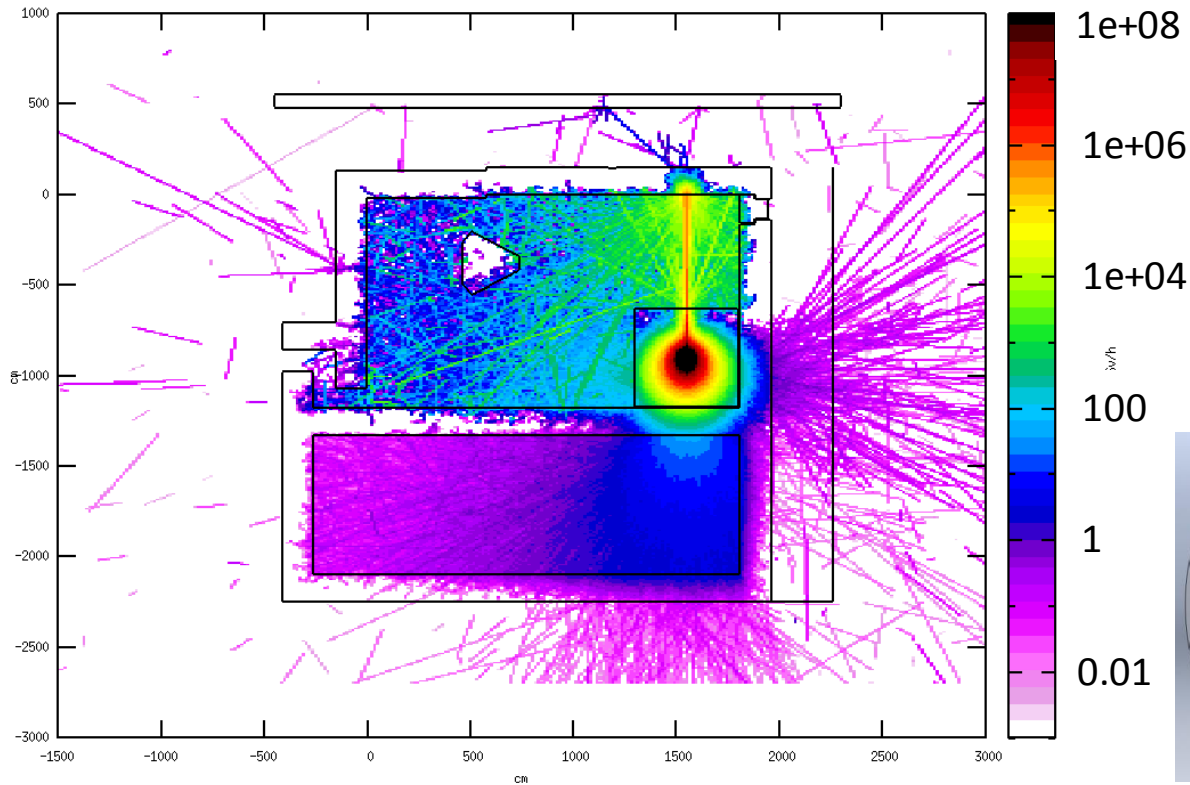
Future MAGNEX hall



# Beam dump inside the MAGNEX hall

**85  $\mu$ A beam of  $^{18}\text{O}$  on Ag**

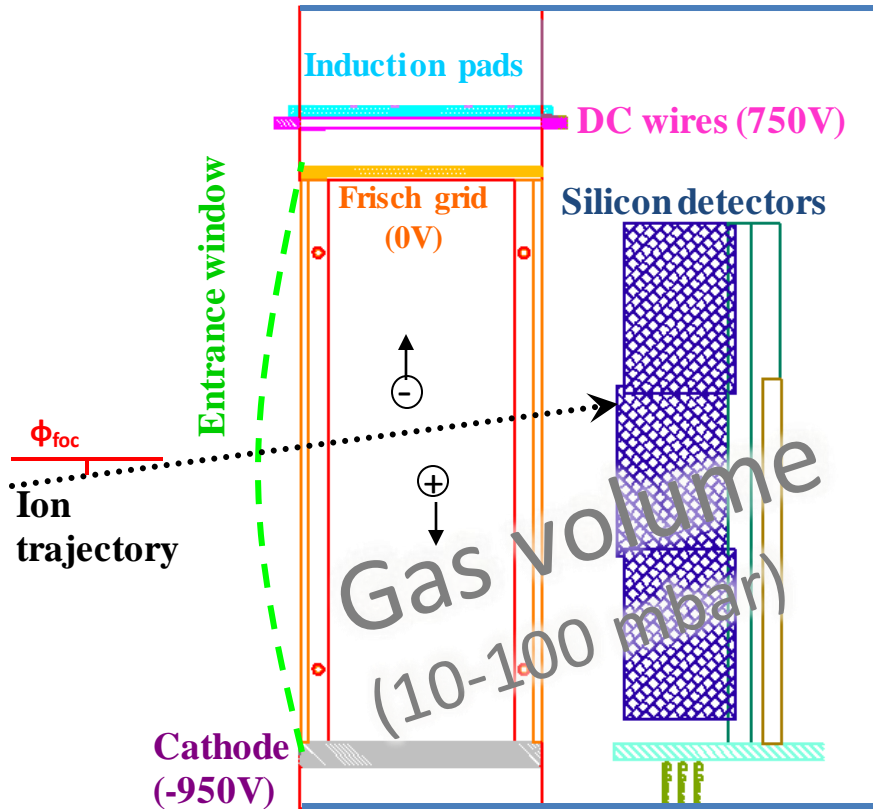
H\*, 0-18, 60MeV/u, 80 microA su BS di Argento (schermo in barite)



From S. Russo (LNS radioprotection service)

# Upgrade of the MAGNEX Focal Plane Detector

Large volume: 1360mm X 200mm X 96mm



Section view



Wall of 60 stopping 7 X 5 cm<sup>2</sup> Silicon detectors  
Covered area 100 X 20 cm<sup>2</sup>  
Thickness 500 – 1000  $\mu$ m

Hybrid detector:

Gas section: proportional wires and drift chambers

+

Stopping wall of silicon detectors

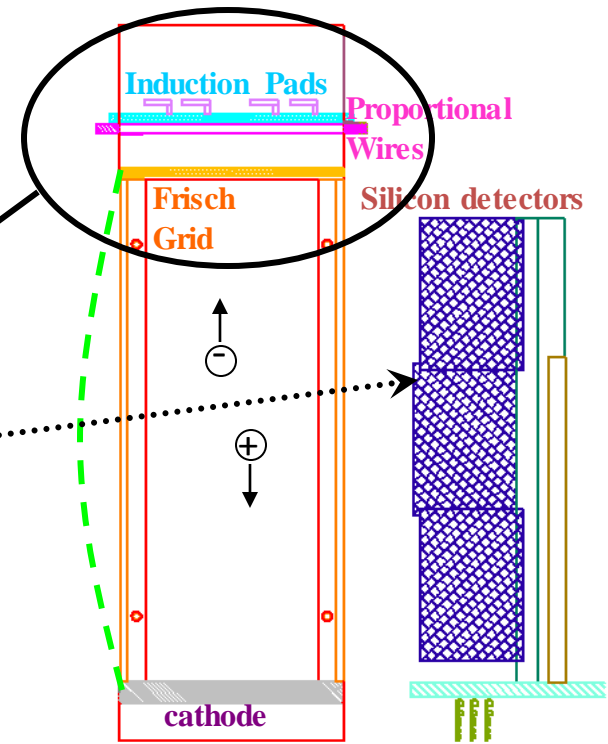
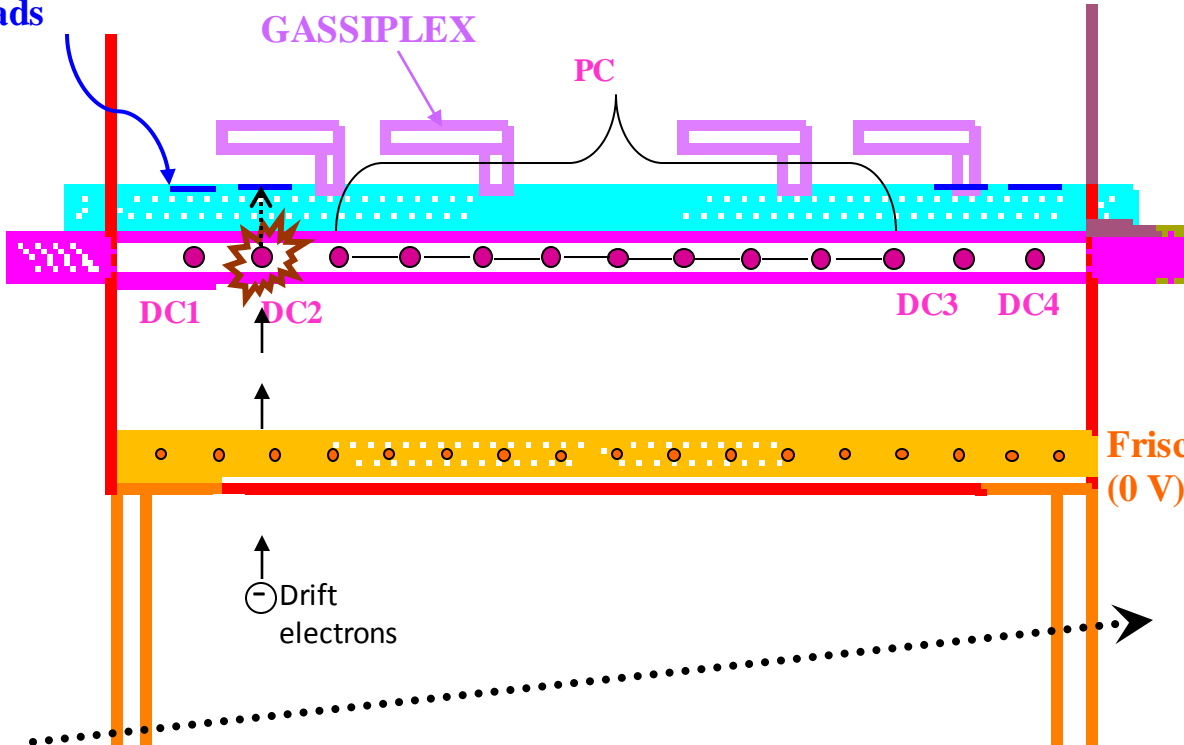
# Upgrade of the MAGNEX FPD: Gas Tracker

Present:  
wire-based gas tracker  
Low pressure (10-100 mbar)  
Rate limit **few KHz**

Induction  
Pads

GASSIPLEX

PC



Proportional  
Wires (750 V)

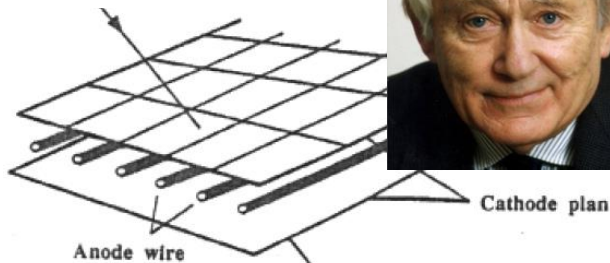
Frisch grid  
(0 V)

Rate from **few kHz to MHz**  
Preserving low pressure  
operations



# Gaseous detectors

**MWPC 1968**  
**G. Charpak**  
**Nobel Prize in 1992**



**Tens-Hundred Microns**

**Multi-Wire Proportional Chamber -MWPC**

## Gaseous detectors: why?

- good stability, robustness and aging compared to solid/liquid detectors
- good space and moderate energy resolution
- three dimensional readout/flexible geometry
- cheap
- still today the only choice whenever large-area coverage with low material budget is required

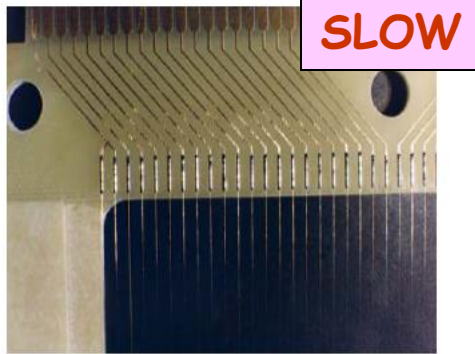
# Limits of wire-based detectors

## Wire-Based Detector:

Secondary effects → Gain limits

Space charge → Counting-rate limits ( $10^4$  Hz/mm<sup>2</sup>)

Aging → Damage after long-term operation



Wire spacing → 1-2 mm

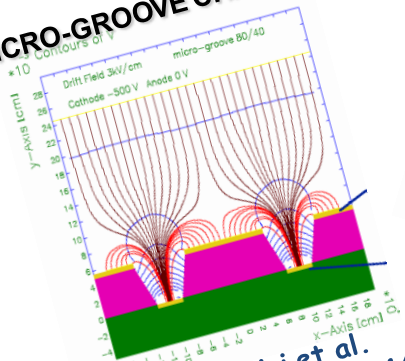


## New Idea:

Move down in size & add cathodes very close to anodes to evacuate ions produced during the avalanche process

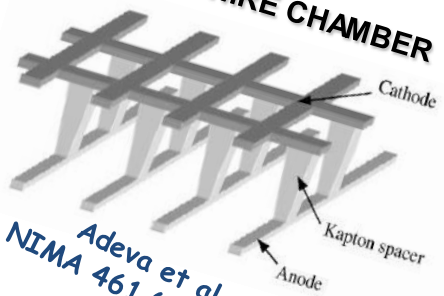
# Micro-Pattern Gaseous Detector

**MICRO-GROOVE CHAMBER**



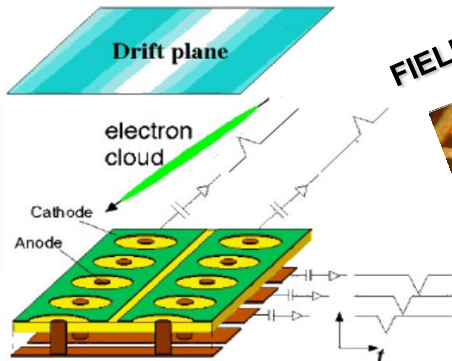
Bellazini et al.  
NIMA 424 (1999) 444

**MICROWIRE CHAMBER**



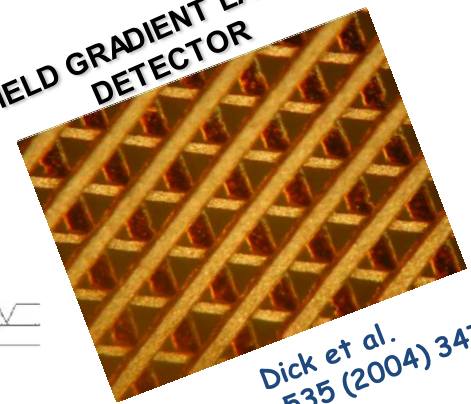
Adeva et al.  
NIMA 461 (2001) 33

**MICRO-PIXEL CHAMBER**



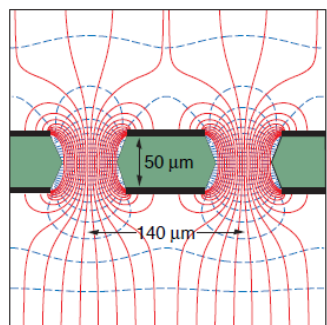
Ochi et al.  
NIMA 471 (2001) 264

**FIELD GRADIENT LATTICE DETECTOR**



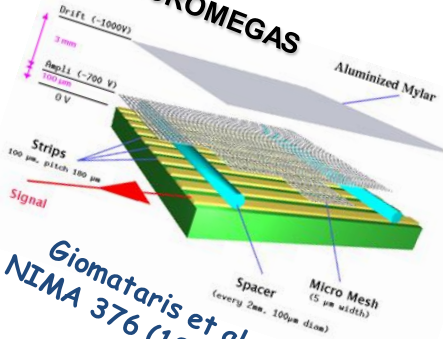
Dick et al.  
NIMA 535 (2004) 347

**GAS ELECTRON MULTIPLIER**



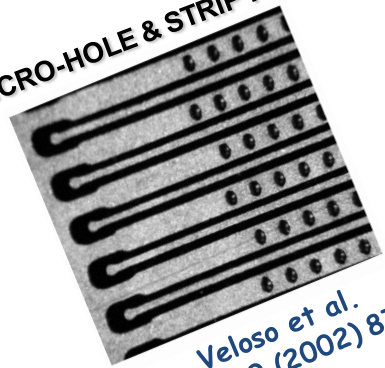
Sauli  
NIMA 386 (1997) 531

**MICROME GAS**



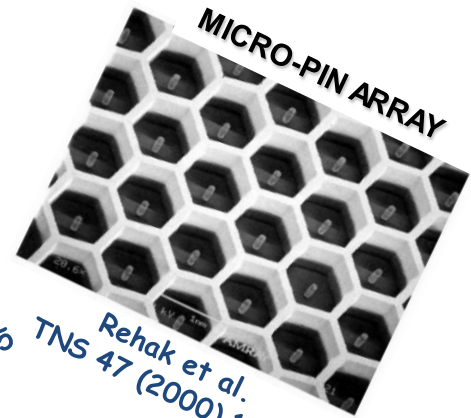
Giomataris et al.  
NIMA 376 (1996) 29

**MICRO-HOLE & STRIP PLATE**



Veloso et al.  
TNS 49 (2002) 875

**MICRO-PIN ARRAY**



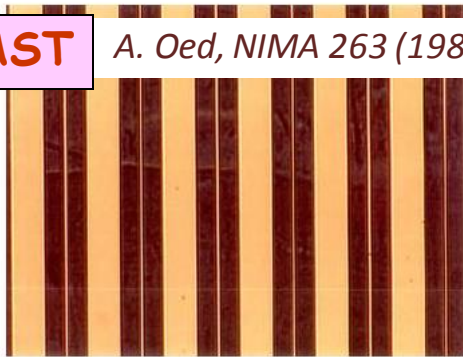
Rehak et al.  
TNS 47 (2000) 1426

.... and many others

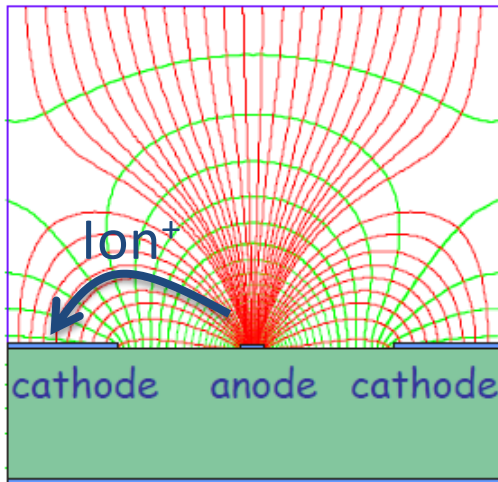
# Micro-strip gas chamber (MSGC)

FAST

A. Oed, NIMA 263 (1988) 351

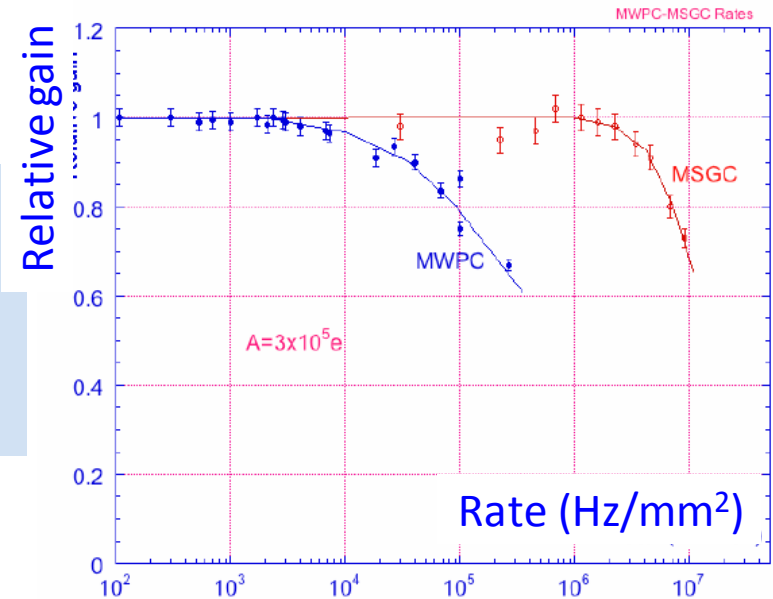


Anode spacing  $\rightarrow$  200  $\mu\text{m}$



Micrometric structures of electrodes (photolithography techniques): Pattern of thin anode and cathode strips on high-resistivity substrate

Rate Capability Limits due to space charge overcome by increasing the amplifying cell granularity



## Limitations:

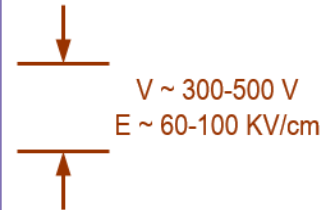
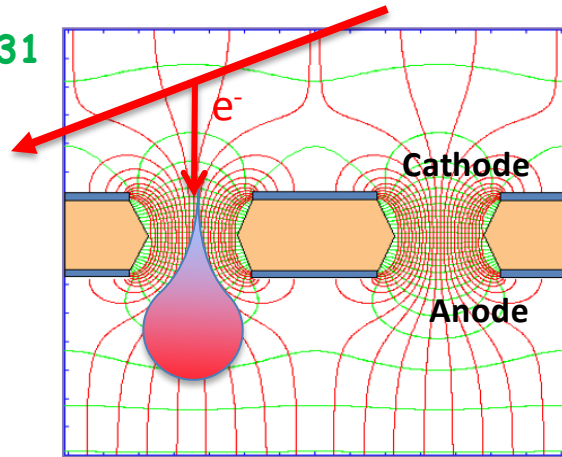
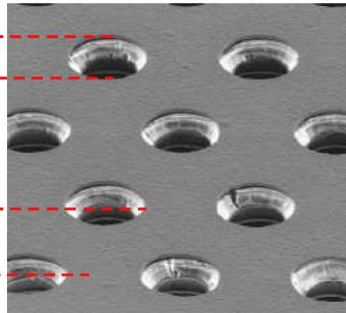
- High E-values at the edge between insulator and strips  $\rightarrow$  **discharges**
- Charge accumulation at the insulator  $\rightarrow$  **gain evolution vs time**



# Gas Electron Multiplier (GEM)

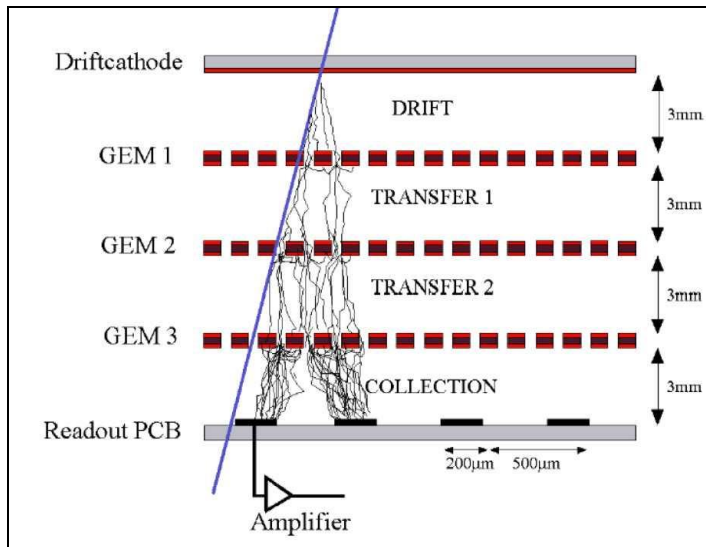
Thin metal-coated polymer (Kapton) foil chemically pierced by a high density of holes

Sauli, NIMA 386 (1997) 531



Confined avalanche within holes  
→ Lesser photon-mediated secondary effects

Multi-stage



## Properties:

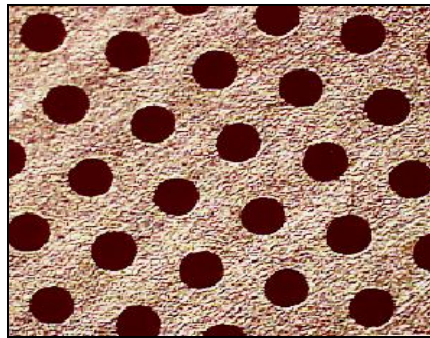
- Large area
- High rate (up to 1 MHz/mm<sup>2</sup>)
- High Spatial Resolution ( $\approx 40 \mu\text{m}$ )
- High gas gain ( $\sim 10^3$ - $10^4$  single-stage,  $10^6$ - $10^7$  multi-stage)
- 15-20% energy resolution (5.9 keV X-rays)
- Flexible detector shape and readout patterns

# Thick-Gas Electron Multiplier (THGEM)

Manufactured by standard PCB techniques of precise drilling in G-10/FR-4 (and other materials) and Cu etching

→ **Simple & Robust**

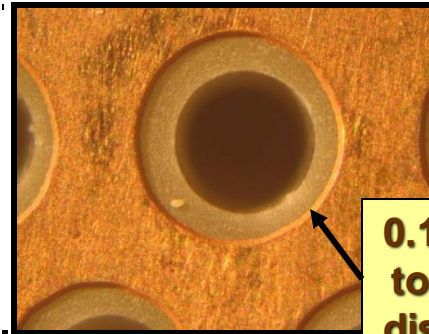
**STANDARD GEM**  
 $10^3$  GAIN IN SINGLE GEM



1 mm

**THGEM**

$10^5$  gain in single-THGEM



0.1 mm rim  
to prevent  
discharges

THGEM geometry:

- ) Thickness = 0.6 mm
- ) Hole  $\varnothing$  = 0.5 mm
- ) Hole Pitch = 1 mm

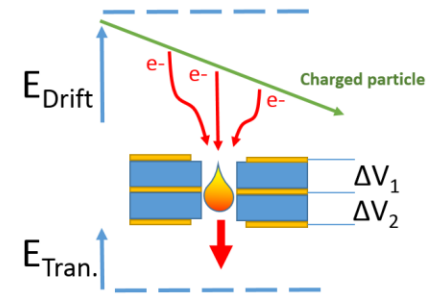
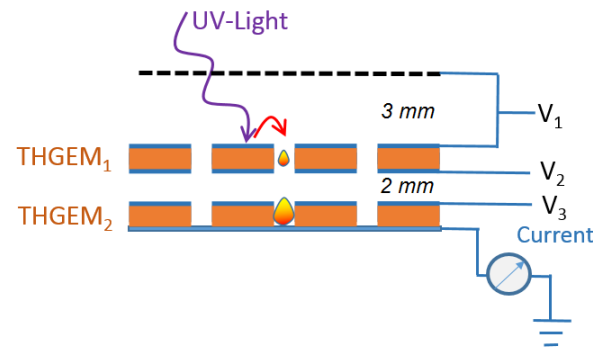
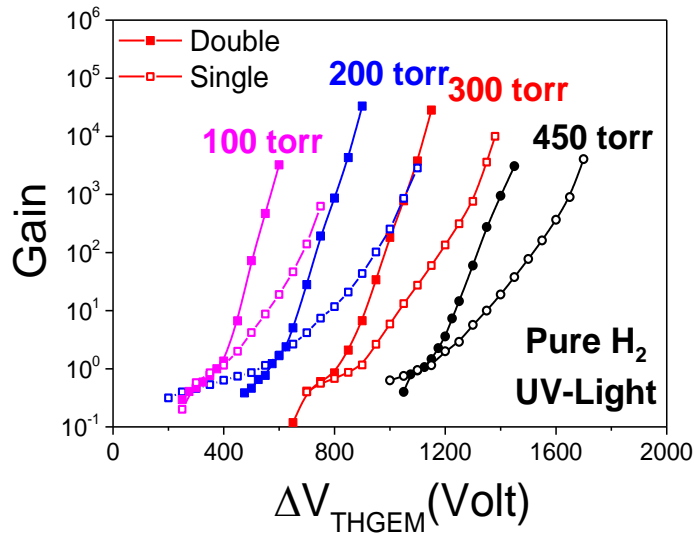
- Effective single-electron detection
- High gas gain  $\sim 10^5$  ( $>10^6$ ) @ single (double) THGEM
- Few-ns RMS time resolution
- Sub-mm position resolution
- **MHz/mm<sup>2</sup> rate capability**
- Cryogenic operation: OK
- Gas: molecular and noble gases
- **Pressure: 1mbar - few bar**

*L. Periale et al., NIM A478 (2002) 377*  
*P. Jeanneret, PhD thesis, Neuchatel U., 2001*  
*P.S. Barbeau et al., IEEE NS50 (2003) 1285*  
*R. Chechik et al., NIMA 535 (2004) 303*

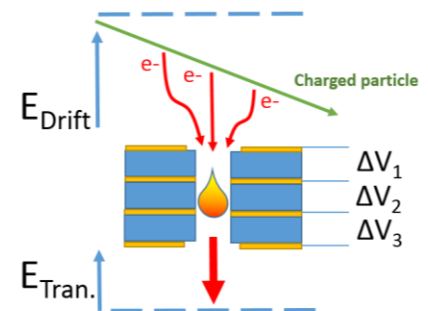
From M. Cortesi

# Operation of THGEM in low-pressure, “pure” Noble Gas

Cortesi et al., 2015 JINST P09020



2-layer THGEM



3-layer THGEM

Large maximum achievable gain at low pressure due to:

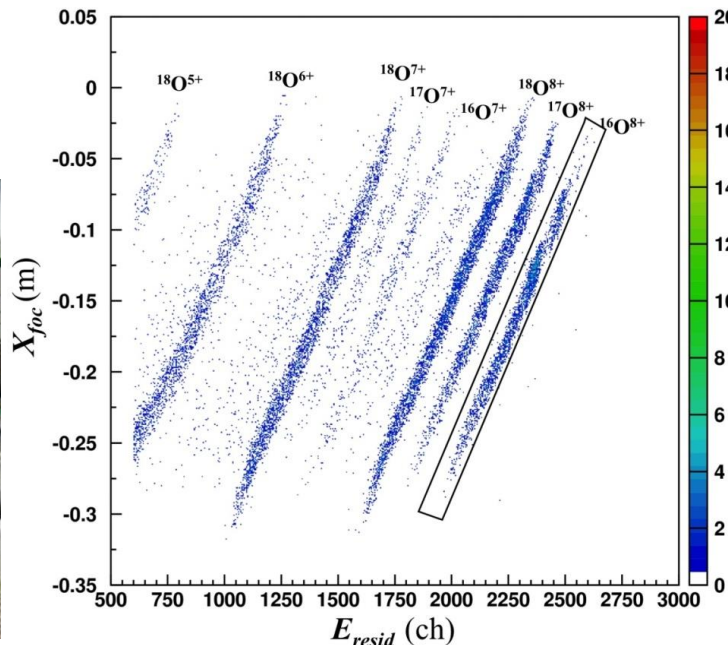
- 1) Extended avalanche volume (larger than the  $e^-$  mean free path)  
→ high  $e^-$  multiplication
- 2) Avalanche confinement within the hole  
→ Lesser photon-mediated secondary effects

# Upgrade of the MAGNEX FPD: The Particle Identification

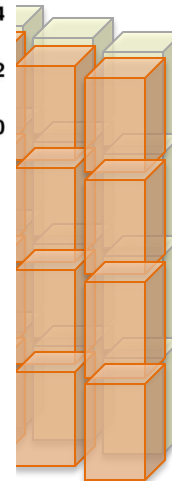
A radiation tolerant stopping wall for particle identification

**Radiation hardness** → expected  $10^{14}$  ions in ten years activity  
(silicon detector dead at  $10^9$  implanted ions/cm<sup>2</sup> (heavy ions not MIP!!))

From wal  
detectors



??



What is the right material??

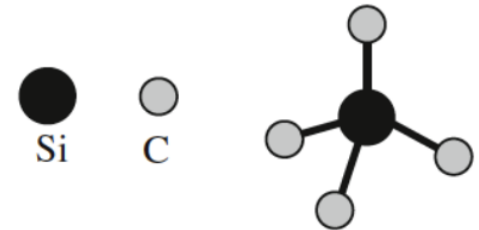
- Radiation hard
- Heavy ions
- Working in gas environment
- Large area
- High energy resolution (1%)
- Timing resolution (few ns)

**A big challenge!**



# Silicon Carbide (SiC)

Tetrahedron of Carbon and Silicon atoms with strong bonds in the crystal lattice. **Very hard and strong material!**



**strong bonds !**

## General Properties of SiC

- high thermal conductivity
- low thermal expansion
- high strength (hardness)
- chemical inertness



**Exceptional thermal shock resistant qualities**

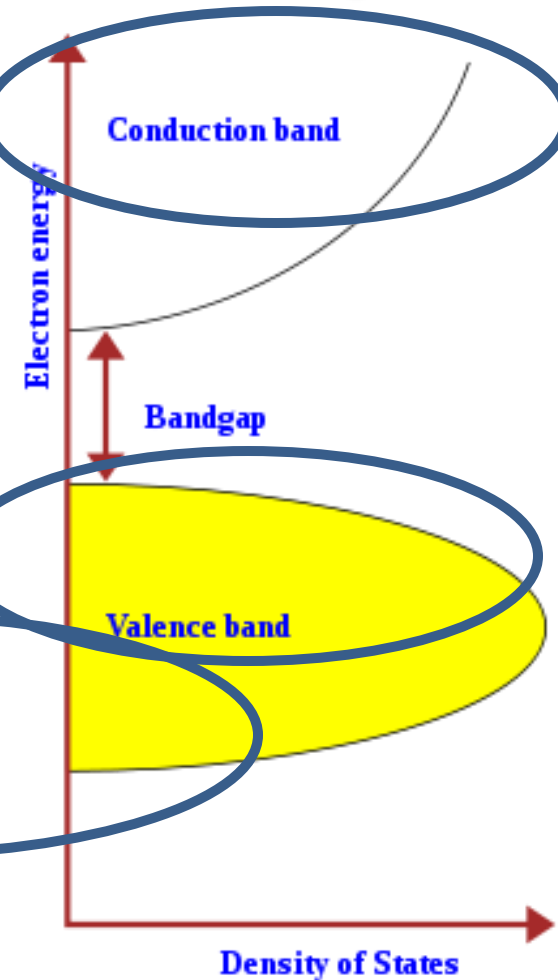
## Applications on ELECTRONIS DEVICES

- High power
- High frequency
- High temperature
- Radiation detectors

# SiC for radiation detectors

Property	Diamond	GaN	4H SiC	Si
$E_g$ [eV]	5.5	3.39	3.28	1.12
$E_{\text{breakdown}}$ [V/cm]	$10^7$	$4 \cdot 10^6$	$3-4 \cdot 10^6$	$3 \cdot 10^5$
$\mu_e$ [ $\text{cm}^2/\text{Vs}$ ]	1800	1000	800	1450
$\mu_h$ [ $\text{cm}^2/\text{Vs}$ ]	1200	30	115	450
$v_{\text{sat}}$ [cm/s]	$2.2 \cdot 10^7$	-	$2 \cdot 10^7$	$0.8 \cdot 10^7$
Z	6	31/7	14/6	14
$\epsilon_r$	5.7	9.6	9.7	11.9
e-h energy [eV]	13	8.9	7.6-8.4	3.6
Density [g/cm <sup>3</sup> ]	3.515	6.15	3.22	2.33
Displacem. [eV]	43	$\geq 15$	30-40	13-15

- Wide band-gap (3.3eV)
- ⇒ Visible blind
- ⇒ Lower Leakage current



- Signal
- ⇒ Less charge than Si,  $\text{SiC} \approx \text{Si}/2$

- Higher displaceme threshold
- ⇒ Radiation harder t

# Silicon Carbide (SiC)

Silicon Carbide technology offers then an ideal response to the challenges of NUMEN, since it gives the opportunity to couple the **excellent properties of silicon detectors** (resolution, efficiency, linearity, compactness) with a **much bigger radiation hardness** (up to five orders of magnitude for heavy ions), thermal stability and insensitivity to visible light.

However...

# Defects in SiC

Challenges in the growth of bulk SiC: to grow large single crystals in large quantities is a problem

## Macroscopic defects

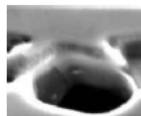
- polytype inclusions
- micropipes
- comets, carrots

## Microscopic defects

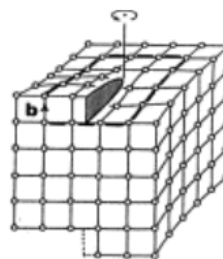
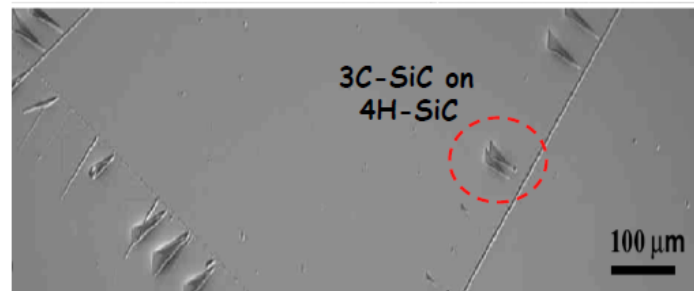
- dislocations
- stacking faults
- interstitial, vacancies
- divacancies, antisites

## Extended defects

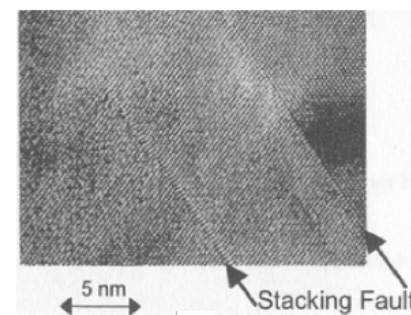
Micro-pipe



polytype inclusions

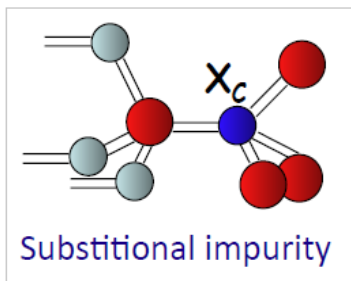
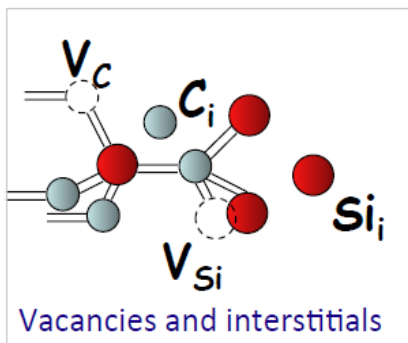


dislocations



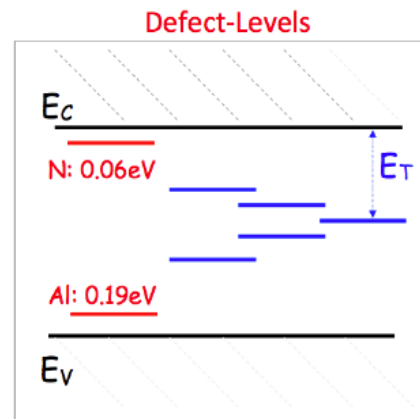
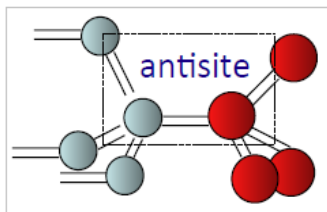
Stacking Fault

## Point and Point-like defects



Donor & Acceptor Impurities

Deep levels in the gap =>



From S. Tudisco

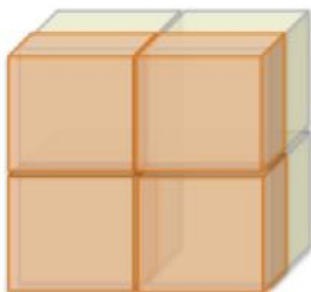


# Silicon Carbide Detectors for Intense Luminosity Investigations and Applications

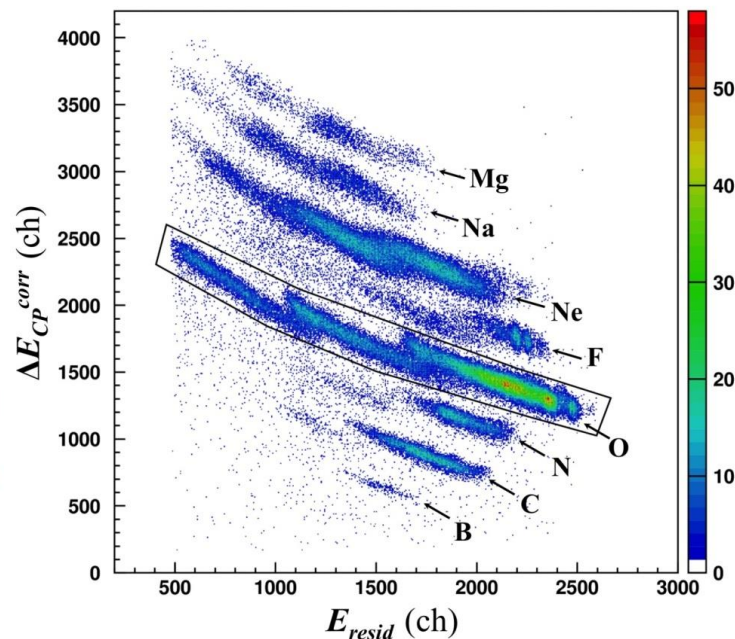


P.I. S. Tudisco

## SiC $\Delta E$ -E telescopes



- ✓ Active area  $1 \text{ cm}^2$
- ✓  $\Delta E$  stage thickness  $\geq 100 \mu\text{m}$
- ✓ E stage thickness  $500 \div 1000 \mu\text{m}$

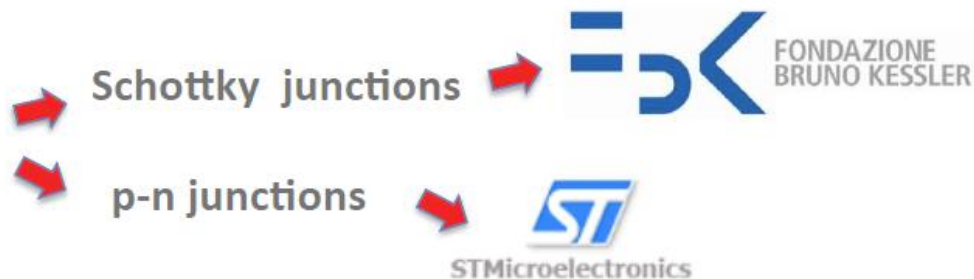


## SiCILIA Strategy



Epitaxial growth SiC: beyond the state of the art (small number of defects)

## New Tecnology



From S. Tudisco



## Participating INFN research units

*INFN Laboratori Nazionali del Sud di Catania (LNS)*

*INFN Sezione di Catania and "Gruppo collegato di Messina" (CT-ME)*

*INFN Sezione di Milano Bicocca (MI-B)*

*INFN Sezione di Milano (MI)*

*INFN Sezione di Firenze (FI)*

*INFN Sezione TIFPA (TN)*

*INFN Sezione Pisa (PI)*

## External institutions

CNR-IMM – Catania

CNR-INO – Pisa

## Companies

Fondazione Bruno Kessler (**FBK**) – Trento

ST Microelectronics – Catania

LPE – Catania (**LPE**)

## Global Deliverables

- Tens of detectors: epitaxial grow SiC (50-150  $\mu\text{m}$  thick) semi-insulating SiC (500-1000  $\mu\text{m}$  thick)
- Study of the performance in the electrons and ions detection (radiation hardness, energetic resolution, timing, etc.)
- Study of the performance in the neutrons and X-ray detection
- Study of the ions identification through the pulses shape analysis
- A wall of tens of SiC telescopes equipped with a VMM ASIC front-end as demonstrator
- Performance of demonstrator in operative conditions

# Reaction targets

**Target** technology for intense heavy-ion beam (10pμA)

Typical present target ladder



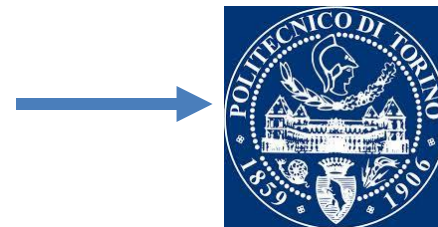
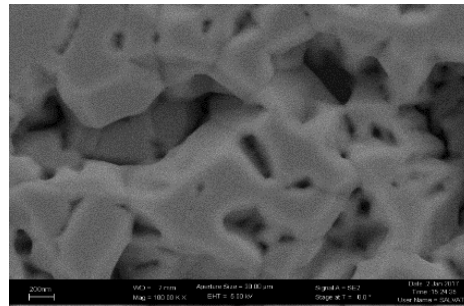
Isotopes candidate for  $0\nu\beta\beta$ :

$^{116}\text{Sn}$ ,  $^{116}\text{Cd}$ ,  $^{76}\text{Ge}$ ,  $^{76}\text{Se}$ ,  $^{130}\text{Te}$ ,  $^{48}\text{Ca}$ , ...

Most of them have **low melting temperature** and **low thermal conductivity**

Idea:

Evaporation on a **backing material** with good properties (Graphen, Diamond, Graphite) and **cooling**



Politecnico Torino  
and INFN-Torino

# The NUMEN challenges

## Theory:

Formal development and calculation of reaction cross sections as a function of the NME

## Detectors:

- Gas tracker for high rate heavy ions at low pressure (MPGD)
- PID wall covering a large area made of radiation hard and high resolution detectors (SiC)

## Targets:

For intense heavy-ion beams

## Mechanics:

Beam dump for zero-degree beam downstream of the spectrometer

Accelerator and beam lines:  
Upgrade of the Superconducting Cyclotron for high power

Integration



- Many **experimental facilities** for  $0\nu\beta\beta$  half-life, but not for the **NME**
- Pioneering experiments shown that **DCE cross sections can be suitably measured**
- First results for the ( $^{18}\text{O}, ^{18}\text{Ne}$ ) and ( $^{20}\text{Ne}, ^{20}\text{O}$ ) are encouraging, showing that **quantitative information on  $0\nu\beta\beta$  NME** are not precluded
- **Experimental campaign** on nuclei candidates for  $0\nu\beta\beta$  and work on the **theory** in the next 5 years
- The **upgrade** foreseen for the INFN-LNS cyclotron and the MAGNEX spectrometer will allow to build a **unique facility** for a systematic exploration of all the nuclei candidate for  $0\nu\beta\beta$